

AD-A202 821

AFAL-TR-88-068

AD:



Final Report
for the period
July 1984 to
March 1988

Prepolymer Characterization

October 1988

Author:
R. J. Laub

San Diego State University
Department of Chemistry
San Diego, CA 92182

F04611-84-K-0016

Approved for Public Release

Distribution is unlimited. The AFAL Technical Services Office has reviewed this report, and it is releasable to the National Technical Information Service, where it will be available to the general public, including foreign nationals.

DTIC
ELECTE
DEC 07 1988
S H D

Prepared for the:

Air Force
Astronautics
Laboratory

Air Force Space Technology Center
Space Division, Air Force Systems Command
Edwards Air Force Base,
California 93523-5000

88 12 6 037

REPORT DOCUMENTATION PAGE				Form Approved OMB No. 0704-0188		
1a. REPORT SECURITY CLASSIFICATION Unclassified			1b. RESTRICTIVE MARKINGS			
2a. SECURITY CLASSIFICATION AUTHORITY			3. DISTRIBUTION / AVAILABILITY OF REPORT Approved for public release. Distribution is unlimited.			
2b. DECLASSIFICATION / DOWNGRADING SCHEDULE						
4. PERFORMING ORGANIZATION REPORT NUMBER(S)			5. MONITORING ORGANIZATION REPORT NUMBER(S) AFAL TR-88-068			
6a. NAME OF PERFORMING ORGANIZATION San Diego State University		6b. OFFICE SYMBOL (if applicable)	7a. NAME OF MONITORING ORGANIZATION Air Force Astronautics Laboratory			
6c. ADDRESS (City, State, and ZIP Code) Department of Chemistry San Diego, CA 92182			7b. ADDRESS (City, State, and ZIP Code) LSSP Edwards AFB, CA 93523-5000			
8a. NAME OF FUNDING / SPONSORING ORGANIZATION		8b. OFFICE SYMBOL (if applicable)	9. PROCUREMENT INSTRUMENT IDENTIFICATION NUMBER FO4611-84-K-0016			
8c. ADDRESS (City, State, and ZIP Code)			10. SOURCE OF FUNDING NUMBERS			
			PROGRAM ELEMENT NO. 62302F	PROJECT NO. 5730	TASK NO. 00	WORK UNIT ACCESSION NO. AN
11. TITLE (Include Security Classification) Prepolymer Characterization (U)						
12. PERSONAL AUTHOR(S) Laub, Richard J.						
13a. TYPE OF REPORT FINAL		13b. TIME COVERED FROM 84/7 TO 88/3		14. DATE OF REPORT (Year, Month, Day) 88/10	15. PAGE COUNT 147	
16. SUPPLEMENTARY NOTATION This report has been divided into two sections, the main report and the appendix. The appendix is being issued as a separate document (AFAL TR-88-068 Supplement 1).						
17. COSATI CODES			18. SUBJECT TERMS (Continue on reverse if necessary and identify by block number) hydroxy-terminated polybutadiene, R-45M, prepolymer characterization, chromatography, mass spectrometry, infrared spectroscopy, viscosity, density, vapor phase osmometry. (M311)			
FIELD 21	GROUP 09	SUB-GROUP 2				
19. ABSTRACT (Continue on reverse if necessary and identify by block number)						
<p>Some fundamental aspects of the physicochemical characterization of propellant prepolymers were explored for the purpose of developing and optimizing analytical procedures for molecular weight, degree of branching, and functionality distributions. Fractional solution fractionation, vapor phase osmometry, viscosity, Fourier-transform infrared and nuclear magnetic resonance spectroscopy, gel-permeation, gas, and "high-performance" column-liquid chromatography, and mass spectrometry were employed with model polystyrene polymers as well as bulk and fractionated R-45M and HMDS-treated R-45M. The methodologies and techniques of analysis ultimately developed make use only of readily-available equipment, are applicable to characterization and routine quality control of virtually any prepolymer system, and can be implemented in any vendor or governmental laboratory.</p>						
20. DISTRIBUTION / AVAILABILITY OF ABSTRACT <input checked="" type="checkbox"/> UNCLASSIFIED/UNLIMITED <input type="checkbox"/> SAME AS RPT. <input type="checkbox"/> DTIC USERS			21. ABSTRACT SECURITY CLASSIFICATION UNCLASSIFIED			
22a. NAME OF RESPONSIBLE INDIVIDUAL Roy Wurzbach			22b. TELEPHONE (Include Area Code) (805) 275-5414		22c. OFFICE SYMBOL LSSP	

TABLE OF CONTENTS

	<u>PAGE</u>
INTRODUCTION	1
CONTEMPORARY METHODS OF MOLECULAR WEIGHT DETERMINATION ..	1
Solvent Partitioning	1
Colligative Properties	2
Gel Permeation Chromatography	2
Comparison of Methods	4
CONTEMPORARY METHODS OF CHAIN-BRANCHING DETERMINATION	4
CONTEMPORARY METHODS OF FUNCTIONALITY DETERMINATION	5
Silica-Gel Column Liquid Chromatography	5
Gelation-Point	5
Wet-Chemical Techniques	5
CONTRACT OVERVIEW. PHASE I: CHARACTERIZATION BY MOLECULAR WEIGHT	6
Task 1. Fractionation and Characterization of Polystyrenes and HTPB	6
Task 2. Mass Spectral Determination of Fraction Molecular Weights	6
CONTRACT OVERVIEW. PHASE II: CHARACTERIZATION BY CHAIN BRANCHING	7
Task 1. Ultra-High Resolution Reverse-Phase Microbore-Column Liquid Chromatography	7
Task 2. Liquid Chromatography/Mass Spectrometry	7
CONTRACT OVERVIEW. PHASE III: CHARACTERIZATION BY FUNCTIONALITY	7
Task 1. Hydroxyl Group Content and Distribution	7
Task 2. Analysis of Lots of R-45M	7
EXPERIMENTAL SECTION	8
Apparatus and Equipment	8
Liquid Chromatographs	8
Gas Chromatograph	8
Mass Spectrometer	8
Infrared Spectrophotometer	8
Density Apparatus	8
Vapor-Phase Osmometer	8
Viscometry Apparatus	8
Water-Bath Thermostat	8
Differential Scanning Calorimeter	9
Nuclear Magnetic Resonance Spectrometer	9
Fractional-Solution Apparatus	9
Materials and Supplies	9
LC Columns	9
Solvents	9
Polystyrene Standards	9
Polybutadiene Standards	10
Sample Lots of R-45M Prepolymer	10
Procedures	10
Clean-Up of Goodyear Polystyrenes Standards	10
Analytical-Scale Chromatography	14



		<input checked="" type="checkbox"/>		
		<input type="checkbox"/>		
		<input type="checkbox"/>		
Availability Codes				
Dist. Avail. for				
A-1				

Preparative-Scale Chromatography	14
Bulk-Scale Fractional Solution of HTPB	14
Single-Stage Fractionation	14
Analytical-Scale Multiple-Extraction	
Fractionation	14
Preparative-Scale Multiple-Extraction	
Fractionation	14
Bulk-Scale Silylation of R-45M	14
Vapor-Phase Osmometry	15
Viscosity	15
Infrared Spectroscopy	16
Derivatization with Formic Acid	16
Nuclear Magnetic Resonance Spectrometry	16
Differential Scanning Calorimetry	16
Inverse Gas Chromatography	16
RESULTS AND DISCUSSION	17
Phase I, Task 1. Fractionation of Polystyrenes	
and HTPB	17
GPC Fractionation of Polystyrenes with THF	
Solvent	17
GPC Fractionation of Polystyrenes with Chloroform	
Solvent	17
Limitations of GPC for Fractionation of	
Polystyrene Homologs	22
Analytical-Scale Reverse-Phase LC Fractionation of	
Polystyrene Homologs	22
Choice of "Good" and "Poor" Solvents	22
Choice of Analytical Column	22
Solvent Optimization for 680M Polystyrene	22
Solvent Optimization for 946M Polystyrene	28
Solvent Optimization for 1350M Polystyrene	28
Solvent Optimization for 1770M Polystyrene	31
Solvent Optimization for 2550M Polystyrene	31
Limitations of Reverse-Phase LC for Fractionation	
of Polystyrene Homologs	31
Semi-Preparative-Scale Reverse-Phase LC Fractionation	
of Polystyrene Homologs	32
Fractionation of 526M Polystyrene	32
Fractionation of 680M Polystyrene	32
Fractionation of 946M Polystyrene	32
Preparative-Scale Reverse-Phase LC Fractionation of	
Polystyrene Homologs	35
Work-Up of Preparative Fractions	35
Analytical-Scale Reverse-Phase LC Characterization	
of Preparative Fractions	38
Analytical-Scale Reverse-Phase LC Fractionation of	
Polybutadiene Homologs	38
Fractionation of 500M Polybutadiene	42
Fractionation of 1000M Polybutadiene	42
Analytical-Scale Reverse-Phase LC Fractionation of	
HTPB Homologs	42
Methanol/Tetrahydrofuran Mobile Phases (RI	
Detection)	42

Water/Tetrahydrofuran Mobile Phases (RI Detection)	45
UV Detection	45
Limitations of Reverse-Phase LC for Fractionation of HTPB Homologs	46
Preparative-Scale Bulk Fractional-Solution Fractionation of HTPB	47
GPC Characterization of Fractionated HTPB	47
Analytical-Scale Reverse-Phase LC Characterization of Fractionated HTPB	47
Characterization of the Polystyrene and HTPB Fractions	48
Analytical-Scale Reverse-Phase LC Characterization of GPC Fractions of Polystyrenes	48
GPC Characterization of Reverse-Phase LC Fractions of Polystyrenes	55
VPO Characterization of Reverse-Phase LC Fractions of Polystyrenes and HTPB	55
Zero Displacement	55
Calibration with Benzil	56
Number-Average Molecular Weights of Bulk Polystyrenes and HTPB	60
Number-Average Molecular Weights of Reverse-Phase LC Fractions of Polystyrenes	60
A Priori Calculation of Number-Average Molecular Weights of Bulk and Fractionated Polystyrenes	60
Systematic Error Inherent in VPO	60
Viscosity Characterization	67
Densities and Viscosities of Solvents	67
Characterization of Bulk and Fractionated HTPB	72
Phase I, Task 2. Mass Spectral Determination of Fraction Molecular Weights	72
Calibration to 2000 Da	72
Characterization of Reverse-Phase LC Fractions of Polystyrenes	72
Characterization of Reverse-Phase LC Fractions of Polybutadienes	76
Bulk PBD	77
Fractionated PBD	77
Characterization of HTPB	77
Liquid Chromatography/Mass Spectrometry	77
Phase II, Task 1. Ultra-High Resolution Reverse-Phase Microbore- Column Liquid Chromatography	77
Microbore-Column LC Fractionation of Poly- styrenes	78
Fractional-Solution Fractionation of Untreated R-45M	78
Analytical-Scale Fractionation	78
Preparative-Scale Fractionation	79
Fractional-Solution Fractionation of Silylated R-45M	79
Silylation of R-45M	79
Fractionation of Silylated R-45M	79

Gel-Permeation Chromatography of Fractionated R-45M	79
Vapor-Phase Osmometry	79
Densities of Standard Solutions of Benzil	82
Calibration Plots with Chloroform and THF Solvents	82
VPO of Polystyrenes Fractions	82
Viscosity	83
Independent Calibration of the Viscometer Tube	83
Importance of Viscometer Cleaning	84
Measurement of Viscosity of Bulk R-45M	84
Comparison of Results with Viscosity Data of Carver	85
Measurement of Viscosity of Fractionated R-45M	86
Measurement of Viscosity of Fractionated HMDS-Treated R-45M	86
Mark-Houwink Constants	86
Branching	86
Type and Extent of Unsaturation	86
Phase II, Task 2. Liquid Chromatography/Mass Spectrometry	90
Mass Spectrometry of R-45M Fractions	92
Inverse Gas Chromatography	92
Reproducibility of the GC Technique	93
Specific Retention Volumes of Probe-Solutes	93
Phase III, Task 1. Hydroxyl Content by FT-IR	103
Direct Measurement of Hydroxyl Content by FT-IR	103
FT-IR of Derivatized R-45M	103
NMR of R-45M Derivatized with Trichloroacetyl Isocyanate	109
6-Undecanol Standard	109
R-45M Fraction 2A	109
NMR of R-45M Derivatized with Formic Acid	109
¹³ C FT-NMR	109
¹ H FT-NMR	112
¹ H CW-NMR	112
Other Derivatizing Agents	112
Other Alcohols	112
DSC of R-45M	112
Phase III, Task 2. Analysis of Lots of R-45M	114
Density Analysis	114
Experimental Sources of Error	116
Reproducibility	116
Linearity of Density with Temperature	117
Regression of the Density Data with Temperature	117
Regression of the Density Data with Prepolymer Molecular Weight	117
Application to Other Lots of R-45M	117
Viscosity Analysis	117
SUMMARY AND CONCLUSIONS	123
REFERENCES	126

LIST OF TABLES

<u>TABLE</u>	<u>CAPTION</u>	<u>PAGE</u>
1	Solvent Compositions Used for Fractional Extraction of HTPB (1)	3
2	Values of M_n for Fractions of R-45M Determined by Vapor-Phase Osmometry and by Gel Permeation Chromatography (10)	4
3	Minimal and Maximal Values of M_n and M_w for Bulk R-45M Determined by Solvent Precipitation and by Gel Permeation Chromatography (11)	4
4	VPO Zero Displacement Measurements Obtained by Two Operators for Identical Drop Sizes of Pure Chloroform Solvent on Each Thermocouple; Drops Changed on Both Sample and Reference Sides for Each Set of Four Measurements; Instrument Zero Not Changed Until Completion of All Measurements. Attenuation of 8 Throughout	56
5	VPO Zero Displacement Measurements Obtained by Two Operators for Identical Drop Sizes of Pure Chloroform Solvent on Each Thermocouple; Drops Changed Only on Sample Side for Each Set of Measurements; Instrument Zero Not Changed Until Completion of All Measurements. Attenuation of 8 Throughout	56
6	VPO Zero Displacement Measurements Obtained by Two Operators for Identical Drop Sizes of Pure Chloroform Solvent on Each Thermocouple; Drops Changed Only on Reference Side for Each Set of Measurements; Instrument Zero Not Changed Until Completion of All Measurements. Attenuation of 8 Throughout	57
7	VPO Zero Displacement Measurements Obtained by Single Operator for Identical Drop Sizes of Pure Chloroform Solvent on Each Thermocouple; Drops Changed on Both Sample and Reference Sides for Each Set of Measurements; Instrument Rezeroed After Completion of Each Measurement. Attenuation of 8 Throughout	57
8	VPO Zero Displacement Measurements Obtained by Single Operator for Identical Drop Sizes of Pure Chloroform Solvent on Each Thermocouple; Drops Changed Only on Sample Side for Each Set of Measurements; Instrument Rezeroed After Completion of Each Measurement. Attenuation of 8 Throughout	57
9	VPO Zero Displacement Measurements Obtained by Single Operator for Identical Drop Sizes of Pure Chloroform Solvent on Each Thermocouple; Drops Changed Only on Reference Side for Each Set of Measurements; Instrument Rezeroed After Completion of Each Measurement. Attenuation of 8 Throughout	58

10.i	Raw VPO Measurements Obtained for Indicated Concentrations (g kg^{-1}) of Benzil by Single Operator. Identical Drop Sizes; Pure Chloroform Reference Solvent Changed after Each Set of Measurements; Instrument Rezeroed After Completion of Each Set of Measurements; Attenuation Settings of 8 Through 64 Used as Required	58
10.ii	Repeat of Measurements Described in Table 10(i)	58
11	Zero-Corrected VPO Measurements Obtained for Indicated Concentrations (g kg^{-1}) of Benzil by Single Operator. Drop Sizes as Indicated; Pure Chloroform Reference Solvent; Instrument Rezeroed After Completion of Each Set of Measurements; Attenuation Settings of 8 Through 64 Used as Required	59
12	Raw and Corrected Areas and Area Percentages for Indicated Polystyrene Blends	64
13	Densities and Viscosities of Chloroform at Indicated Temperatures	69
14	Densities of Chloroform Solutions of Bulk HTPB at Indicated Temperatures	69
15	Densities of Chloroform, Bulk HTPB, and 10% Fraction HTPB at Indicated Temperatures	69
16	Molecular Formulas and Weights of Polystyrene Homologs	75
17	Summary of Preparative-Scale Amounts/% (wt/wt) and GPC Peak-Maximum Molecular Weights/ Da for Indicated HMDS-Treated and Untreated Fractions of R-45M	81
18	Densities of Listed Chloroform Solutions of Benzil at Indicated Temperatures	82
19	Successive Raw Fall Times and Resultant Calculated Viscosities n/cS of 27.3054 m Solution of 580M Polystyrene in Chloroform at 15°C (Tube Not Cleaned Between Runs; B constant of $0.002842 \text{ cS sec}^{-1}$)	84
20	Comparison of Intrinsic Viscosity Data $[\eta]/\text{cm}^3 \text{ g}^{-1}$ at 30°C for Indicated HMDS-Treated and Untreated Fractions of R-45M Obtained at 35°C with Mixtures of IPA + Benzene	88
21	Comparison of GPC Molecular Weights (M/Da) with Those Calculated from Best-Fit Mark-Houwink Constants ($\text{M}-\text{H}$) for Indicated R-45M Fractions	89
22	Cis-, Trans-, and Vinyl-Contents of Silylated R-45M Fractions Obtained by ATR FT-IR	92
23	Smoothed (van't Hoff) Specific Retention Volumes $V_0^0/\text{cm}^3 \text{ g}^{-1}$ for Listed Probe Solutes at Indicated Temperatures with Lot AFAL of R-45M	94
24	Slopes m , Intercepts b , and Correlation Coefficients r for van't Hoff Plots of $\text{Ln } V_0^0$ of Listed Probe-Solutes Against 10^3 T^{-1} with Lot AFAL of R-45M	95

25	Smoothed (van't Hoff) Specific Retention Volumes $V_g^0/cm^3 g^{-1}$ for Listed Probe Solutes at Indicated Temperatures with Lot 1A-200 of R-45M	96
26	Slopes m , Intercepts b , and Linear Regression Correlation Coefficients r for van't Hoff Plots of $\ln V_g^0$ of Listed Probe-Solutes Against $10^3 T^{-1}$ with Lot 1A-200 of R-45M	97
27	Smoothed (van't Hoff) Specific Retention Volumes $V_g^0/cm^3 g^{-1}$ for Listed Probe Solutes at Indicated Temperatures with Lot 1B-108 of R-45M	98
28	Slopes m , Intercepts b , and Linear Regression Correlation Coefficients r for van't Hoff Plots of $\ln V_g^0$ of Listed Probe-Solutes Against $10^3 T^{-1}$ with Lot 1B-108 of R-45M	99
29	Smoothed (van't Hoff) Specific Retention Volumes $V_g^0/cm^3 g^{-1}$ for Listed Probe Solutes at Indicated Temperatures with Lot 2A-404 of R-45M	100
30	Slopes m , Intercepts b , and Linear Regression Correlation Coefficients r for van't Hoff Plots of $\ln V_g^0$ of Listed Probe-Solutes Against $10^3 T^{-1}$ with Lot 2A-404 of R-45M	101
31	Experimental and Calculated Hydroxyl Contents of Indicated Fractions of R-45M and ARCO Hydroxy-Terminated Polybutadiene Resins	105
32	Experimentally-Observed Densities for Indicated Lots of R-45M at 30-65°C	114
33	Experimentally-Observed Densities and Linear Least-Squares Fitting Parameters for Indicated Lots of R-45M at 20-65°C	115
34	Comparison of Densities Observed Experimentally for R-45M Lot 14LM at Increasing and Decreasing Temperatures over the Range: 20-65°C	116
35	Best-Fit Linear Regression Parameters for Density Data of Table 32	118
36	Best-Fit Quadratic Regression Parameters for Density Data of Table 32	118
37	Comparison of Experimentally-Observed Densities with Values Calculated from Best-Fit Linear and Quadratic Relations (Cf. Text) for Indicated Lots of R-45M at 30-65°C	119
38	Apparent Number-Average Molecular Weights M_n/Da of Indicated Lots of R-45M Calculated from Data of Table 33	122
39	Raw Viscosity Data for Indicated Lots of R-45M at 30°C Except as Noted	122

LIST OF FIGURES

<u>FIGURE</u>	<u>CAPTION</u>	<u>PAGE</u>
1	Proton NMR spectrum of 580M PL polystyrene as received. Instrument: Varian HA-100 NMR; amplitude: 600; sweep time: 5 min; filter: 0.5 sec; RF power: 0.1 mG; solvent: deuterated chloroform. Spectrum taken at room temperature	11
2	Proton NMR spectrum of 500M polystyrene as received from Goodyear Chemical. Remaining conditions as in Figure 1	12
3	Proton NMR spectrum of Goodyear 500M polystyrene after clean-up; arrow indicates trace amount left of unknown peak at ca. 1.3 ppm. Remaining conditions as in Figure 1	13
4	Gel-permeation chromatogram of concentrated polystyrene (680 Da) solution in THF with the PL column of 7.5 mm i.d. by 60 cm in length (Polymer Laboratories). THF solvent at 0.5 cm ³ min ⁻¹ ; 25°C temperature; UV detection at 254 nm; chart speed (CS) as noted. Fraction-collection region spans fractions B ₁ through G ₁	18
5	As in Figure 4; more concentrated solute solution	19
6	Summary illustration of the gel-permeation chromatogram of unfractionated polystyrene of nominal molecular weight 680 Da, and the positions of the peak maxima B through F collected as described in Figures 4 and 5	20
7	Summary illustration of the gel-permeation chromatogram of unfractionated polystyrene of nominal molecular weight 680 Da, and the positions of the peak maxima B through F collected as described above	21
8	Isochratic reverse-phase LC separation of 680M polystyrene. Column and conditions: 80% v/v THF/H ₂ O mobile phase; column: 25-cm Spherisorb C ₁₈ 5-um; flow rate: 1 cm ³ min ⁻¹ ; chart speed: 1 min cm ⁻¹ ; room temperature; 10-mm ³ injection-loop volume	24
9	As in Figure 8; 60% THF/H ₂ O mobile phase	25
10	As in Figure 8; 70% THF/H ₂ O mobile phase	26
11	Gradient reverse-phase LC separation of 680M polystyrene. Column: 25-cm Spherisorb C ₁₈ 5-um; flow rate: 1 cm ³ min ⁻¹ ; chart speed: 2 min cm ⁻¹ ; room temperature; 10-mm ³ injection-loop volume. Mobile-phase gradient: 5 min at 5% H ₂ O/95% MeOH isochratic, then to 10% THF/90% MeOH (contained in a separate reservoir) at 2% v/v reservoir change per min	27

12	Step-change gradient reverse-phase LC separation of 680M polystyrene. Column: 25-cm Spherisorb C ₁₈ 5-um; flow rate: 2 cm ³ min ⁻¹ ; chart speed: 4 min cm ⁻¹ ; 25°C column temperature; 10-mm ³ injection-loop volume. Mobile-phase program: (a) 10% H ₂ O/90% MeOH, then to (b) 5% H ₂ O/95% MeOH, then to (c) pure MeOH	29
13	Step-gradient reverse-phase LC separation of 680M polystyrene. Column and conditions as in Figure 12. Mobile-phase program: (a) 7.5% H ₂ O/92.5% MeOH, then to (b) 2.5% H ₂ O/97.5% MeOH, then to (c) pure MeOH	30
14	Reverse-phase LC separation of 526M polystyrene. Column: 50-cm Partisil C ₁₈ 10-um; flow rate: 10 cm ³ min ⁻¹ ; chart speed: 2 min cm ⁻¹ ; room temperature; 150-mm ³ injection-loop volume. Mobile phase: 60% v/v THF/H ₂ O isocratic	33
15	As in Figure 14; reinjection of fractions 5-7. Chart speed: 1 min cm ⁻¹	34
16	Reverse-phase LC separation of 526M polystyrene. Column: 30-cm Partisil C ₁₈ 10-um; flow rate: 27.7 cm ³ min ⁻¹ ; chart speed: 4 min cm ⁻¹ ; 0.5-cm ³ injection-loop volume. Mobile phase: 55% v/v THF/H ₂ O isocratic	36
17	Isochratic reverse-phase preparative LC separation of 580M polystyrene. Column: 2.54 by 30-cm Partisil C ₁₈ 10-um; flow rate: 27.7 cm ³ min ⁻¹ ; chart speed: 4 min cm ⁻¹ ; room temperature; 2.5-cm ³ injection-loop volume. Mobile phase: pure MeOH. Detector: UV at 222 nm (a) at 2.0 AUFS and (b) at 0.5 AUFS	37
18	Isochratic reverse-phase LC of 580M polystyrene. Column: 25 cm by 4.6-mm i.d. 5-um Spherisorb ODS. UV detection at 222 nm; (a) 2.0 AUFS and (b) 1.0 AUFS; 10-mm ³ sample loop; flow rate of 1 cm ³ min ⁻¹ ; room temperature; chart speed of 2 min cm ⁻¹ . Mobile phase: 100% methanol	39
19	Isochratic reverse-phase analytical chromatograms of 580M polystyrene fractions 1-4. Column and conditions as in Figure 18	40
20	Isochratic reverse-phase analytical chromatograms of 580M polystyrene fractions 5-7. Column and conditions as in Figure 18	41
21	Isochratic reverse-phase analytical LC of Goodyear PBD, 500 Da. Column: 25 cm by 4.6-mm i.d. 5-um Spherisorb ODS; room temperature; 10-mm ³ injection loop; UV detection at 240 nm; chart speed: 2 min cm ⁻¹ . Mobile phase: 20% H ₂ O/80% MeOH at 4 cm ³ min ⁻¹	43
22	Repeat runs of analytical-scale reverse-phase LC fractionation of 1000M PBD. Column: 25-cm Spherisorb ODS 5-um; injector: Rheodyne valve with 10-mm ³ loop; detector: UV at 240 nm (0.5 AUFS); chart speed: 2 min cm ⁻¹ . Mobile phase: 80% MeOH/25% H ₂ O at 4 cm ³ min ⁻¹ flow rate. Dots indicate fractions collected	44

23	Isochratic reverse-phase LC separation of 680M polystyrene. Column: 25-cm Spherisorb C ₁₈ , 5- μ m; flow rate: 1 cm ³ min ⁻¹ ; chart speed: 2 min cm ⁻¹ ; 25°C column temperature; 10-mm ³ injection-loop volume. Mobile phase: 65% v/v THF/H ₂ O	49
24	As in Figure 23; GPC fraction C ₁	50
25	As in Figure 23; GPC fraction D ₁	51
26	As in Figure 23; GPC fraction E ₁	52
27	As in Figure 23; GPC fraction F ₁	53
28	As in Figure 23; GPC fraction G ₁	54
29	Plots of VPO data for benzil and indicated polystyrenes	61
30	Plots of VPO data for benzil and HTPB	62
31	VPO data plots for benzil (standard; chloroform solvent); polystyrene 580M fractions 2, 4, and 6; and bulk 580M polystyrene	63
32	Plot of relative error, 10 ² (VPO - true)/true, against true molecular weight for indicated polystyrene blends. Error bars represent $\pm 3\%$ on molecular weight, $\pm 10\%$ on VPO data. Solid curve: three datum points; dashed line: four datum points	66
33	Plots of density against weight percent of solutions of Table 14	70
34	Plots of density against temperature t/°C for Bulk and Fractionated HTPB	71
35	Plots of density against temperature for indicated concentrations of HTPB in chloroform	73
36	Mass spectrum of polystyrene fractions 3+4. AEI MS-902 double-focussing mass spectrometer; 70 eV electron impact ionization; 8kV accelerating potential	74
37	Summary bar-graph of the preparative-scale amounts (% w/w) obtained for each extraction of R-45M. Solvents: IPA, fraction 1, + 5% (v/v) increments of benzene (subsequent fractions). Intrinsic viscosities (right-hand ordinate: THF, 30°C) superposed as connected dots (see later)	80
38	Intrinsic viscosities of fraction 10A of R-45M at indicated temperatures	87
39	ATR FT-IR spectrum of fraction 1A	91
40	Plots of the specific retention volumes $V_g^0/cm^3 g^{-1}$ obtained for the indicated probe-solutes n-pentane (n-C ₅), acetone (MMK), dichloromethane (DCM), 3-methylpentane (3MC ₅), 1-hexene(1-C ₆), and n-hexane (n-C ₆) with fractions 1A and 10A and bulk R-45M	102
41	FT-IR Beer's-law plot for 6-undecanol in CCl ₄	104

42	Plot of hydroxyl content $C_{OH}/\text{meq g}^{-1}$ of R-45M fractions against GPC molecular weight M/Da	106
43	Thin-film FT-IR spectrum of neat underivatized R-45M	107
44	Thin-film FT-IR spectrum of R-45M derivatized with formic acid	108
45	NMR spectrum of 6-undecanol in CCl_4 showing peak integrations	110
46	NMR spectrum of TCI-derivatized 6-undecanol	111
47	^1H FT-NMR spectrum of derivatized R-45M. The formate band occurs at ca. 8 ppm	113
48	Isochratic reverse-phase analytical LC of Goodyear PBD, 500 Da. Column: 25 cm by 4.6-mm i.d. 5- μm Spherisorb ODS; room temperature; 10- mm^3 injection loop; UV detection at 240 nm; chart speed: 2 mjn cm^{-1} . Mobile phase: 20% $\text{H}_2\text{O}/80\%$ MeOH at 4 $\text{cm}^3 \text{min}^{-1}$	120
49	Plot of density against temperature for R-45M Lot 10LM	121

INTRODUCTION

Polymeric binder materials are used at the present time as composite propellants in a number of Defense systems. These include: polyneopentyl glycol azelate (NPGA) in HAWK; hydroxy-terminated polybutadiene (HTPB) in VIPER, PATRIOT, MET ROCKET, GSRs, PERSHING, and HELLFIRE; polybutadiene acrylic acid (PBAA) in PERSHING and SPARTAN; and polyethylene glycol (PEG), polyethylene glycol adipate (PEGA), and polycaprolactone (PCL) in composite smokeless propellants currently under development (1,2). However, the polydisperse nature of these binders results in significant changes in the various combustion properties of the respective propellant, hence the engine itself. For example, Carver (1) has recounted the multimillion-dollar costs associated with reevaluation of several thousand HAWK motors that was necessitated by variations encountered in amounts of insoluble matter in the propellant binder.

Further compounding the problem is that, since the analytical procedures currently employed for characterization of the respective prepolymers are difficult and time-consuming, they are frequently neglected by propellant vendors (2). It was also concluded in one instance that operator variations were greater than raw-material variations (3). Moreover, there is considerable disagreement at the present time regarding interpretation of the results of such analyses even when performed in good faith, and correlation of these with properties (e.g., curing and aging) of the resultant polymer (4-8).

This Contract was therefore initiated to explore and to clarify the situation regarding the analysis of propellant prepolymers and, in particular, to develop and optimize strategies pertaining to speciation according to molecular weight (Phase I); to degree of branching (Phase II); and to functionality distribution (Phase III). The methods employed centered largely upon fractional solution/dissolution of bulk materials; colligative properties; column-liquid, gel, and gas chromatography; and mass spectrometry. Other instruments, such as DSC and NMR were also employed. In addition, much of the work was based upon R-45M. However, the fundamental analytical developments and resultant practical methodologies and techniques developed in the Contract are applicable to analysis and routine quality control of virtually any prepolymer system.

CONTEMPORARY METHODS OF MOLECULAR-WEIGHT DETERMINATION

Much of the unclassified (U) literature from 1965 through 1978 concerning assay and fractionation of prepolymers such as HTPB has been abstracted and assembled by the Chemical Propulsion Information Agency (5). A more detailed bibliography covering the period 1958 through 1973 (537 citations) has also been published (6). Methods of analysis used for the molecular-weight characterization of such species today include solvent/solvent partitioning, vapor-phase osmometry, viscosity, and gel-permeation chromatography.

Solvent Partitioning

Fractionation on the basis of solubility has been employed for many years for polymer analysis, and in fact was the method of choice prior to the advent of gel permeation chromatography. More recently, Myers (9), Ramey (10), and Blanks, Shephard, and Stephens (11) have used the technique for fractionation of HTPB.

Two variations of solvent fractionation are in principle possible: in the first, called fractional precipitation (or dissolution), the composition of a binary solvent is adjusted in a step-gradient manner so as to yield successively-insoluble fractions of prepolymer.

Since solubility is presumed to be a function of molecular weight, the precipitated fractions obtained are in order of decreasing M . An alternative and entirely equivalent method comprises fractional extraction (solution) wherein neat sample is extracted into solvent mixtures of increasing solubilization strength (decreasing "polarity", since lower molecular-weight homologs of species such as HTPB are less soluble in more "polar" solvents). As above, solubility of the prepolymer is said to be a function of M , hence the fractions thereby obtained are in order of decreasing molecular weight. The latter technique has proved over the years to be more convenient in the instance of crystalline polymers, since fractions are taken up in solution (thence removed) as opposed to requiring isolation by filtration. (The converse was found to be true in this work with liquid polymers.) Table 1 provides illustration of the conditions employed by Blanks, et al. for HTPB.

Colligative Properties

A number of techniques based upon colligative properties have been used for molecular-weight determination. These consist primarily of variants of vapor-phase osmometry, high-speed membrane osmometry, boiling-point elevation, and freezing-point depression. The result in each case is a distribution of absolute M_n , although the accuracy of such measurements is subject to some uncertainty (particularly at high M) (7). Vapor-phase osmometry has been applied to HTPB inter alia by Dilts and coworkers (12), by Muenker and Hudson (13), and by Johnson (14). Several workers have also compared the results obtained from VPO with those of GPC (see later).

Gel-Permeation Chromatography

GPC is today by far the most frequently-employed technique for the fractionation of prepolymers. The two most recent texts concerning the pertinent theory and instrumentation are those by Yau, Kirkland, and Bly (15) and Kremmer and Boross (16). In the particular instance of analysis of HTPB and similar materials, Styragel packings (polystyrene-divinylbenzene) seem at present to be preferred. Either chloroform or THF appear to be suitable solvents, although any solvent will do provided that it swells the gel and dissolves (but does not react with) the prepolymer. It is also commonplace to connect columns of gels of different pore size in tandem. For example, Carver (2) utilized as many as three or four columns of gels of 100 to 10^5 Angstroms. He has also described and discussed the importance of various system variables, such as sample size, injection volume, flow rate, temperature, and so forth.

Detection of prepolymers is commonly carried out by UV, refractive-index (RI), low-angle laser-light scattering (LALLS), or by some combination of these and/or with FT-IR or NMR. LALLS offers the advantage of direct determination of M_w , whereas UV and RI instruments provide near-universal detection. However, all suffer characteristically from poor response time and sensitivity. Nevertheless, split-stream (parallel) or series detection utilizing UV and RI has been reported to hold some advantage in terms of selectivity if the prepolymer hydroxyl groups are appropriately derivatized (10).

Calibration of GPC columns is of real and practical concern in the fractionation of materials such as HTPB since suitable standards for construction of elution volume/log molecular weight nomographs have yet to be defined for other than polystyrene. Accordingly, the "universal calibration" technique of Grubisic, Rempp, and Benoit (8) has been resorted to on occasion, where plots of adjusted elution volume $V_R' = V_R - V_M$ against $\log M_w [\eta]$ ($[\eta]$ being an intrinsic viscosity) seem to be independent of the prepolymer under consideration so long as each is linear. The technique has been described and discussed at length by Yau and coworkers (15), and utilized, for example for HTPB analysis, by Carver (2) and by Law (4). Fully-characterized polystyrene standards have been described by Cazes and Dobbins (17) for use in construction of "universal" plots.

TABLE 1. Solvent Compositions Used for Fractional Extraction of HTPB (11)

Fraction	Composition (% w/w)		% (w/w) Extracted	$\frac{\bar{M}_w}{\bar{M}_n}$	$\frac{\bar{M}_n}{\bar{M}_w}$	$\frac{\bar{M}_w}{\bar{M}_n}$
	Benzene	2-Propanol				
1	0	100	15.21	10,895	5,917	1.84
2	20	80	22.08	9,607	5,004	1.92
3	30	70	20.66	7,410	4,152	1.78
4	38	62	20.18	4,336	2,381	1.82
5	50	50	21.87	3,047	1,421	2.14

\bar{M}_n GPC

Comparison of Methods

Detailed comparisons of molecular weights obtained for identical samples of HTPB with different techniques have been made by Ramey (10) and by Blanks and his coworkers (11). Unfortunately, the results are not encouraging. Table 2 presents the values of VPO- and GPC-determined M_n found by Ramey for solvent-precipitated fractions of R-45M, while Table 3 contrasts minimal and maximal values of M_n and M_w as found by solvent precipitation and by GPC.

TABLE 2. Values of M_n for Fractions of R-45M Determined by Vapor-Phase Osmometry and by Gel Permeation Chromatography (10)

Fraction	M_n		$\Delta, \%$
	VPO	GPC	
A	1,340	1,650	18.8
B	2,130	2,260	5.7
C	2,700	2,900	6.9
D	4,020	3,900	-3.0
E	5,200	4,800	-7.7
F	9,900	7,000	-29.2

TABLE 3. Minimal and Maximal Values of M_n and M_w for Bulk R-45M Determined by Solvent Precipitation and by Gel Permeation Chromatography (11)

	Solvent Pre- cipitation	GPC	$\Delta, \%$
\bar{M}_n (min)	1,427	1,449	1.5
\bar{M}_n (max)	5,917	9,178	35.5
\bar{M}_w (min)	3,047	2,866	-6.3
\bar{M}_w (max)	10,895	23,817	54.3

CONTEMPORARY METHODS OF CHAIN-BRANCHING DETERMINATION

The type and extent of prepolymer chain-branching are important from a Defense standpoint, insofar as they affect the properties of the resultant polymer quite substantially. It is thought that there are at least four gradations of branching type, namely, random short- and long-chained, star, and comb-like. However, instrumental methods for quantitating the distribution (or for that matter the presence or absence) of each are virtually non-existent. (Somewhat related to the question of branching is chain-folding, about which nothing is known with regard to R-45M prepolymers.) Of the very few methods of characterizing chain-branching in such species today, one of the more

useful is the technique developed by Drott and coworkers (18) that involves deviations in the change of viscosity with prepolymer molecular weight (where the latter is determined by gel-permeation chromatography). ^{13}C -NMR has also been shown to provide at least some distinction between lots of R-45M on the basis of branching as well as functionality (19). In addition, Coleman and Fuller (20) were able to obtain an empirical reiterative fit of viscosity data which in turn gave a function with which various types and distributions of branches could at least be estimated.

CONTEMPORARY METHODS OF FUNCTIONALITY DETERMINATION

As with molecular weight and branching, the functionality distribution of prepolymers is an important factor in determining the properties of the resultant polymer. Silica-gel chromatography, gelation-point, and wet-chemical techniques are today the most commonly used methods for evaluation of this parameter, although are hardly the most optimal.

Silica-Gel Column Liquid Chromatography

Fractions said to correspond to this or that functionality have been obtained by silica-gel column chromatography for many years (e.g., refs. 12,13,21). The method commonly employed is that developed by Muenker (22) and DiMilo (23) wherein prepolymer is eluted from LC columns under linear- or step-gradient conditions (increasing solubilization strength; decreasing solvent polarity). Much of this work must be regarded with some skepticism, however, since it has been shown for example by Myers (7) that HTPB undergoes structural changes when contacted with silica for any length of time.

Gelation-Point

The onset of incipient gelation has been used to characterize prepolymer functionality e.g., by Ramey (10) and by Anderson and coworkers (19) following the studies of Consaga (24). However, Ramey (25) concluded in subsequent work that the method is insufficiently precise for the assessment of functionality, and it is not widely used at the present time.

Wet-Chemical Techniques

The most popular wet-chemical technique for determination of the absolute number of functional groups (hence M_{eq} and F_n) appears to be reaction of the prepolymer with a functional-group-specific reagent, followed by determination either of unreacted (excess) reagent or by spectroscopic quantitation of the derivatized groups. For example, HTPB has been acetylated with acetic anhydride in pyridine, and the excess reactant and resultant acetic acid product back-titrated with alcoholic potassium hydroxide (15,16). However, Dee, Biggers, and Fiske (26) have shown that this method provides overestimation of functionality, presumably due to the water content of the polymer and reactant and sample decomposition. As a consequence, other derivatizing agents have been employed over the years for hydroxyl groups, including trifluoroacetic anhydride (TFAA) (4), 3,5-dinitrobenzoyl chloride (DNBC) (1,4), and toluenesulfonyl isocyanate (TSNCO) (4,10). DNBC suffers from the drawback of incomplete reaction even in the presence of pyridine and toluene at 100°C for 24 hr (2), while IR and ^{19}F -NMR derived results for TSNCO, TFAA, and AA (the latter determined by back-titration) present serious disagreement (4,10).

There are nonetheless promising developments in this field. Of particular interest is the work of Law (4) wherein RI and UV LC detectors were placed in tandem such that a

prepolymer molecular weight distribution was said to be obtained from the first while the second was specific for the functional group. Thus, overlaying the two chromatograms provided simultaneously both the molecular-weight and the functional-group distributions. However, since no standards were available, it was not possible to construct calibrated response nomographs nor could the linearity of the detectors be assessed with any degree of certainty.

CONTRACT OVERVIEW. PHASE I: CHARACTERIZATION BY MOLECULAR WEIGHT

There have been very many advances over the years in the characterization of prepolymers of Defense-related interest, as described above. Further, since the most useful physical properties of such species for correlation with the chemical and rheological characteristics of the resultant polymers are the molecular-weight, chain-branching, and functionality distributions, most studies have been concentrated in these areas. However, Tables 1-3 amply illustrate that there remain very many uncertainties surrounding such data and, indeed, the methods themselves. Moreover, in seeking to assess the physicochemical properties of materials such as HTPB, it must be recognized that no suitable standards are available for comparative purposes. Thus, the primary objective of the initial Phase of this work was the fractionation and characterization according to molecular weight, by various means, of suitable standards of polystyrenes and HTPB. This was carried out by fractional solution/dissolution, vapor-phase osmometry, viscosity, LC, GPC, and MS techniques as described and discussed in what follows.

Task 1. Fractionation and Characterization of Polystyrenes and HTPB

It was readily apparent from preliminary work that what are commonly supposed to be "pure" polystyrene standards in fact represent blends of polydisperse molecular weight. The first goal of this work was therefore the isolation of gram-quantities of narrow molecular-weight distribution of each "pure" polystyrene standard. This task was accomplished by cutting narrow fractions of commercially-obtained materials with conventional- and preparative-bore reverse-phase LC columns. Fractional solution was also employed for HTPB. Gram-amounts of fractions were isolated. Gel-permeation chromatography, viscosity, and vapor-phase osmometry were then used to characterize bulk as well as fractionated polystyrene and HTPB in order to gauge batch-to-batch differences in the nominal M_n of each.

Task 2. Mass Spectral Determination of Fraction Molecular Weights

Unambiguous determination of lower molecular-weight homologs of the polystyrene standards and HTPB fractions, collected as described above, was carried out by mass spectrometry. In addition, the double-focussing capabilities of the MS902 instrument provided resolution of oligomers such that mapping of overlapping series of molecular-ion fragments was possible up to 2000 Da. Also carried out at this point was off-line LC/MS. Sufficient expertise was gained with the elution patterns at least of polystyrenes so as to obviate MS detection, that is, such that molecular-weight distributions could be determined solely from chromatographic spectra.

CONTRACT OVERVIEW. PHASE II: CHARACTERIZATION BY CHAIN BRANCHING

The primary objective of the second Phase of the Contract was further fractionation according to branching, and then the characterization, of prepolymers fractionated earlier in Phase I by molecular weight. This was carried out by fractional solution/dissolution, viscosity, and GPC.

Task 1. Ultra-High Resolution Reverse-Phase Microbore-Column Liquid Chromatography

Each of the (narrow-cut) GPC fractions of polystyrene was used to develop gradient-elution LC with high-resolution fractional-dissolution columns. Suitable "poor" and "good" solvents were water/THF and methanol/THF. The systems were then used for further analysis of narrow-cut fractions of HTPB. The number and kinds of peaks subsequently obtained were thought initially to be a function mainly of branching (recall that each GPC fraction should be of apparent identical molecular weight), since reverse-phase LC packings are not adsorbent, and only secondarily of hydroxyl content.

Task 2. Liquid Chromatography/Mass Spectrometry

The lower molecular-weight (400-2000 Da) fractions of the polystyrene standards and HTPB were used next in conjunction with fractional-dissolution (reverse-phase) microbore-column systems to initiate high-resolution LC/high-resolution (50,000) MS. Since the flow rate from microbore columns is routinely only $5 \text{ mm}^3 \text{ min}^{-1}$, it was thought that microbore-LC column effluents could be fed without sample splitting directly into the ion source of instruments such as double-focussing mass spectrometers.

CONTRACT OVERVIEW. PHASE III: CHARACTERIZATION BY FUNCTIONALITY

The primary objective of the third Phase of the Contract (as amended) was to characterize prepolymers fractionated in Phase II according to hydroxyl content; and, subsequent to this, to establish the most accurate technique for the determination of functionality. The task was carried out by Fourier-transform infrared spectroscopy (FT-IR), nuclear magnetic resonance spectrometry (NMR) (including FT-NMR), differential scanning calorimetry (DSC), and inverse gas chromatography (GC).

Task 1 - Hydroxyl Group Content and Distribution

As indicated in the amended Statement of Work for the Contract, Fourier-transform IR with fractionated HMDS-treated as well as untreated HTPB was used to determine the prepolymer hydroxyl group distribution. Other derivatizing agents and methods of detection, such as inverse GLC, NMR, and DSC were also investigated. The most accurate technique for determination of the functionality distribution was then established.

Task 2 - Analysis of Lots of R-45M

Application of most of the characterization techniques evaluated as described above was carried out as the last part of the Contract on a number of lots of R-45M provided by AFAL.

EXPERIMENTAL SECTION

Apparatus and Equipment

Liquid Chromatographs. The analytical liquid chromatographs utilized throughout the work for LC as well as GPC were Varian Models 5000 and 8500. The preparative LC pump was from Altex, which was fitted with a solvent-delivery head that was capable of $27.7 \text{ cm}^3 \text{ min}^{-1}$ flow rate. The detectors were a Varian Vari-Chrom variable-wavelength UV-Vis, an LDC Model 1205 UV of 254 nm fixed wavelength, or a Knauer Model 98 differential refractometer as specified. The injectors were from Valco and Rheodyne; and comprised 10-mm³ (or larger) external sample loops fabricated from stainless-steel tubing. The recorders were from Linear and Houston Instruments. The column thermostat was a Neslabs Model RTE-8 water-bath, water (or water + methanol for low temperature studies) from which was pumped through a column water-jacket fabricated from a length of glass pipe to which had been attached inlet- and outlet ports. Seals were made at the column ends with rubber stoppers, into one end of which was also bored a no. 00 hole for a thermometer probe. In the case of the Knauer RI detector, water was passed from the column through the detector and then returned to the bath.

Gas Chromatograph. The high-precision gas chromatograph has been described and evaluated elsewhere (27).

Mass Spectrometer. The mass spectrometer was an MS-902, updated with solid-state electronics controls, computer system, and turbomolecular pumping from Mass Spectrometry Services, Ltd., Manchester, U.K. The instrument was modified for fast-atom bombardment (FAB) ionization with a Frazer Scientific (Vacuumetrics, Los Angeles, CA) FAB gun equipped with a self-contained sample probe. The FAB gas was argon.

Infrared Spectrophotometer. The IR was a Mattson Cygnus Series FT-IR. Thin-film liquid cells were employed with conventional NaCl windows. The instrument was also equipped with a Mattson Model "Universal Optics" package of optics and cells; an attenuated total reflectance (ATR) unit comprised of a KRS-5 crystal (thallium bromide-iodide); and a cylindrical internal-reflectance (CIRCLE) cell (Spectra-Tech, Inc.), the rod being zinc selenide.

Density Apparatus. Density measurements were carried out to 2 parts in 10^4 with a Mettler-Paar Model DMA-45 density meter.

Vapor-Phase Osmometer. The vapor-phase osmometer was a Knauer Model VPO supplied by AFAL. The device was equipped with a timer and a temperature read-out, the latter being accurate to $\pm 0.1^\circ\text{C}$. The temperature was also checked occasionally with a Hewlett-Packard platinum-resistance thermometer ($\pm 0.02^\circ\text{C}$).

Viscometry Apparatus. The viscometer tube was a certified (i.e., calibrated) Ubbelohde No. 0C (Cannon Instruments Co., State College, Pa.). The water-bath used for the viscometer was a 5-dm³ tall-form beaker which was insulated with molded asbestos tape, and to which was also fitted a clamp such that the viscometer tube was true-vertical when put in place. Temperature control was achieved by passing thermostated water through approximately 10 ft of coiled quarter-inch copper tubing that was rested roughly 1 in from the bottom of the container. The entire apparatus was mounted on top of a stirring motor, where a large stirring bar was placed directly on the bottom of the beaker. Stirring was carried out at a speed just below vortex formation.

Water-Bath Thermostat. The thermostat was a Neslabs Model RTE-8 Endocal water-bath capable of $\pm 0.05^\circ\text{C}$ precision. Water (or water + methanol for low temperature studies) from the bath was controlled at 35°C for the fractional-solutions work, or at $15^\circ\text{--}40^\circ\text{C}$ for the viscosity measurements. Temperature measurements were made to $\pm 0.02^\circ\text{C}$ with the Hewlett-Packard Model 2802A platinum-resistance system mentioned above, or to $\pm 0.1^\circ\text{C}$ with a Neslabs DB-2 thermocouple system.

Differential Scanning Calorimeter. The DSC was a Perkin-Elmer Model DSC-7, equipped with liquid-nitrogen cooling facilities, a "Delta" computer data acquisition/reduction system, and a Hewlett-Packard Model 7470A plotter.

Nuclear Magnetic Resonance Spectrometer. The NMR instruments were a Chemagnetics 220-MHz superconducting FT-NMR, and a conventional Varian EM-390 90-MHz continuous-wave (CW) NMR.

Fractional-Solution Apparatus. The analytical-scale fractional-solution vessel was a water-jacketed 250-cm³ separatory funnel; while semi-preparative-scale fractionation was carried out with a 2-dm³ water-jacketed round-bottom flask.

Materials and Supplies

LC Columns. The initial GPC column was a TSK Gel Type G3000H8, obtained from Varian, and was 7.5 mm i.d. by 50 cm in length. The manufacturer's stated exclusion limit of this column was 60,000 Da. The column packing material was claimed to be spherical cross-linked polystyrene/divinylbenzene of 8 to 10 μ m particle size. The second GPC column was a Polymer Laboratories Type PL-GEL, and was 7.5 mm i.d. by 60 cm in length. The manufacturer's stated exclusion limit was 20,000 Da. The column packing material was claimed to be spherical cross-linked polystyrene/divinylbenzene of 5 μ m particle size. The analytical microbore LC columns were 50 cm in length by 1 mm i.d. and contained 10- μ m Micro-sphere C₈ or C₁₈ silica, two of the former of which were connected in series with three of the latter for an overall length of 2.5 m. The columns were obtained from Jones Chromatography (Columbus, Ohio). The conventional analytical LC columns were also from Jones Chromatography and were 4.6-mm i.d. by 25-30 cm in length. The packings were in each case 5- μ m Spherisorb ODS or as noted. The semi-preparative column was from Whatman, and was 9.4-mm (0.5-in.) i.d. by 50 cm in length. The packing was 10- μ m Partisil ODS-2, and was claimed by the manufacturer to be a much higher degree of derivatization than conventional reverse-phase packings. The preparative column was from HP Chemical Co. (St. Louis, Missouri), and was 25.4 mm (1-in.) i.d. by 30 cm in length. The column packing material was claimed to be 10- μ m particulate ODS silica. The glass-bead column, 4.6-mm i.d. by 25 cm, was fabricated with 8- μ m glass beads (22% claimed standard deviation) from Duke Scientific (Palo Alto, California). Packing was carried out by the tap-and-fill method, further compaction then being obtained by pressurizing the column to 350 atm with the Varian 5000 LC.

Solvents. The solvents, acetone, carbon disulfide, toluene, tetrahydrofuran (THF), chloroform, methanol (MeOH), iso-propyl alcohol (IPA), and benzene were "HPLC" grade from Fisher Scientific or were ACS reagent-grade. Water was deionized and doubly-distilled. Hexamethyldisilazane (HMDS) was purchased from Aldrich.

Polystyrene Standards. Two sets of polystyrene prepolymer standards (1-g amounts) were used initially. The first, obtained from Varian, was a Standard Polystyrene Kit from Toyo Soda Manufacturing Co., Ltd., Tokyo; while the second was a Polystyrene Calibration Kit obtained from Polymer Laboratories, Inc. Polystyrene standards from the former of these were designated by the manufacturer as A-500 (500 Da), A-1000 (1000 Da), A-2500 (2800 Da), A-5000 (6200 Da), F-1 (10,300 Da), F-2 (16,300 Da), F-4 (43,000 Da), and F-10 (98,900 Da). Standards from the latter kit were designated as I, II, III, ..., X and were of claimed molecular weight, respectively, of 680, 1050, 1350, 1770, 2550, 3550, 5100, 7800, 12,500, and 17,000 Da. Extensive characterization bulletins were provided with the Toyo standards, including batch numbers. In contrast, no information (other than GPC peak-maximum molecular weight data) was sent with the Polymer Laboratories standards. Subsequently, new 10-g amounts of members of the PL kit were received for preparative-scale fractionation. Repeated requests for the data sheets for all of the polymers finally yielded documentation that included GPC, light-scattering, viscosity, and NMR tracings and graphical data reduction sheets.

Also received later in the work were 10-g amounts of polystyrenes from Goodyear Chemicals, Inc., purchased as recommended by AFAL. The chemical purity of these materials was found to be particularly bad, especially in view of the fact that they are represented by Goodyear as "standards". The data sheets indicated that each batch was in fact contaminated with insoluble catalyst residues as well as volatile solvent(s).

Polybutadiene Standards. Polybutadiene (PBD) prepolymers were obtained from AFAL. All were from Goodyear; the lowest molecular-weight material was labeled as No. CDS-B-1, 500 Da. It was a clear liquid of viscosity on the order of water, and was brown in color. The remaining PBD were of nominal molecular weight 1000 (CDS-B-2), 2500 (CDS-B-3), and 22,000 (CDS-B-4) Da. The molecular-weight data comprised the only documentation available for the materials.

Sample Lots of R-45M Prepolymer. Also received from AFAL was ca. 4 dm³ of R-45M of nominal molecular weight 6800 Da (GPC peak maximum). Additional HTPB prepolymers were obtained from Morton Thiokol via AFAL, and were labeled as Nos. 1A-200, 1B-108, and 2A-404. There was virtually no documentation provided for any of these materials. Additional lots of R-45M received from AFAL at the end of the Contract were labeled nos. 403225, 602185, 810255, 810265, and 905175. Additional materials were also obtained from United Technologies, and were labeled Lots 33 and 38.

Procedures

Clean-Up of Goodyear Polystyrenes Standards. Clean-up of several of the polystyrene "standards" obtained from Goodyear was attempted as follows (the results were independent of the nominal molecular weight). First, because the polymers were white opaque solids (whereas the TSK and PL polymers were clear viscous liquids), 5 g of Goodyear material was taken up in benzene. This resulted in a dispersion of white insoluble solid in the solution, which was removed by filtration. Approximately 1 g of solid was thereby obtained (i.e., 20% of the total weight of the polymer). The solid was also found to be somewhat soluble in water. Next, most of the benzene comprising the polymer-benzene filtrate was driven off with a heat gun, following which the remainder was removed at room temperature on a vacuum manifold (Edwards high-vacuum pump; 10⁻³ torr). The resultant polymer was a viscous liquid which, however, still contained noticeable amounts of white solid dispersed in it.

Figure 1 illustrates the ¹H-NMR spectrum of PL 580M polystyrene whereas, for comparison, Figure 2 provides the spectrum of Goodyear 500M as received. The only noticeable impurity in the former is a peak corresponding to a trace amount of acetone which was used to rinse the NMR tube; the spectrum is otherwise as expected. In contrast, the latter figure shows a large peak at ca. 1.3 ppm, the identity of which is not known. In any event, solution in benzene (followed by filtration) appeared to be an effective method of removing it, as demonstrated by the NMR spectrum of the polymer provided in Figure 3, after it was subjected to the clean-up procedure described above.

In an effort to cause coagulation of the colloidal suspension of particulate matter, a hot saline wash (with vigorous stirring) of Goodyear polymers dissolved in benzene was next carried out. The benzene layer was then drawn off, washed with distilled water, dried over magnesium sulfate, and then filtered. Since the solution was still somewhat cloudy, it was passed through a glass buret containing column LC silica, where the eluent was 90:10 hexane:THF. The eluate was less cloudy than before and also, was water-white in color. (In addition, there were several yellow-to-brown bands left on the column.) Thus, there was what appeared to be a second kind of impurity present in the Goodyear material that was benzene-soluble, and that coeluted from silica with the polystyrene. This might well have been either a second group of impurities, or simply a finer suspension of the first kind. In any event, microfiltration was then attempted since, unless the solid matter were removed, it would plug the inlet frits of the HPLC systems.

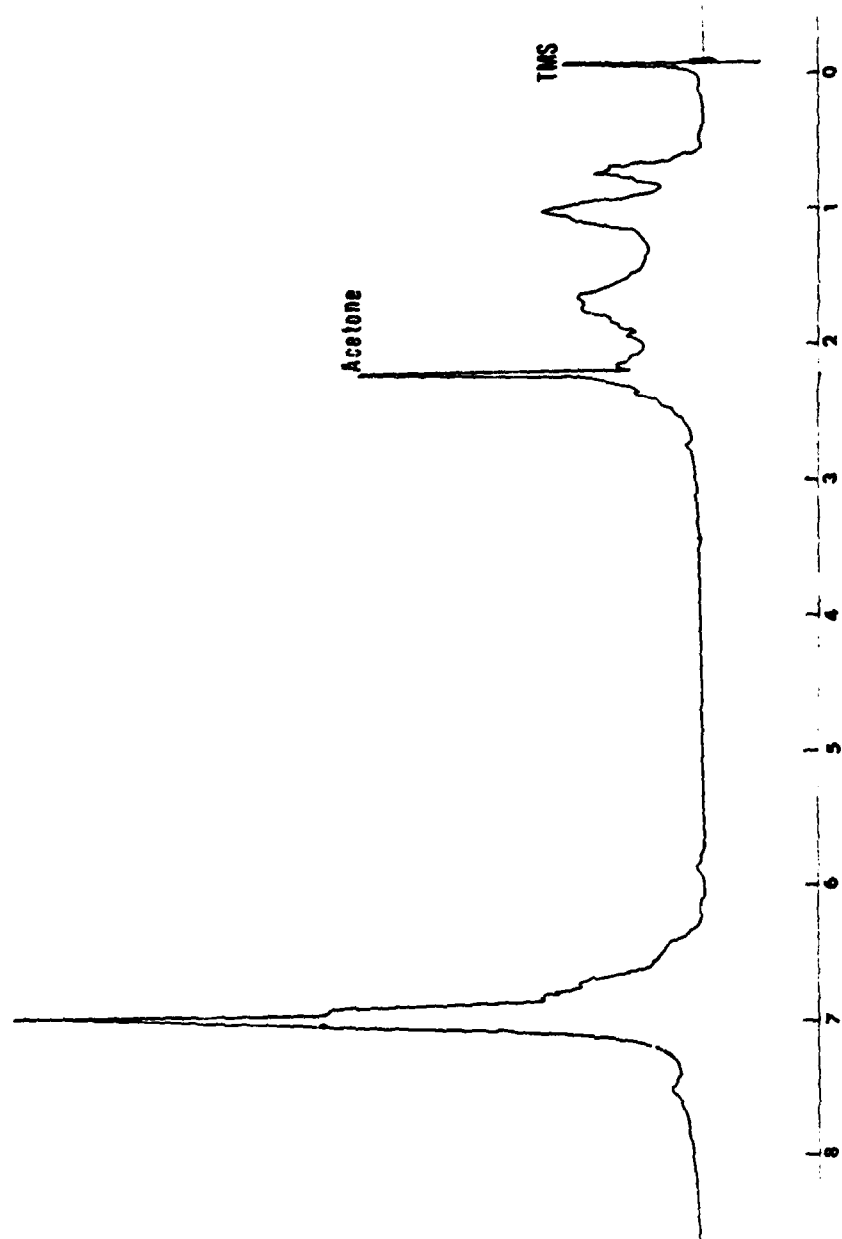


FIGURE 1. Proton NMR spectrum of 580M PL polystyrene as received. Instrument: Varian HA-100 NMR; amplitude: 600; sweep time: 5 min; filter: 0.5 sec; RF power: 0.1 mG; solvent: deuterated chloroform. Spectrum taken at room temperature.

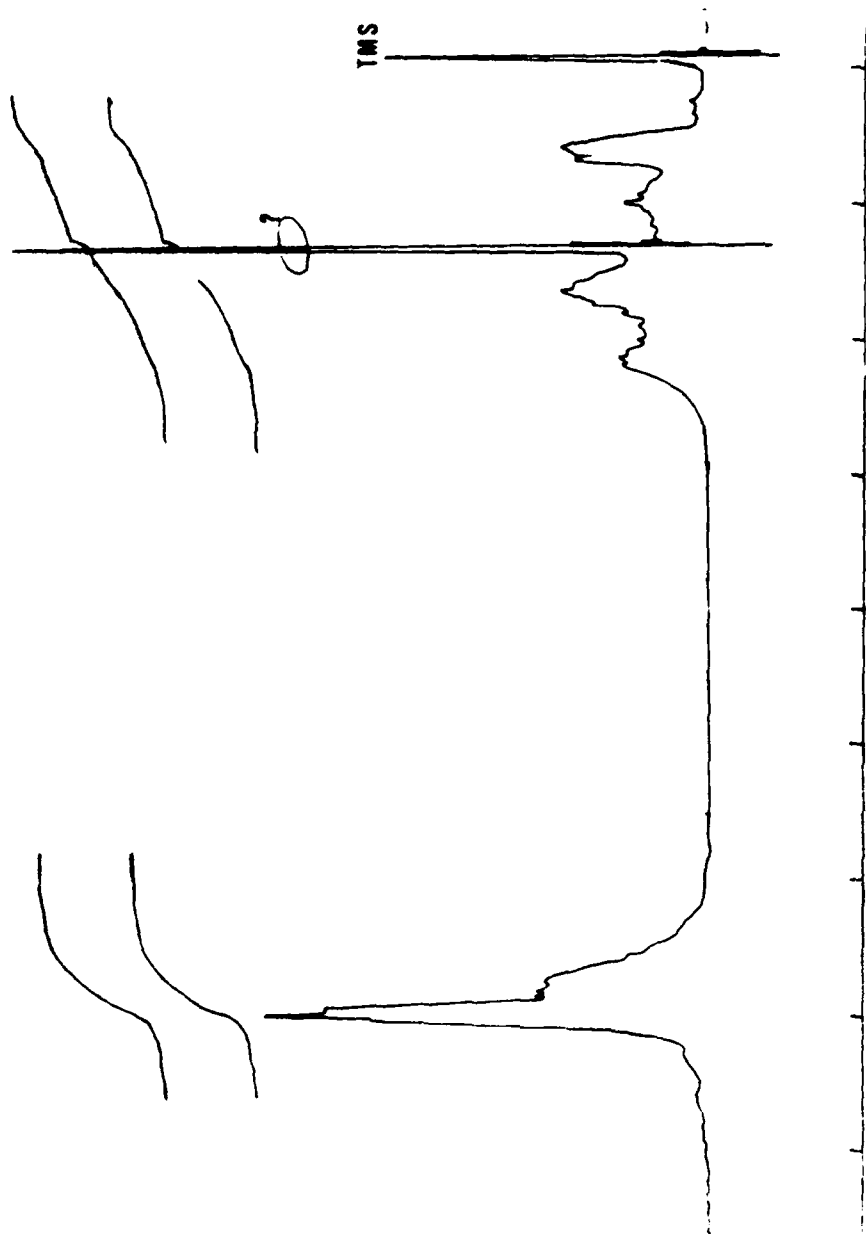


FIGURE 2. Proton NMR spectrum of 500M polystyrene as received from Goodyear Chemical. Remaining conditions as in Figure 1.

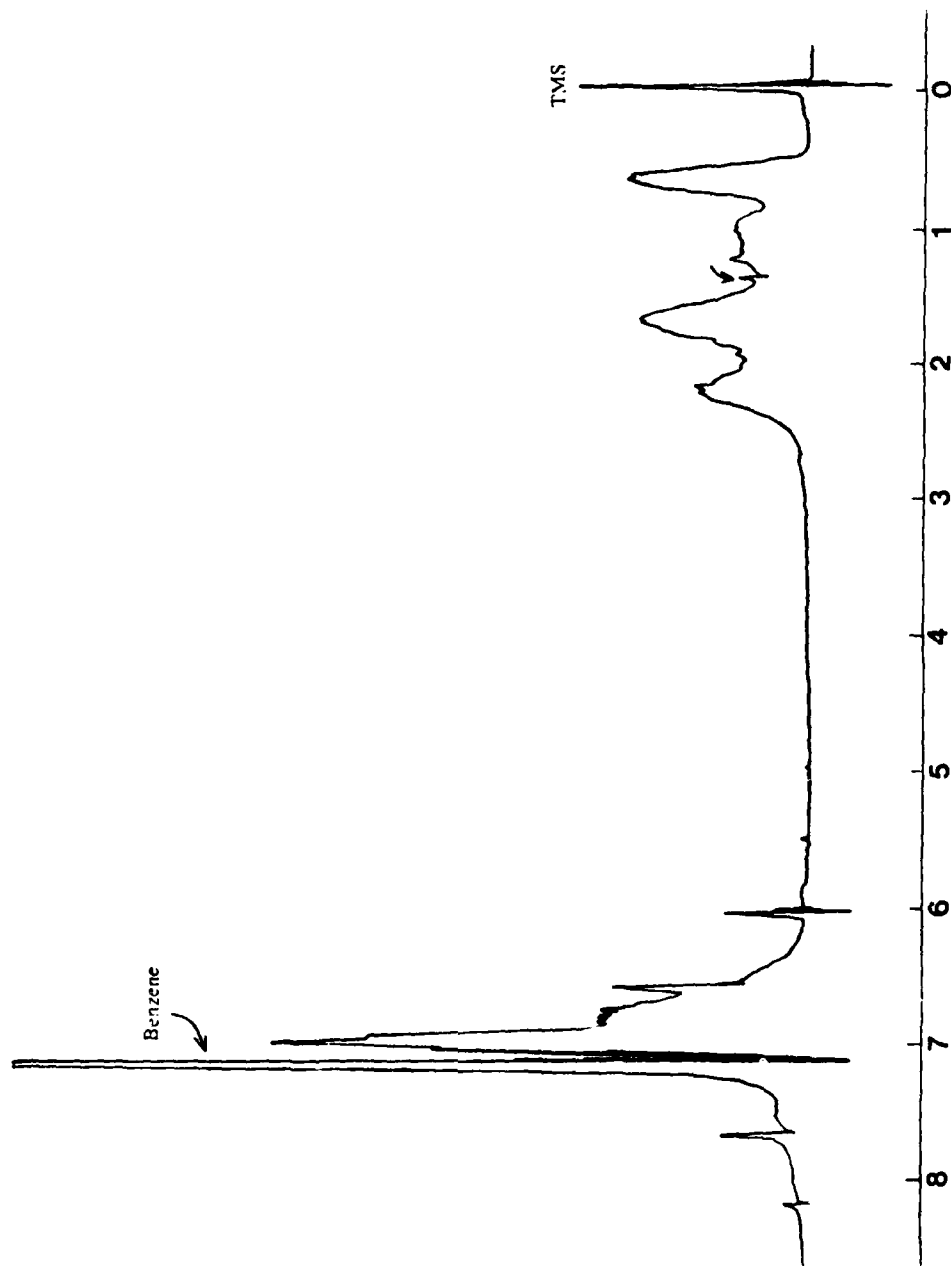


FIGURE 3. Proton NMR spectrum of Goodyear 500M polystyrene after clean-up; arrow indicates trace amount left of unknown peak at ca. 1.3 ppm. Remaining conditions as in Figure 1.

Ultimately, it was found that filtration through 0.2-um filters removed a considerable amount more of the solid. However, there did not appear to be any readily-applied means of getting rid of all of the contaminant.

Analytical-Scale Chromatography. Each standard, as well as mixtures of standards, were made up in THF solvent. The solutions were then diluted serially until approximately three-quarter-scale response was obtained at a detector sensitivity of 0.05 UV absorbance units (AU) or gave peaks of better than half-scale recorder response at range settings of 64-128 with the RI detector. The chart speed and flow rate were as noted. Nominal flow rates were occasionally checked by passing the eluent into a thermostated buret. The column and flow-meter temperatures were set as noted. The mobile phase was brought to temperature prior to entering the column.

Preparative-Scale Chromatography. Solutions of the polystyrenes used in the fractionation work were made up in acetone. This was found to be useful in preventing gumming of the injection valve. The concentrations were either $1/3 \text{ g cm}^{-3}$ or $1/5 \text{ g cm}^{-3}$, and were such that the main bands exhibited absorbances of in excess of 2 AUFS, the maximum capability of the detector. Fractions were collected manually in glass flasks and recovered by rotary evaporation.

Bulk-Scale Fractional-Solution Fractionation of R-45M. In the initial work of this portion of the Contract, a single-stage bulk-scale solvent fractionation of R-45M was carried out. Later, multiple-extraction fractionation was used.

Single-Stage Fractionation. The initial attempt at solvent fractionation of hydroxy-terminated polybutadiene was carried out as follows: 10 g of R-45M was first taken up in a volume of THF contained in the 250-cm^3 water-jacketed separatory funnel. Following this, a second volume of MeOH was added so as to yield a final solution consisting of 5%, 10%, or 20% v/v THF. The solution was shaken vigorously for a few minutes and then allowed to stand overnight. The high molecular-weight R-45M that settled out of solution as a lower layer was drawn off and discarded. The THF/MeOH solution containing the low molecular-weight fraction of R-45M was then subjected to rotary evaporation; residual solvent was removed by placing in a vacuum line in series with an Edwards mechanical pump (10^{-3} torr). Approximately 60 g of crude R-45M was required to isolate 4 g of fractionated HTPB that was soluble in 10% THF/90% MeOH.

Analytical-Scale Multiple-Extraction Fractionation. Multiple-stage fractional-solution fractionation of R-45M was next carried out on an analytical test scale as follows. Approximately 50 g of R-45M was placed in the thermostated separatory funnel, following which was added the appropriate solvent (IPA or a mixture of IPA + benzene). The mixture was next stirred for 4 h, and phase separation then allowed to take place over at least 18 h. The upper layer was siphoned off; the solvent was removed by rotary evaporation; and the fraction was transferred to a screw-cap vial with methylene chloride. The solution was then subjected to vacuum, first by water aspiration to remove most of the methylene chloride and, secondly, by a two-stage rotary-vane vacuum pump capable of 10^{-3} torr. Pumping with the latter was continued for at least 3 h. The recovered and tared R-45M was then flushed with nitrogen, sealed, and stored in the dark. Virtually all fractions were very-pale-yellow to colorless, and clear.

Preparative-Scale Multiple-Extraction Fractionation. For preparative-scale fractionation (2-dm^3 vessel; 500-g amounts of R-45M), 1-dm^3 amounts of extractant solvent were employed, i.e., the fractionation was scaled up by a factor of 10.

Bulk-Scale Silylation of R-45M. A 500-g amount of R-45M was also silylated, and then fractionated as described above. Thus, this amount of material was placed in a 2-dm^3 one-neck round-bottom flask equipped with a heating mantle and reflux condenser. A solution of 100 cm^3 HMDS in 900 cm^3 dried (Na; molecular sieves) toluene was then added and the solution refluxed for 48 h. Following this, the solvent was removed by

rotary evaporation and then single-stage vacuum distillation (Edwards vacuum pump; ca. 10^{-2} torr). The product was orange-brown in color, and was clear.

Vapor-Phase Osmometry. The initial procedures used with the VPO were as described in Technical Memorandum AFAL TM-84-025 (June 1984). However, because of protracted difficulties with the Knauer VPO, the accuracy of measurements made with it were also assessed. The first aspect of the instrument that gave rise to large errors was temperature control of the samples cell. Thus, two additional heat pumps were installed in the laboratory that enabled ambient room temperature to be controlled to $76 \pm 2^\circ\text{F}$. The VPO cell temperature could then be maintained to better than $\pm 0.1^\circ\text{C}$, as measured with the Hewlett-Packard thermometer. However, the heat pumps caused a draft around the instrument, which also affected the measurements. The entire instrument was therefore encased in a Plexiglass housing. The instrument then zeroed quite well on an attenuation setting of 4. Also, after making a series of measurements, then replacing the solutions drop with one of pure solvent, the instrument returned to zero to within ± 0.2 units, again on an attenuation setting of 4. (The sample thermocouple required at least three washings with pure solvent.) Thus, overall, control of the room temperature, elimination entirely of drafts, and careful washing of the instrument thermocouple posts, yielded readings that were in fact of very good precision.

Viscosity. Viscosity measurements were made with the apparatus described above and in accordance with ASTM Methods D-445 and D-446. The specific procedures were as follows. First, an open thermostat (i.e., the 5-dm³ tall-form insulated beaker) had the advantage of ease of access when changing solutions and when removing the viscometer tube for cleaning. (The disadvantage of the system was that approximately $\frac{1}{2}$ h was required, in order to change the bath temperature by 5° .) Next, the sample was placed in a 25-cm³ volumetric flask that was also suspended in the water-bath so as to ensure that it was at the same temperature as the thermostat itself. The use of a volumetric flask had several advantages. First, all solutions were made up by weight, with the volumetric flask resting on an analytical balance. Thus, a weight of polymer was added to the tared volumetric, following which it was diluted to the mark with solvent (initially chloroform and, later, THF). The weight of added solvent could thereby also be calculated. Since the weight of the solution as well as its volume were known at this point, the density of the solution at the balance (i.e., room) temperature could also be calculated. In addition, when a quantity of solution was removed from the volumetric flask for analysis, and then later returned to the flask, a small volume of solvent was inevitably lost due to evaporation. This was replaced simply by the addition of more solvent to bring the solution back to the mark in the volumetric. A small amount of prepolymer was of course also lost in transferring volumes of the solutions, due to adsorption onto the walls of the pipet as well as the viscometer tube. The pipet and viscometer tube were therefore washed with the solvent that was used to bring the solution back to volume in an attempt to minimize this although, even so, some material was undoubtedly still not recovered. However, the loss was negligible in comparison with the concentration-change of the solution due to evaporation of the solvent.

Prior to use of the viscometer tube as well as between each run, it was cleaned with fresh hot chromic acid cleaning solution. This procedure was not required for reproducible results with the solvent itself (see below), but was absolutely necessary for any of the polymer solutions. Also, if the chromic acid solution (normally brown) showed any hint of green, it was discarded. Washing was carried out as follows. The tube was filled with chromic acid and was placed in a large beaker containing hot water. The beaker and tube were then placed under a hot-water (ca. 70°C) tap, the flow from which was directed directly into the capillary arm while the chromic acid was draining through all three tubes. Roughly 10 min was required to drain all of the cleaning solution through the capillary. Following this, the tube was rinsed thoroughly with distilled water, acetone, and chloroform (or THF); and then blown dry.

In filling the viscometer tube, 15 cm³ of the liquid mixture was transferred from the (thermostated) volumetric flask via a 15-cm³ Class A pipet to the large arm of the viscometer clamped in place in the water-bath. Thus, the solution was exposed to room temperature for only a very short time. Even so, the filled apparatus was allowed to stand for ca. 1/2 h in order to ensure thermal equilibrium. During this time all three arms of the viscometer were capped with rubber serum septa to prevent solvent loss. The solution was then drawn up into the capillary arm of the viscometer and the fall time measured by the procedure given in the Cannon literature. The fall of the capillary meniscus was timed with a Siliconix Model ET 200 electronic stopwatch, accurate to ± 0.001 sec.

An important finding was that, with the (three-arm) Ubbelohde-model viscometer tube, true-vertical standing was relatively unimportant, as confirmed by measuring the fall-times of chloroform with and without the tube being at true-vertical: it had to be as much as 5° out before the fall-times changed measurably.

Infrared Spectroscopy. The branching studies by solution IR were conducted as specified in ARCO T & D NO. 8004, with CS₂ solvent. The ATR studies required only that the R-45M fraction under consideration be smeared, neat, onto both faces of the ATR crystal. No special precautions were observed in doing so, as it was found that reproducible spectra were obtained independent of the layer thickness as well as the manner of application. Thus, for example, no effort was made to exclude air bubbles. The CIRCLE method involved simply filling the boat with the sample of interest.

Quantitation of hydroxyls by FT-IR was carried out as described by Dee and Emanuel (28). Briefly, a Beer's-law calibration plot was constructed from measurements of the OH peak of the recommended standard, 6-undecanol, at 3628 cm⁻¹ (CCl₄ solvent). The hydroxyl content of R-45M was then determined at 3620 cm⁻¹ with this plot. The optimal conditions for determination of hydroxyls by this method with the Mattson FT-IR were found to be 128 scans at 4 cm⁻¹ resolution, operated at 2% aperture opening and scanning from 3800 to 1400 cm⁻¹. For the Perkin-Elmer instrument, 100 scans were taken at 4 cm⁻¹ resolution over 4000 to 1200 cm⁻¹. In either case, the spectrum of neat carbon tetrachloride was subtracted such that the peak at 1549 cm⁻¹ was nulled.

Derivatization with Formic Acid. R-45M hydroxyls were converted virtually quantitatively to formate esters via a modification of a procedure for formate ester derivatization of bile acids (29). Thus, a stirred solution of ca. 2 g polymer in 10 cm³ of 95-97% formic acid containing 2 drops of 70% perchloric acid was warmed to 55°C for 1/2 h on an oil-bath. The solution was then allowed to cool to ca. 40°C, whereupon acetic anhydride was added dropwise at a rate sufficient to maintain the solution temperature at between 55-60°C. The addition was continued until the onset of effervescence. The solution was then cooled to room temperature and poured into 30 cm³ water. Thirty cubic centimeters of methylene chloride was added, the water layer drawn off, and the lower organic layer washed twice more with water. The solution was then washed with 20 cm³ 5% sodium bicarbonate solution, once more with water to neutrality, and then dried over anhydrous sodium sulfate. The methylene chloride was then removed by vacuum aspiration, the last remnants being taken off on a vacuum line.

Nuclear Magnetic Resonance Spectrometry. NMR spectra were taken in the usual way. Tetramethylsilane (TMS) was occasionally added as an internal standard.

Differential Scanning Calorimetry. DSC was carried out for the most part with aluminum pans and crimp seals. Stainless-steel pans with threaded caps and rubber O-ring seals were also used for some solutions; however, the heat capacity of the cells was high, which resulted in very broad transition peaks and, in turn, inaccuracies in the transition temperatures. They were therefore not used further.

Inverse Gas Chromatography. The procedures used for high-precision GC data acquisition and reduction were as described elsewhere (27).

RESULTS AND DISCUSSION

Phase I, Task 1. Fractionation of Polystyrenes and HTPB

In the initial portion of the work of Phase I, the fractionation of several low molecular-weight polystyrenes was carried out by gel permeation chromatography. The results obtained with tetrahydrofuran and chloroform solvents are described and discussed below.

GPC Fractionation of Polystyrenes with THF Solvent. Shown in Figures 4 and 5 are representative gel-permeation chromatograms of concentrated THF solutions of polystyrene of molecular weight 680 Da with the PL GPC column (THF mobile phase) (note that the chart speed was changed during the course of the runs so as to yield a manageable strip-chart length). (The concentration of the polymer solution was purposely higher in the latter case so as to yield different peak heights and widths of the main band as well as the smaller bands.) Indicated at the top of the figures are the fraction identification numbers, A_1 - I_1 and A_2 - I_2 , respectively. It was subsequently found (analytical GPC) that fractions A_1 through G_1 were identical; the large peaks to the extreme right of each main peak were assumed to be solute and/or solvent impurities, and were not investigated further. The smaller peak to the extreme left of each main peak corresponds to an injection pulse. Each collected fraction corresponds to 1 min of chart distance, or, since the flow rate was $0.5 \text{ cm}^3 \text{ min}^{-1}$, 0.5 cm^3 of mobile phase. The data are summarized in Figure 6, which illustrates the analytical GPC of unfractionated PS of 680 Da together with the band maxima (vertical lines) of each of the fractions.

GPC Fractionation of Polystyrenes with Chloroform Solvent. THF was found to be deleterious to the PL column and, as a result, the mobile phase was changed during the course of this portion of the work to chloroform and the fractionation work repeated with this solvent.

First, two gel-permeation chromatograms were run of an individual concentrated solution of the 680M polystyrene. The same nomenclature was used as before for the fraction numbers, although it was assumed at the outset that these would most likely not correspond to those collected previously with THF. As before, it was found that fractions A and B were virtually equivalent, as were G, H, and I. Only fractions B through G were therefore considered in further detail.

Since the analytical gel-permeation chromatograms of the collected fractions were taken from injections of the same solution of the polystyrene, they provided a good test of the reproducibility of the collection procedures. Fractions B_1 and B_2 were found to be identical both in terms of peak retentions as well as areas. The band symmetry was also quite good, in contrast to that found previously with fractions B collected with THF solvent. The same was true also of fractions C_1 and C_2 , and D_1 and D_2 . Moreover, the areas under these peaks were quite substantially greater than those under fractions B. The bands of fractions E were comprised of two partially-separated peaks. The retentions of these were the same on passing from E_1 to E_2 ; however, the first was smaller than the second in E_1 , while both peaks were of nearly the same height in E_2 . Fractions F also exhibited two partially-resolved peaks as well as several shoulders. Those in F_2 were of very different height, while the peaks in F_1 were only marginally so. Fractions G were virtually identical in terms of the partially-resolved peaks and shoulders evident in both. However, the area under G_2 was slightly less than that under G_1 .

The data are summarized in Figure 7, where the GPC of the unfractionated polymer is shown together with vertical lines indicating the various fractions collected in this portion of the work. The latter clearly corresponded to different regions (times or volumes) of the unfractionated material; in addition, virtually the entire peak appeared to have been satisfactorily cut.

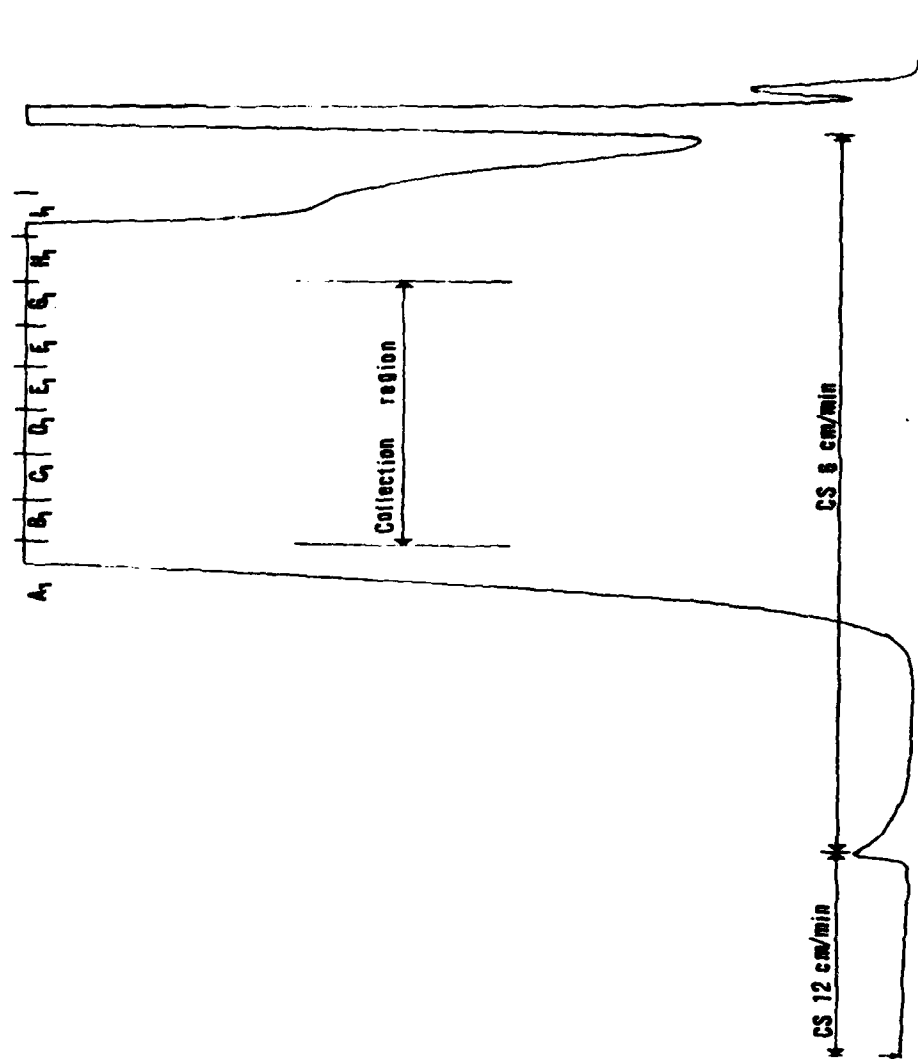


FIGURE 4. Gel-permeation chromatogram of concentrated polystyrene (680 Da) solution in THF with the PL column of 7.5 mm i.d. by 60 cm in length (Polymer Laboratories). THF solvent at $0.5 \text{ cm}^3 \text{ min}^{-1}$; 25°C temperature; UV detection at 254 nm; chart speed (CS) as noted. Fraction-collection region spans fractions B₁ through G₁.

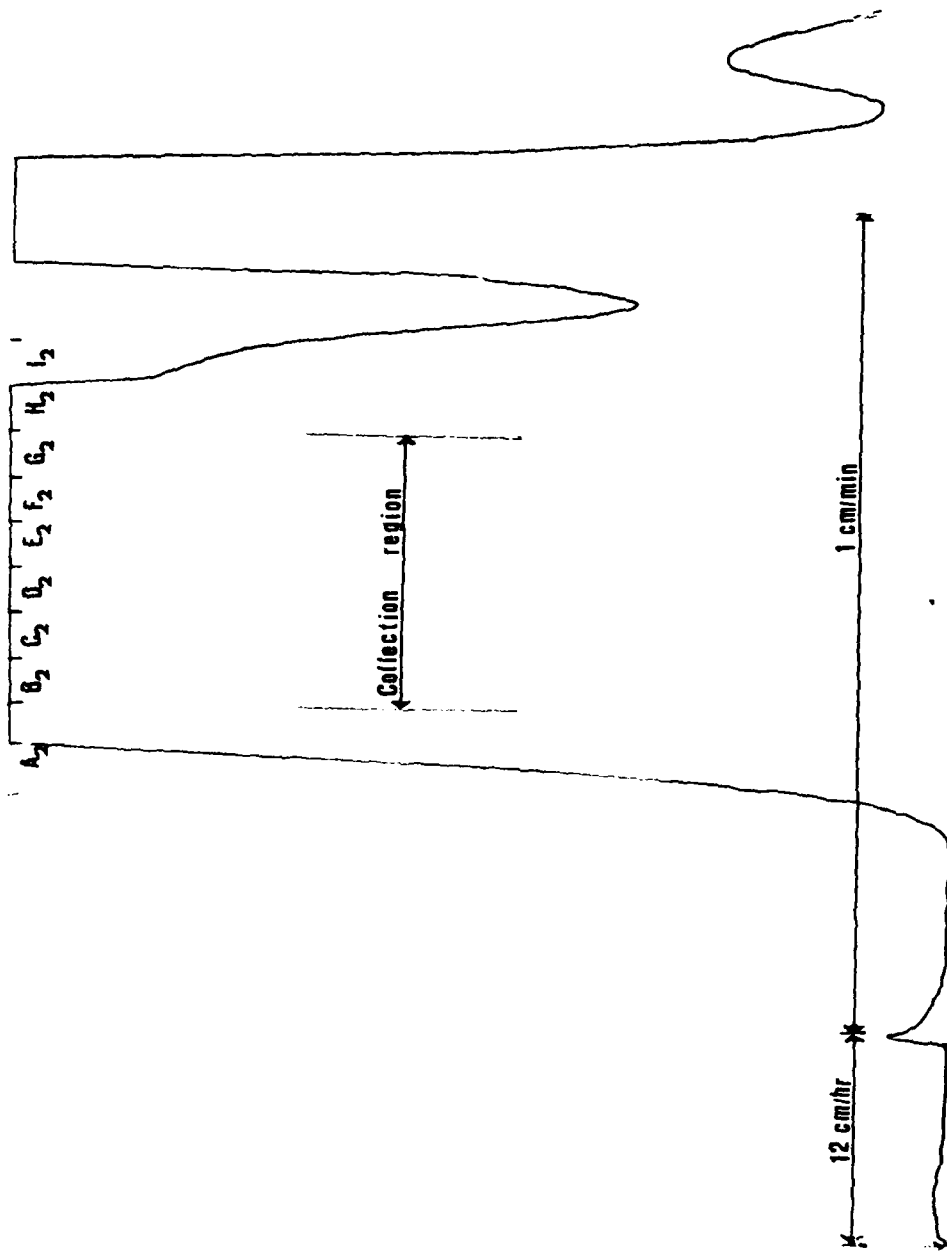


FIGURE 5. As in Figure 4; more concentrated solute solution.

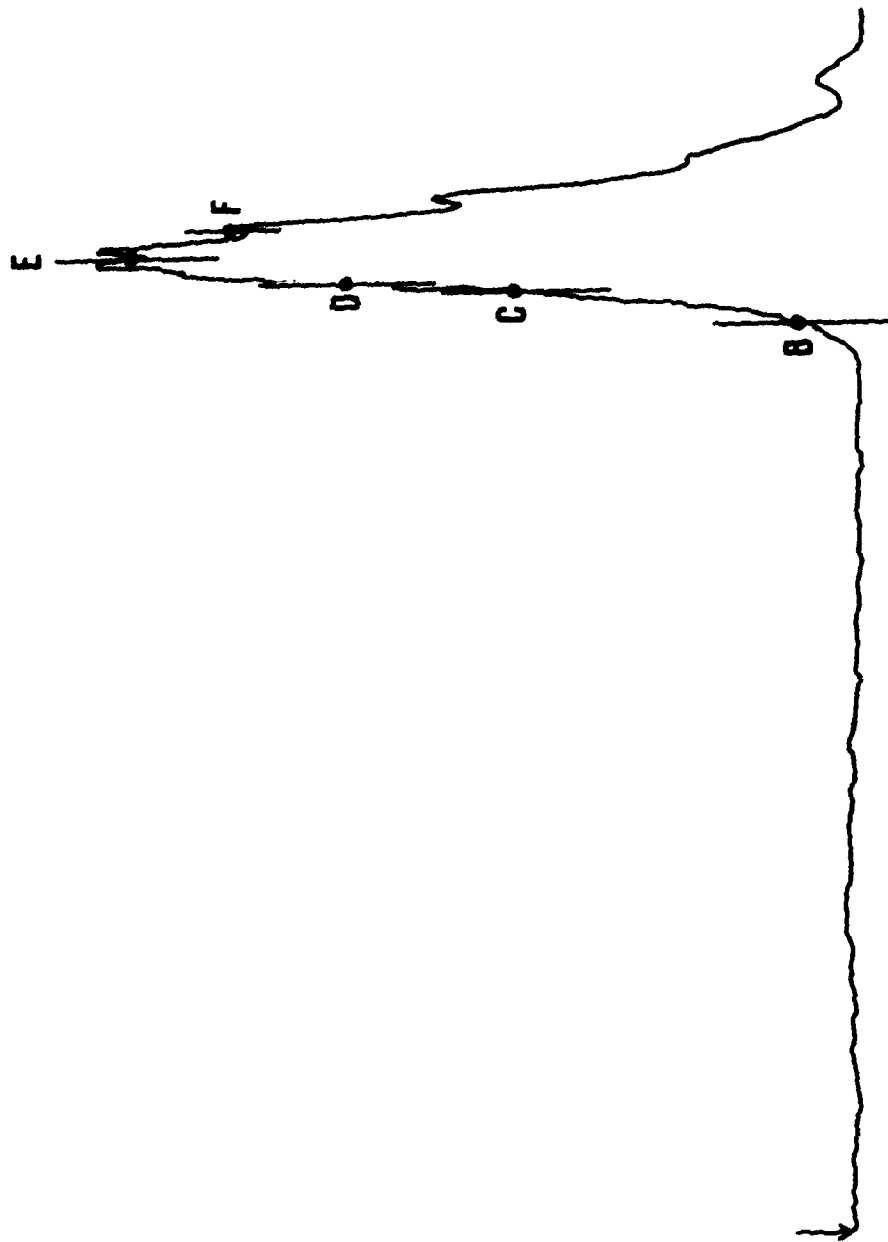


FIGURE 6. Summary illustration of the gel-permeation chromatogram of unfractionated polystyrene of nominal molecular weight 680 Da, and the positions of the peak maxima B through F collected as described in Figures 4 and 5.



FIGURE 7. Summary illustration of the gel-permeation chromatogram of unfractionated polystyrene of nominal molecular weight 680 Da, and the positions of the peak maxima B through F collected as described above.

Limitations of GPC for Fractionation of Polystyrene Homologs. The GPC fractionation of low molecular-weight prepolymers, as exemplified by the work with 680M polystyrene described above, clearly is of limited utility even on the analytical scale: no separation of individual isomers was observed; moreover, what differences were found between peak shoulders amounted to microliters on elution volumes of 10-20 milliliters, i.e., very small differences on rather large volumes. Thus, and despite very careful evaluation and control of the GPC systems, it was concluded at this point that gel-permeation chromatography was inappropriate for the first Task of this Contract, namely, the isolation of gram-amounts of individual polystyrene and HTPB prepolymer homologs.

[In retrospect, the lack of separation of homologs is understandable in terms of the solute partition coefficients K_R . For example, assume that the K_R values of two of the 680M polystyrene homologs are 0.600 and 0.605, which are entirely reasonable in view of the summary separations shown earlier, and below. The alpha value is then $0.605/0.600 = 1.008$. Accordingly, the number of theoretical plates required N_{req} to effect 6 σ (baseline) separation, assuming capacity factors of in excess of 10 (which is most likely naive), is approximately 600,000, i.e., well in excess of the 40,000 theoretical plates exhibited by the PL Gel column. Also, the lower molecular-weight materials represent by far the easiest (i.e., most favorable) cases.]

Analytical-Scale Reverse-Phase LC Fractionation of Polystyrene Homologs. In view of the above findings, the GPC fractionation studies were abandoned at this point, and the method of fractional solution outlined and discussed in the initial Contract Proposal was begun. In essence, this technique amounts to depositing a sample at the top of a reverse-phase LC column, flowing through which is a solvent that is very "poor". Thus, the sample should ideally precipitate at the system entrance. Moreover, the column packing should be completely inert to the sample, that is, a derivatized-silica packing is called for. (The capacity of the column is then governed, literally, by the surface area within the column onto which the solutes can precipitate.) Then, by changing the mobile phase to a "good" solvent, the sample is eluted with concomitant fractionation. Polymer homologs are therefore eluted in order of low to high molecular weight.

[The opposite technique, fractional dissolution, has in the past been used for polymer separations with a separatory funnel as described at the outset of this Report: the polymer is taken up in a good solvent, followed by titration with a poor solvent. This amounts to a one-stage (one theoretical plate) separation; the order of precipitation in this case is high to low molecular weight.]

Choice of "Good" and "Poor" Solvents. A commonly-reported solvent pair for use with polystyrenes is some or other combination of THF + water. Thus, this was the first set of solvents to be evaluated for the reverse-phase LC separations in this work. As will be shown later, however, and despite recent claims in the literature to the contrary, this was by no means the best pair.

Choice of Analytical Column. The analytical LC columns were from Jones Chromatography. Five-micron Spherisorb ODS analytical columns from this company routinely yield ca. 25,000 theoretical plates (that is, nearly 100,000 plates per meter) and so, were used as the fractional solution support system.

Solvent Optimization for 680M Polystyrene. In carrying out initial separations of 680M isomers, a mobile-phase gradient was employed. This was: isocratic for 3 min at 25% v/v THF/H₂O, followed by a linear gradient over 10 min to 80% THF/H₂O. The result was dramatically superior to any chromatogram obtained in the previous work with any of the GPC columns: at least 12 peaks were seen in the polymer envelope (the large initial peak is thought to be due to THF; see below). Also, the baseline did not rise very much over the starting point. It therefore remained at this point only to optimize the mobile-phase combination(s), preferably isocratic, in order to separate the homologs.

Figure 8 illustrates the separation obtained with 80% THF isochratic. This was too "good" a solvent, as all of the polystyrene eluted in one very large peak. In contrast, Figure 9 illustrates the separation obtained with 60% THF: the resolution is too good, that is, the mobile phase is too "poor". Also, longer-retained peaks (not shown) were broadened almost to the point of disappearing into the baseline, and the elution times of what peaks were seen were extraordinarily long. Even so, some separation was achieved.

A compromise between the results of Figures 8 and 9 was achieved with 70% THF, as shown in Figure 10. The separation is excellent, with only a slight baseline rise from the beginning to the end of the polymer envelope. Moreover, twelve PS peaks can be seen in the chromatogram, with the later ones comprising the bulk of the total-polymer chromatogram area. (That is, the area centroid of the polystyrene band actually occurs in the vicinity of isomer nos. 7-8, and not isomer nos. 4-5.)

THF impurities that appeared in the chromatograms were eliminated at this point by going over to pure acetone solvent for the polystyrene sample. Acetone was also found to prevent gumming of the injection valve. The resultant chromatogram of 680M was not quite as good as those obtained with pure THF solvent because of the better solution strength of acetone. Even so, a substantial improvement in terms of "cleaning up" the injection-pulse region was evident.

Because of the slight overlap with acetone solvent, a decrease in the THF content of the mobile phase was indicated, viz., 68% THF. The resultant chromatograms showed some improvement, but better separation was nevertheless desired. The mobile phase was therefore adjusted to 65% THF. The separation was very nearly baseline, although with some sacrifice of visualization of the high end of the polymer envelope.

Nevertheless, and despite the good analytical separations found thus far, it became clear at this point that solvent systems comprised solely of the traditionally-used pair THF + H₂O were unsatisfactory for separation of all but the lowest molecular-weight polystyrene standards. Moreover, the requirement of ca. 70% THF for 680M portended that, eventually, the solvent strength would have to be increased to pure THF for ca. 2000M and higher. That is, no further speciation would be possible under conditions of isochratic elution. Another way to view the situation is that pure THF is too good a solvent for polystyrenes, while pure water is too poor a solvent. Moreover, it is difficult to work on the borderline of solubility of these polymers when attempting fractional solution with this solvent pair. A modifying (i.e., intermediate-strength) solvent hence was called for, for which methanol was chosen. The results thereby obtained were quite satisfactory, as described and discussed in the Sections that follow.

The results obtained for 680M polystyrene with 5% THF/95% MeOH (acetone for the sample) indicated that the mobile phase was far too "good", but the column efficiency, peak sharpness, and so forth, were clearly superior to anything seen with THF/H₂O. That is, the choice of THF with methanol was very much in the right direction in terms of solvent strength. However, chromatograms obtained with 2% THF/MeOH, 0.2%, and pure MeOH indicated that even the latter was too "good" a solvent.

Gradient elution was therefore resorted to at this point. Figure 11 illustrates the result: the resolution of all peaks is considerably greater than baseline, which was required for preparative separations. (The preparative system gave poorer efficiency because it was operated in the overload mode.)

Two additional gradients were subsequently tried. In the first, the finishing solvent was slightly stronger than in the latter; however, there was very little from which to choose between the two. Moreover, neither was as good (particularly at the back end) as that formulated initially. Thus, the gradient indicated in Figure 11 was the best of those tried in this portion of the work.

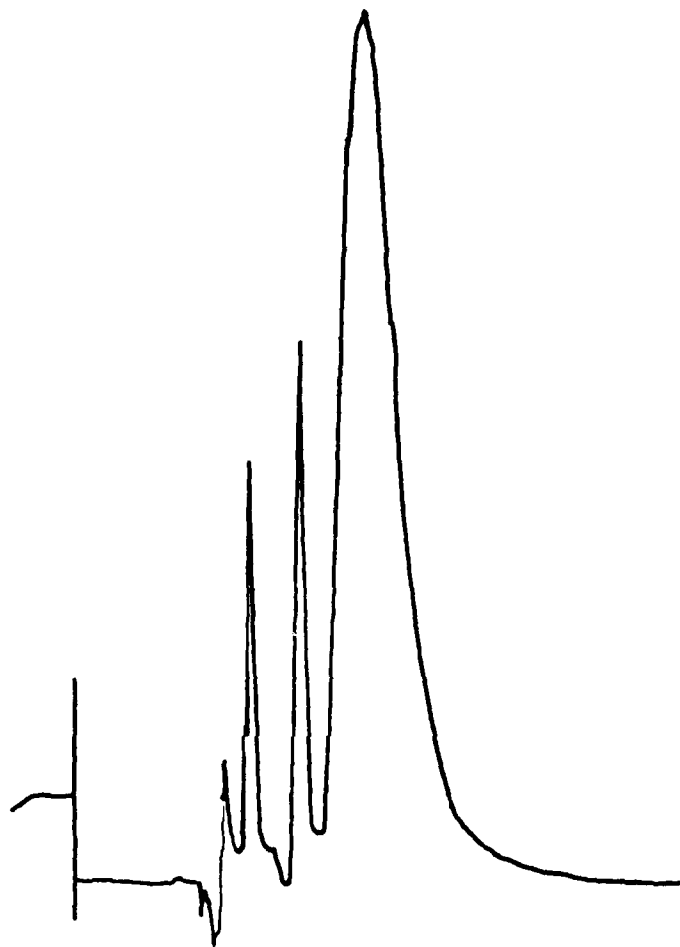


FIGURE 8. Isochratic reverse-phase LC separation of 680M polystyrene. Column and conditions: 80% v/v THF/H₂O mobile phase; column: 25-cm Spherisorb C₁₈ 5- μ m; flow rate: 1 cm³ min⁻¹; chart speed: 1 min cm⁻¹; room temperature; 10-mm³ injection-loop volume.

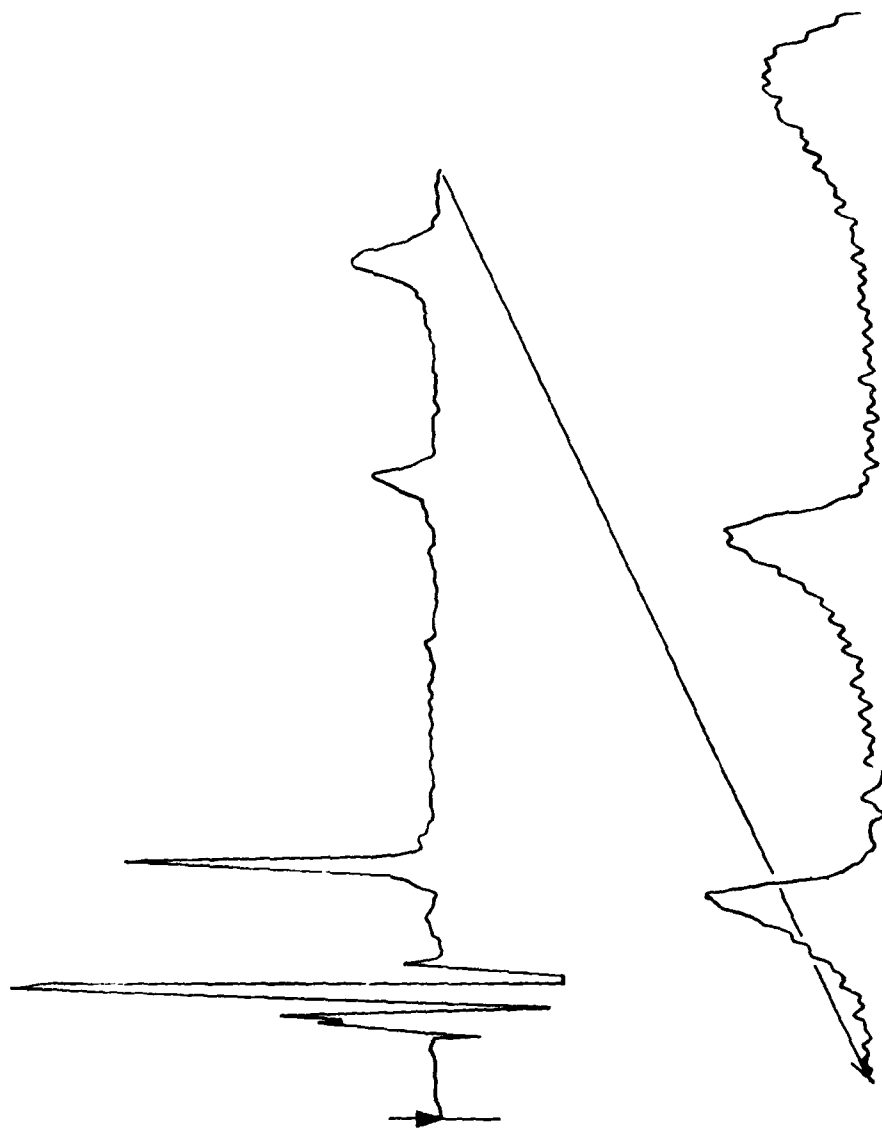


FIGURE 9. As in Figure 8; 60% THF/H₂O mobile phase.

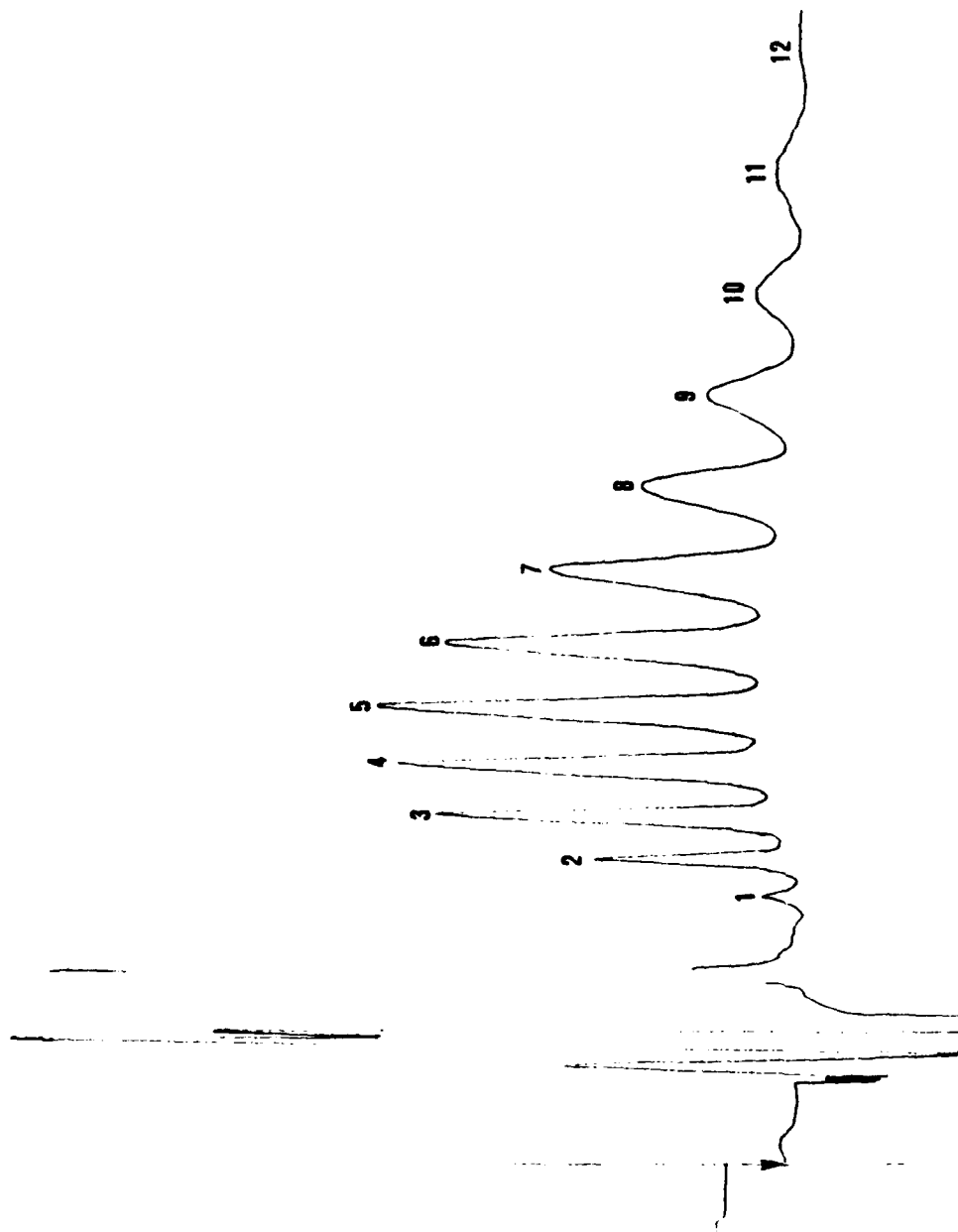


FIGURE 10. As in Figure 8; 70% THF/H₂O mobile phase.

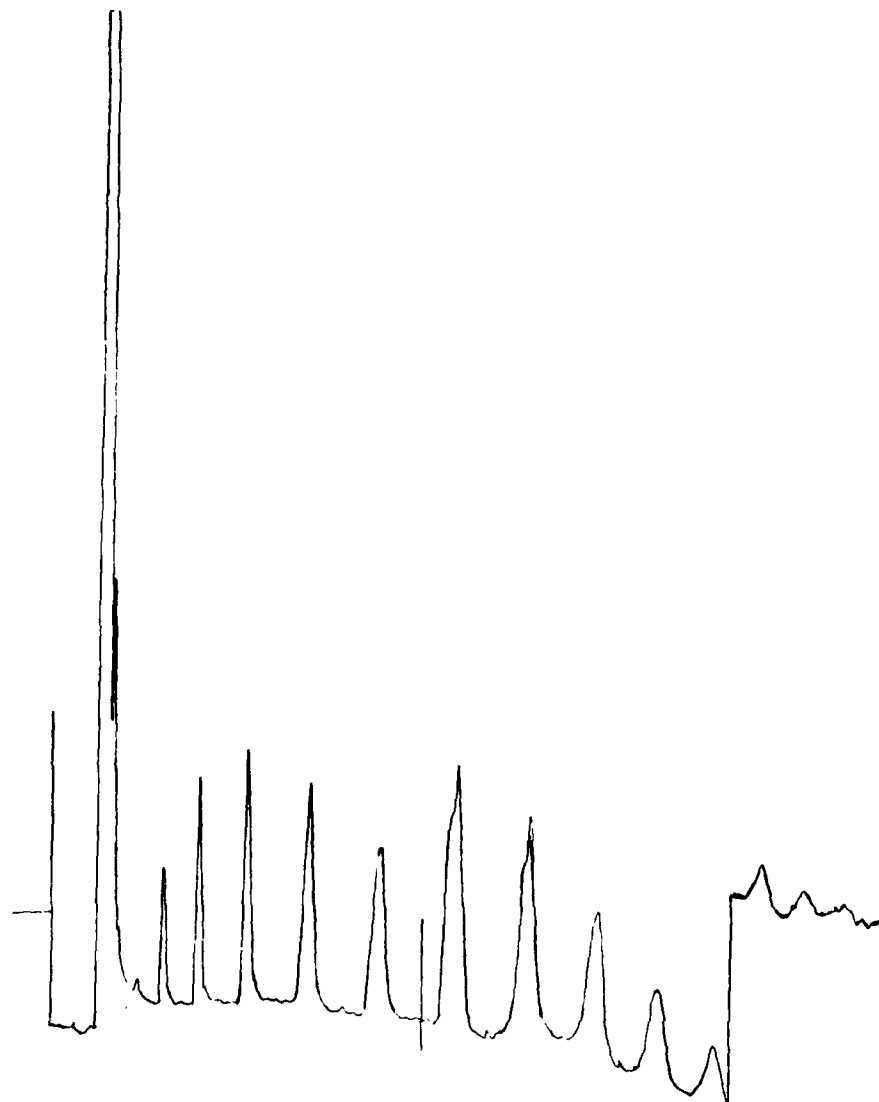


FIGURE 11. Gradient reverse-phase LC separation of 680M polystyrene. Column: 25-cm Spherisorb C_{18} 5- μ m; flow rate: $1 \text{ cm}^3 \text{ min}^{-1}$; chart speed: 2 min cm^{-1} ; room temperature; 10-mm^3 injection-loop volume. Mobile-phase gradient: 5 min at 5% $\text{H}_2\text{O}/95\%$ MeOH isocratic, then to 10% THF/90% MeOH (contained in a separate reservoir) at 2% v/v reservoir change per min.

Despite the above successes, the use of continuous gradients (or, worse, multiple gradients) was not in fact considered practicable from the standpoint of preparative-scale fractionation. Now, while it is true that gradient preparative solvent delivery systems are available (that from Rainin appears to be the best), the costs are on the order of \$10⁴, i.e., prohibitive in this Contract work. Thus, a simple device was implemented that consisted of a mixing chamber for solvents prior to their entry into a single pump head. The flow into the chamber (equipped with a magnetic stirrer) was controlled by manifolded stopcocks, and by raising or lowering the (siphon) containers of pure solvents. The reproducibility of the technique left much to be desired, however, and so, solvent optimization on the analytical scale was reconsidered with the view of defining step-gradient changes that would effect the desired separations. This technique is obviously considerably simpler than continuous-gradient elution, since one has merely to immerse the pump-inlet line into each of a series of solvent containers without having to be concerned with the volume in (or level of) each reservoir. Moreover, constructing this type of system required only that a three-way solvent drain line be connected between the pump and the injection valve so as to be able to purge the lines with the new mobile phase. (There was no flow in the column during the purging process but, since the diffusion of polymers in liquids is slow, resolution was not affected.)

The results of a step-gradient fractional solution experiment for 680M polystyrene with 5% H₂O/95% MeOH, incremented to 100% MeOH, showed that the first half of the chromatographic separation was quite good, but the second solvent was too "strong", i.e., there was considerable overlap. Accordingly, a three-step gradient of 10% H₂O/90% MeOH, then 5% H₂O/95% MeOH, then pure MeOH was used next. The chromatogram is shown in Figure 12(a,b,c), and is quite good: fully 16 peaks are virtually baseline-resolved in the run and, most importantly, the resolution far exceeds baseline in very many instances. Thus, at least with polymers of this molecular weight, the column could be seriously overloaded while maintaining excellent separation. This result was improved even further by small modifications of the step-gradient concentrations, as shown in Figure 13(a,b,c). In the latter instance 17 fully-resolved bands were obtained.

Solvent Optimization for 946M Polystyrene. Having achieved some success with ca. 70% THF/H₂O for 680M polystyrene, roughly the same solvent system was used initially (isochratic mode) for the separation of 946M polystyrene. There was not much to choose from the results obtained with 72% THF vs. 70% THF; both provided near-baseline resolution of the isomers, and each showed roughly 15 peaks. Unfortunately, the retentions were much too long and the peaks much too low and broad for anything less than 70% THF to be of use.

The step-gradient strategy was applied next. The same changes as above were effected in the step-gradient compositions. The separation with the first appeared to be superior to the second in terms both of resolution and analysis time.

Solvent Optimization for 1350M Polystyrene. The isochratic separation of 1350M polystyrene was next attempted, beginning as above with THF/H₂O. Separations were achieved with 75% THF, 73%, 71%, and 70%. The first two of these, 75% and 73% THF, showed the usual polymer envelope, but resolution of the isomers was far from satisfactory. A very considerable improvement was found with 71%, which illustrated how sensitive these separations are to mobile-phase composition when operating on the edge of the polymer solubility in the mobile phase. In any event, 71% THF turned out to be the optimum for 1350M polystyrene.

Recalling that mobile phases of methanol containing small amounts of THF had previously proved useful for the lower molecular-weight polystyrenes, isochratic combinations of these solvents were next investigated for the 1350M polystyrene. Chromatograms were obtained with the Spherisorb ODS analytical column and 5% THF/95% MeOH, 3% THF, and pure MeOH carrier. The first of these contained too

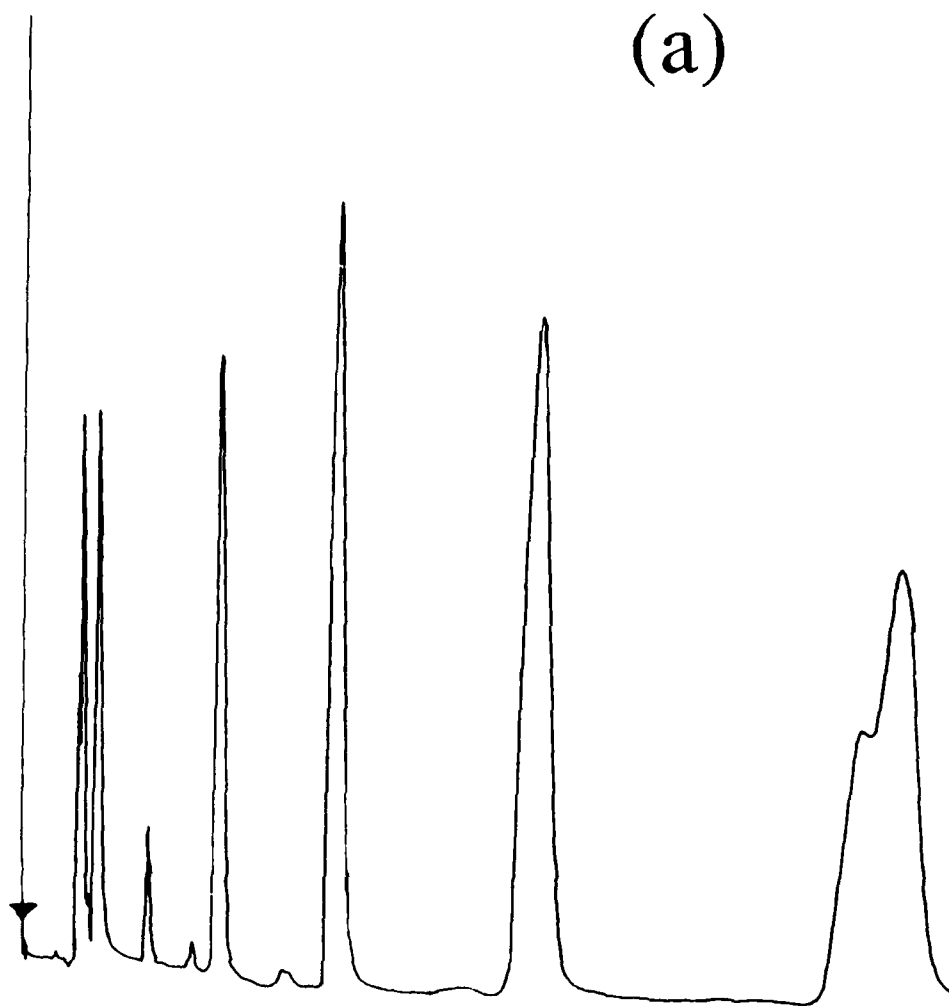
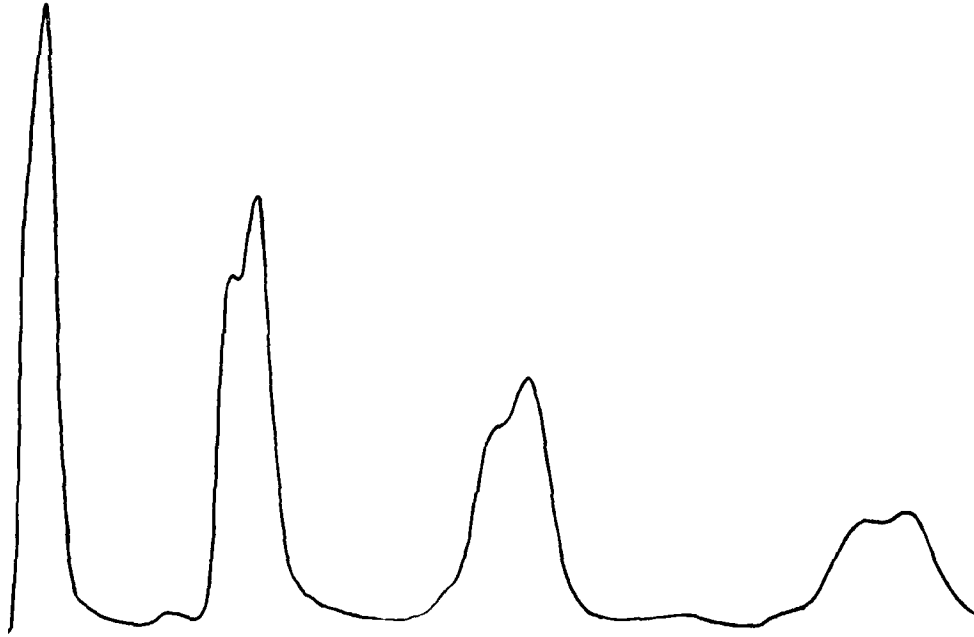
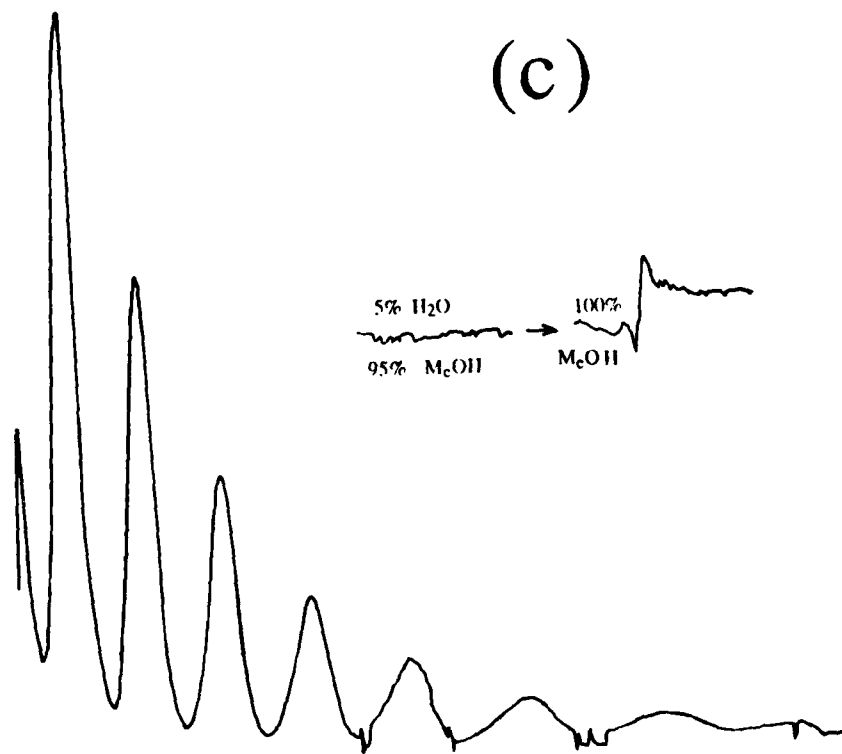


FIGURE 12. Step-change gradient reverse-phase LC₃ separation of 680M polystyrene. Column: 25-cm Spherisorb C₁₈ 5- μ m; flow rate: 2 cm³ min⁻¹; chart speed: 4 min cm⁻¹; 25°C column temperature; 10-mm³ injection-loop volume. Mobile-phase program: (a) 10% H₂O/90% MeOH, then to (b) 5% H₂O/95% MeOH, then to (c) pure MeOH.

(b)



(c)



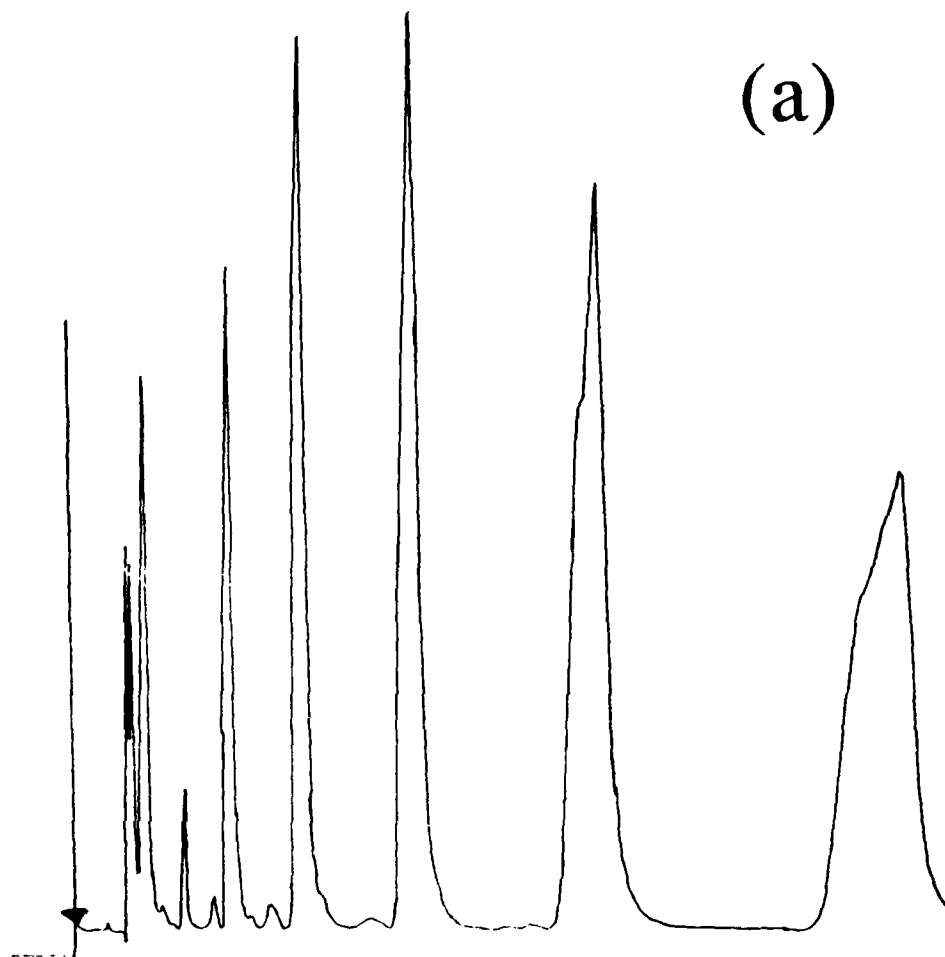
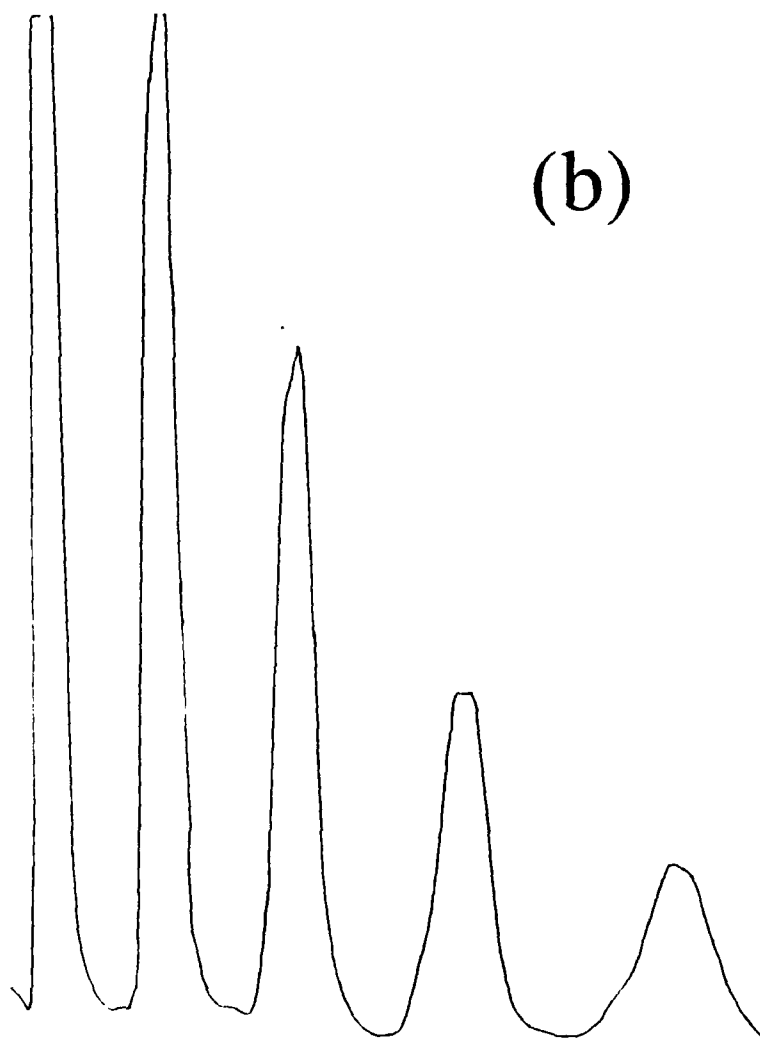
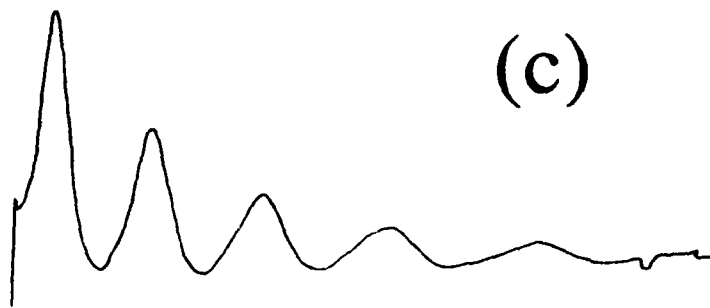


FIGURE 13. Step-gradient reverse-phase LC separation of 680M polystyrene. Column and conditions as in Figure 12. Mobile-phase program: (a) 7.5% H₂O/92.5% MeOH, then to (b) 2.5% H₂O/97.5% MeOH, then to (c) pure MeOH.





much of the "good" solvent (THF); the trace was nonetheless useful in showing that this polystyrene contains fully 22 peaks. Better separation of at least the first 17 of these was obtained by reducing the amount of THF, with even better separation still without THF at all. Clearly, however, gradient elution was called for, a series of which were run. However, none of those tried were satisfactory in terms of baseline resolution of all peaks in a reasonable period of time.

Solvent Optimization for 1770M Polystyrene. Despite the obvious increase in difficulty of separation of polystyrenes on passing from 680M to 1350M, the characteristics of the 1770M material were nevertheless evaluated. Based upon the results obtained as described above, the analytical-scale separation was attempted with a mobile phase of pure MeOH. The result was that not only were fewer peaks visible than was the case with 1350M, but the trace failed to return to the original baseline. That is, there were apparent very many peaks toward the end of the chromatogram that were manifested only as a large "hump".

Solvent Optimization for 2550M Polystyrene. Attempts made at solvent optimization for the separation of this polymer were only partially successful due, in part, to the difficulties mentioned above. There were an extraordinary number of peaks present in the sample, only a fraction of which could be made visible even by severe changes in the mobile-phase flow rate. Another difficulty encountered was that material remaining on the column caused a large increase in the pressure drop. The Spherisorb column in fact became plugged after only three injections of analytical amounts of the 2550M polystyrene, which necessitated thorough flushing with acetone. (It was found that fully 150 cm³ of this solvent had to be passed through the analytical column before the pressure drop returned to normal.)

Limitations of Reverse-Phase LC for Fractionation of Polystyrene Homologs. Much has been made in the literature over the years regarding the mechanism(s) of what has heretofore been assumed to be fractional-solution separations carried out with reverse-phase (i.e., ODS silica) LC of polystyrenes. It was in fact demonstrated repeatedly in this work that the solubility of polystyrenes above ca. 1500 Da or so in mixtures of MeOH with THF is an "all-or-nothing" phenomenon, that is, the polymers are either freely soluble, or are completely insoluble, in the solvent, depending upon its composition. Further, the break-point of solubility appears to be very sharply defined for higher molecular-weight materials, much like the titration curve of a strong acid with a strong base where the slope of the curve at the equivalence point is infinite.

An interesting ancillary aspect of the "all-or-nothing" solubility phenomenon is that reverse-phase LC packings are normally assumed not to interact with polystyrene solutes. If this were indeed the case, the fan-shaped distribution of peaks found in this work (due to molecular-weight homologs) should also be observed with a column containing bare glass beads. Moreover, exactly the same mobile-phase composition as used with the ODS silica column should yield precisely the same chromatogram. Such a column was therefore fabricated as described in the Experimental Section. The chromatogram of 580M PL polystyrene (acetone solvent) found with this column with pure MeOH mobile phase bore no resemblance to that obtained with pure MeOH and the Spherisorb ODS column, that is, the reverse-phase column provided separations on some basis other than (or in addition to) fractional solution. This result was unexpected since, as noted above, conventional wisdom has it that reverse-phase columns will separate polystyrenes of at least low molecular weight based solely on their solubility. However, the results of this portion of the work demonstrated clearly that this is not so. Nor can it be claimed that a slightly poorer mobile phase might yield the desired result (required, e.g., because of the lower capacity of the glass-bead column), as was verified by chromatograms obtained with 7.5% H₂O/92.5% MeOH and 15% H₂O/85% MeOH mobile phases. Thus, the mechanism(s) of the separations process of polystyrene homologs with reverse-phase packings remains open to question at this time.

Semi-Preparative-Scale Reverse-Phase LC Fractionation of Polystyrene Homologs. Having at this point found what appeared to be the appropriate solvent conditions for at least small-scale fractionation and collection of the lower molecular-weight polystyrenes, the semi-preparative (9.4-mm i.d. by 50 cm in length) reverse-phase column was assembled into an LC system. It was then evaluated with regard to 526M, 680M, and 946M polystyrenes, the results of which are reported in turn below.

Fractionation of 526M Polystyrene. Shown in Figure 14 is the fractional-solution chromatogram of 526M obtained with 60% THF/H₂O. The flow rate was 10 cm³ min⁻¹ (the manufacturer's recommended optimum flow was 3 cm³ min⁻¹) and the loop size was 150 mm³. The solvent system was not quite good enough to produce baseline resolution; fractions 1-17 were collected nevertheless, as indicated on the chromatogram. Fractions 5-7 were then worked up by evaporation to dryness, followed by solution of the residue (a few milligrams) in benzene, washing this twice with water, and then concentrating the benzene layer to less than a cm³. (It was found subsequently that solution of the polystyrene residues, followed by washings, was facilitated if methylene chloride were substituted for benzene. This was due to partial emulsion formation of benzene/water mixtures.) Reinjection of the combined solutions containing fractions 5-7 produced the chromatogram shown in Figure 15 where, as expected, the major peak was not as pure as was desired. Even so, the major peak was clearly isolated from the rest of 526M polystyrene, that is, the fraction collection/isolation procedures appeared to be satisfactory, and required only that each peak be cut closer to its maximum.

Another interesting aspect of fraction separation was also evaluated, namely, alteration of the mobile phase during the course of a run. For example, 526M was run at a faster chart speed and with 65% THF/H₂O initially as the mobile phase. Then, during the run, the mobile phase was changed to 55%, thus slowing down the elution times but also, providing better separation of the next isomer. The elution times were next speeded up again by changing to 60% THF/H₂O. Thus, virtually any isomer, at least of 526M, could be isolated during the course of a run for collection.

Fractionation of 680M Polystyrene. Semi-preparative scale fractional solution of the 680M polystyrene standard was attempted next. For this portion of the work, a solution of 17.65 mg cm⁻³ was made. Separations were carried out with a 10-mm³ loop and with 65% THF/H₂O mobile phase. The flow rate was also adjusted to 3 cm³ min⁻¹ so as to correspond more closely to the van Deemter optimum for the column. The results were disappointing: only a single peak was found. Moreover, there was very little (if any) separation of the isomers. The mobile phase was therefore changed to 80%, and eventually to 75% THF/H₂O. The latter separation was considered good enough to attempt the use of the 150-mm³ loop. The resultant chromatogram revealed that the resolution had deteriorated badly, that is, the column was overloaded sufficiently to degrade almost completely the separation. Verification of this was also obtained with a repeat run of 680M with the 10-mm³ loop. As a result, the mobile-phase composition was again altered, this time to 70% THF. The chromatograms obtained with the 150-mm³ and 10-mm³ loops exhibited the same phenomenon, namely, 150-mm³ injection volumes comprising as little as 18 mg cm⁻³ of sample overloaded the column. The situation only worsened with polystyrene standards of higher molecular weight.

Fractionation of 946M Polystyrene. The trace obtained for 946M polystyrene as a concentrate from the 150-mm³ loop was very poor; dilution of the sample by a factor of 20 improved matters considerably, however: the resolution in this case was nearly baseline. It was found once again, therefore, that the semi-preparative column was overloaded with ca. 10 mg of sample; moreover, the sample in these instances consisted of at least 10 isomers. Thus, the overload level for each amounted to ca. 1 mg. This was a very unsatisfactory result, since it was the intent of this portion of the work to collect gram-amounts of these materials. A much larger preparative-scale LC column system was therefore called for.

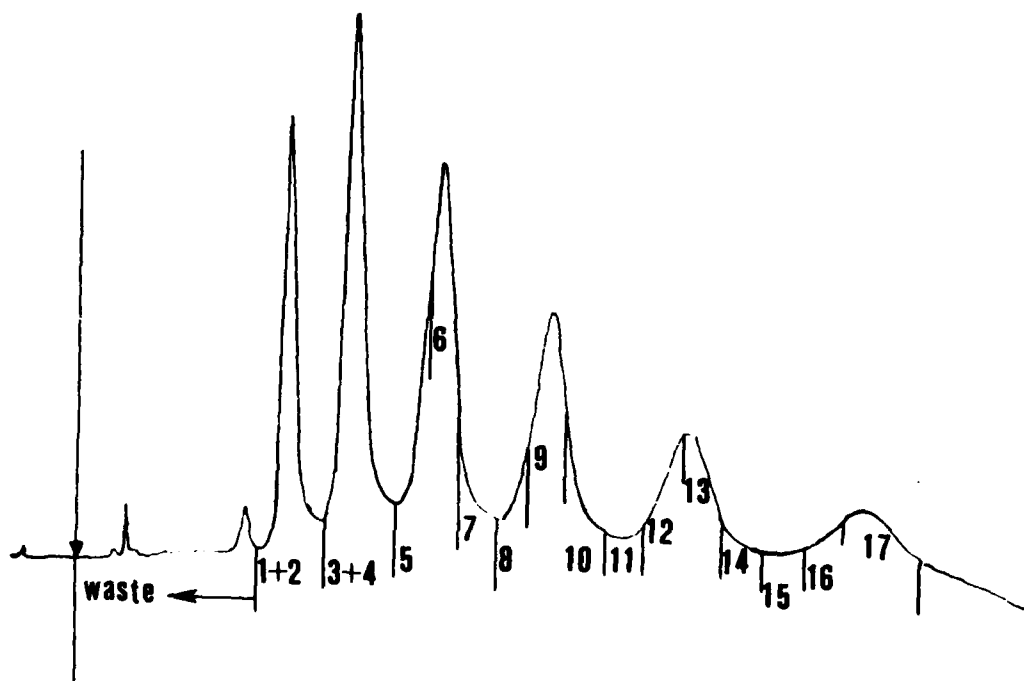


FIGURE 14. Reverse-phase LC separation of 526M polystyrene. Column: 50-cm Partisil C₁₈, 10- μ m; flow rate: 10 cm³ min⁻¹; chart speed: 2 min cm⁻¹; room temperature; 150-mm³ injection-loop volume. Mobile phase: 60% v/v THF/H₂O isocratic.

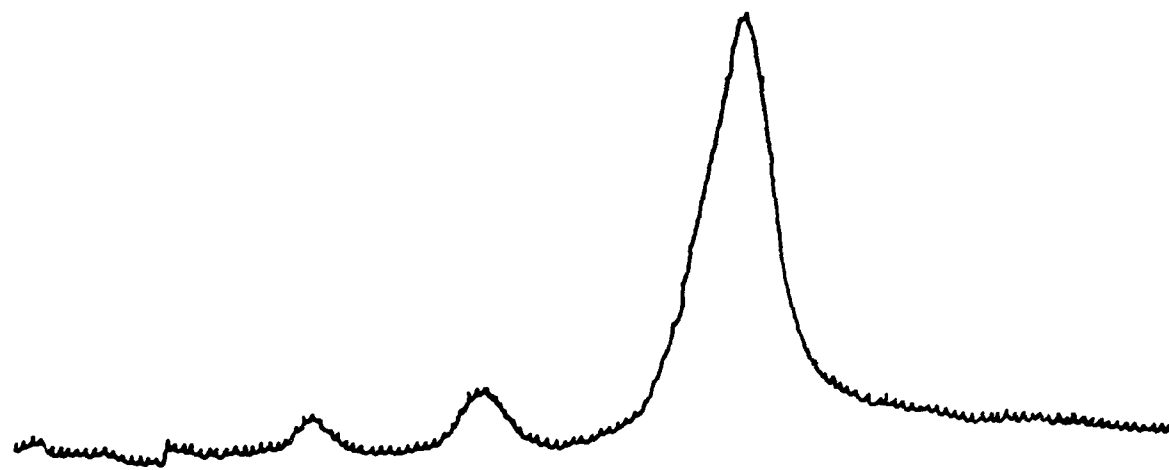


FIGURE 15. As in Figure 14; reinjection of fractions 5-7. Chart speed: 1 min cm⁻¹.

Preparative-Scale Reverse-Phase LC Fractionation of Polystyrene Homologs. At roughly this point in the Contract work a preparative-scale column was obtained. It was fitted, first, with a 0.5-cm³ loop. The first polystyrene used with it was 526M; resolution of the homologs of a concentrated solution (ca. 0.5 g cm⁻³) of this standard (acetone solvent) was not quite baseline but, given the very large sample size, was satisfactory, Figure 16 presents the chromatogram. Thus, the column was fitted next with a 2.5-cm³ loop in order to try at least one injection of the remaining amount of 526M polystyrene. The peaks (ca. 0.2 g each) were somewhat distorted; nevertheless, the scale-up from analytical to gram-scale preparative fractional solution had clearly been achieved, that is, preparative-scale fractional solution of the polystyrenes standards was to hand.

The preparative-scale column mobile phase was changed to pure methanol at this point, since it had previously proved useful on both the analytical- as well as semi-preparative scales. Also, having exhausted the supply of 526M polystyrene, the first polystyrene to be fractionated repetitively on the preparative-scale was PL 580M. Ultimately, it was in fact found that this material contained homologs up to 1618 Da, that is, the molecular-weight range of interest in this portion of the work.

A representative chromatogram of the 40 or so obtained for 580M polystyrene with pure MeOH mobile phase (2.5-cm³ loop; acetone solvent) is presented in Figure 17. As shown, seven fractions were collected, where the last consisted of an acetone wash of the column to prevent the buildup of noneluted material. There is of course some overlap of the peaks; however, while the later-collected fractions contained most of the homologs, the earliest-collected fractions were comprised in the main of at most two or three homologs. That is, the earliest fractions were freed of the later-eluting substances, as confirmed by analytical characterization of the materials (see later.)

Work-Up of Preparative Fractions. Each of the collected fractions except the second was cloudy, and all varied from light yellow to light brown in color, that is, appeared to contain some impurities. It was thought initially that these might have arisen as a result of concentrating, literally, gallons of mobile phase for each (rotary evaporation; 60°C). However, it might also have been that the discoloration arose from passage of the samples through the UV beam of the LC detector with the result of formation of semiquinones along the polystyrene backbone. This latter possibility would seem to be remote, however, in view of the fact that the flow rate was ca. 28 cm³ min⁻¹ and the detector cell volume was only 8 mm³ i.e., the time of exposure of the polymers to the UV beam amounted to less than a hundredth of a second. In any event, further clean-up was called for.

The first procedure used to remove the discoloration was treatment with activated charcoal. Accordingly, fraction no. 7 was taken up in benzene, activated charcoal added, the solution filtered, and the benzene removed by evacuation. This was completely ineffective. Next, the fraction was taken up in chloroform, the solution washed with water, and then dried over magnesium sulfate. Once again, no change was observed in the polymer color. Washing the neat fraction with 50:50 water:methanol was also found to fail to remove the coloration. A small amount of LiChroprep Si60 column silica was then placed in a funnel fitted with a fine glass frit and the fraction in chloroform eluted through it. The eluent was initially colorless, but several yellow-to-brown bands could be seen eluting down the (short) LC column. However, for the most part, these coeluted with the polystyrene, leaving behind a small amount of very dark brown material sorbed onto the silica. The polystyrene recovered at this point was yellow, having been separated from the dark-brown materials.

The latter were flushed off of the silica, and were found to be soluble in acetone, methylene chloride, and methanol; but were insoluble in hexane and water. Accordingly, a 3.5-cm silica LC column was prepared from a standard laboratory buret and the polystyrene eluted through it with pure hexane. The first fraction collected was clear and

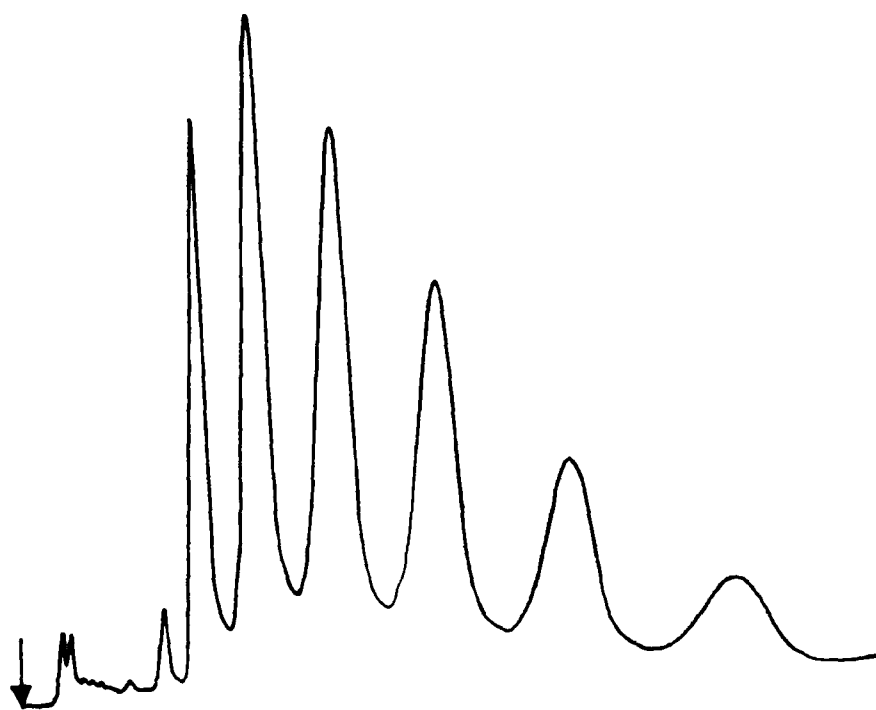


FIGURE 16. Reverse-phase LC separation of 526M polystyrene. Column; 30-cm Partisil C₁₈ 10- μ m; flow rate: 27.7 cm³ min⁻¹; chart speed: 4 min cm⁻¹; 0.5-cm³ injection-loop volume. Mobile phase: 55% v/v THF/H₂O isocratic.

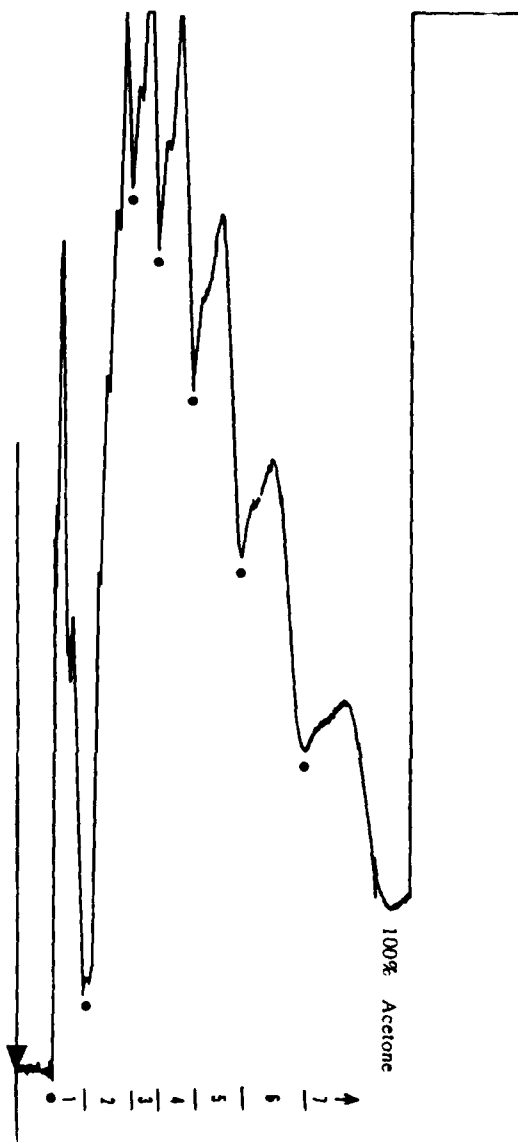


FIGURE 17. Isochratic reverse-phase preparative LC separation of 580M polystyrene. Column: 2.54 by 30-cm Partisil C₁₈ 10- μ m; flow rate: 27.7 cm³ min⁻¹; chart speed: 4 min cm⁻¹; room temperature; 2.5-cm³ injection-loop volume. Mobile phase: pure MeOH. Detector: UV at 222 nm (a) at 2.0 AUFS and (b) at 0.5 AUFS.

and colorless (200 cm³ hexane), but amounted only to ca. 70 mg, i.e., less than 10% of the total weight of fraction no. 7. An additional 280 cm³ hexane recovered approximately 20 mg more polymer, which was also colorless. In addition, the column clearly exhibited three distinctly-colored bands, these being light brown, dark yellow, and light yellow, the former being retained the more strongly. At this point, and in order to recover all of fraction no. 7, the small silica column was washed thoroughly with hexane + ca. 1% THF, and a new 3.5-cm silica column was constructed. Polystyrene fraction no. 7 was eluted from this so long as the dark-brown and dark-yellow-colored bands were seen to remain on the column. The procedure was then repeated once more with a fresh 3.5-cm column. All washings were evaporated at this point, resulting in the recovery of virtually all of fraction no. 7 which, now, was pale yellow in color.

A 20-cm silica column was fabricated next, and the entire amount of fraction no. 7 eluted through it with 250 cm³ of the hexane-THF mixture. Two distinctly-yellow bands were seen during the course of elution which, however, coeluted with the polystyrene. The additional washing of this longer column, first with more hexane-THF and then with acetone, also produced minute quantities of two more yellow-to-brown residues.

Because the amounts of impurities in the fractions were found to be very small (much less than 1%), the remaining fractions 1-6 were simply taken up in chloroform and extracted only with water. The chloroform solutions were then dried over magnesium sulfate and taken to dryness.

Analytical-Scale Reverse-Phase LC Characterization of Preparative Fractions. Following clean-up, each of the preparative fractions was characterized by analytical-scale liquid chromatography (Spherisorb ODS 5-u). Figure 18 provides the trace found for 580M (acetone solvent) prior to fractionation. Here, the peaks are numbered 1 through 12. Figure 19 then shows typical results for polystyrene fraction nos. 1-4; while those for fraction nos. 5-7 are presented in Figure 20.

The first fraction appeared at first glance to be very clean indeed, since the chromatogram showed only a trace of peaks 1 and 3. However, only a very small amount (ca. 50 mg) of this material was actually recovered, and what material was isolated was a dark brown color. This sample was therefore considered to be an impurity. The second fraction showed the presence of peaks 2-4 in about equal amounts. There was also a trace of peaks 1 and 5. In excess of a gram of this fraction was obtained. Moreover, it was a clear liquid, although is somewhat yellow in color. It was somewhat more viscous than the first fraction. The third fraction also contained three peaks, namely, 3-5, with a noticeable amount of peak 2 as well. This fraction was pale brown, cloudy and, notably, substantially more viscous than fraction no. 2. The fourth fraction, slightly less than a gram, contained peaks 2 through 6, although was comprised mostly of 4-6. It, like the third fraction, was pale brown and cloudy, and was very viscous. The fifth fraction, about 2/3 of a gram, contained one more peak than the previous fraction, that is, 2 through 7. It was also a darker brown than the previous two, was more viscous, and was cloudy. The sixth fraction, about half a gram, contained peaks 2 through 8, i.e., one more than its predecessor. It had about the same color and viscosity as the fifth fraction. The seventh fraction, about 2/3 of a gram, contained all 12 peaks present in the polymer. It was also as viscous as the original polymer, but was cloudy and lemon-yellow in color.

Analytical-Scale Reverse-Phase LC Fractionation of Polybutadiene Homologs. As a prelude to attempts at the reverse-phase LC fractionation of HTPB, speciation of the model prepolymer polybutadiene (PBD) was investigated. PBD was thought to represent a material of difficulty intermediate between polystyrene and HTPB, insofar as the former is a relatively simple straight-chain hydrocarbon that presumably is comprised only of conjugated diene groups, i.e., similar to HTPB except for the hydroxyl content of the latter.

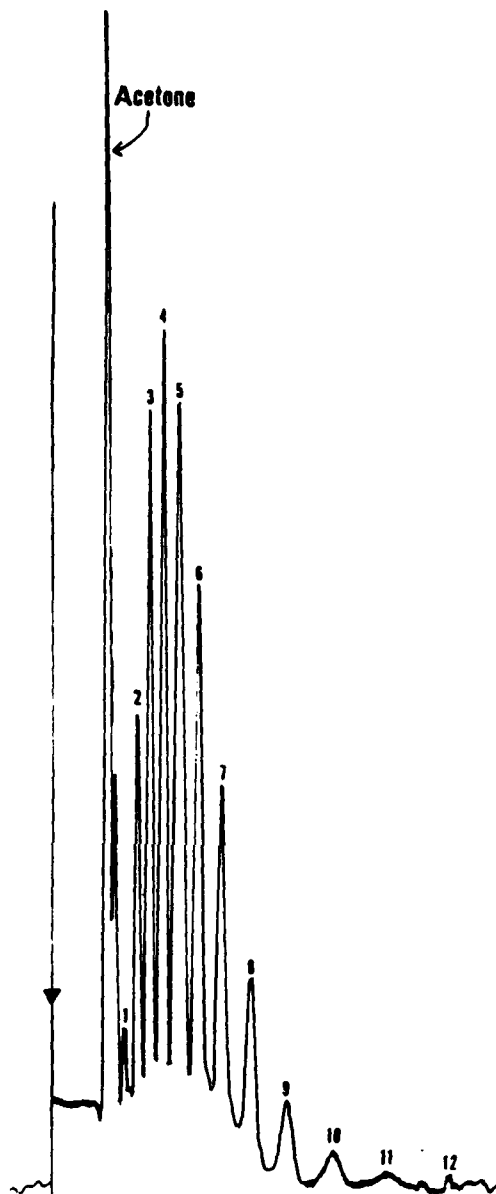


FIGURE 18. Isochratic reverse-phase LC of 580M polystyrene. Column: 25 cm by 4.6-mm i.d., 5- μ m Spherisorb ODS. UV detection at 222 nm; (a) 2.0 AUFS and (b) 1.0 AUFS; 10- mm^3 sample loop; flow rate of 1 $\text{cm}^3 \text{min}^{-1}$; room temperature; chart speed of 2 min cm^{-1} . Mobile phase: 100% methanol.

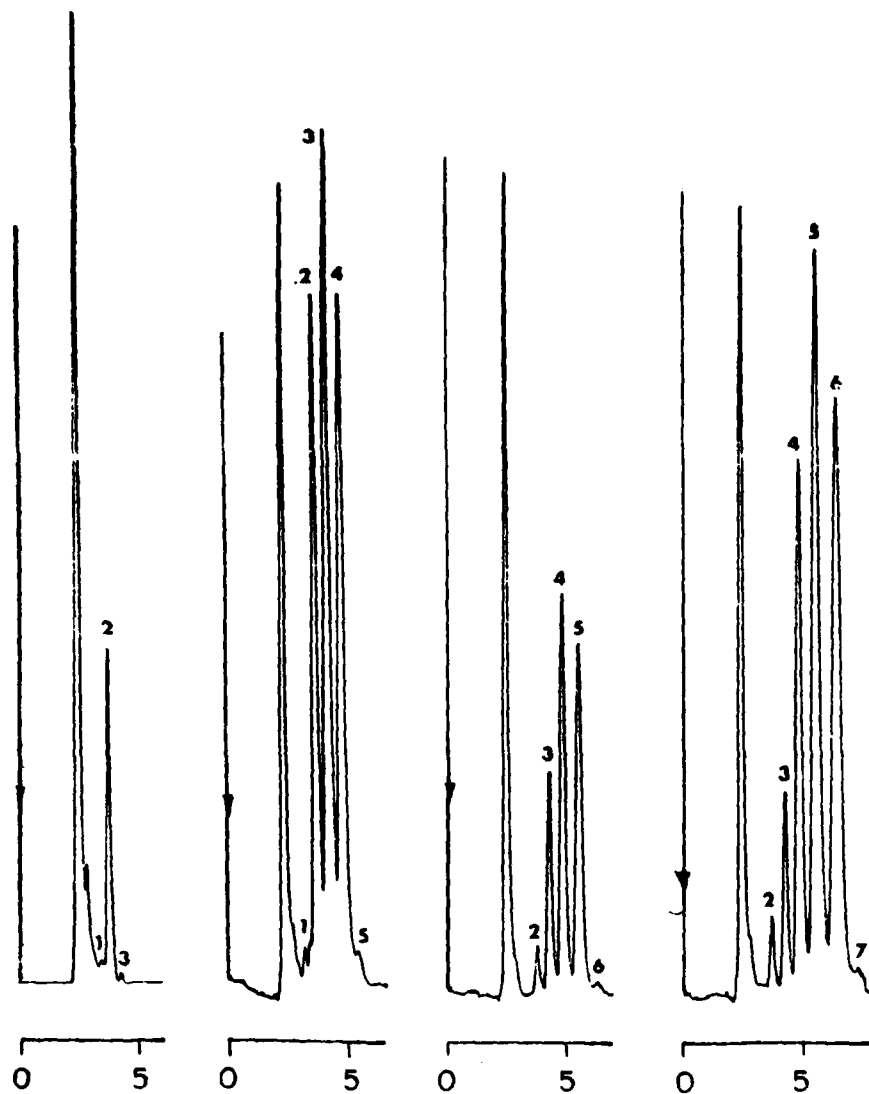


FIGURE 19. Isochratic reverse-phase analytical chromatograms of 580M polystyrene fractions 1-4. Column and conditions as in Figure 18.

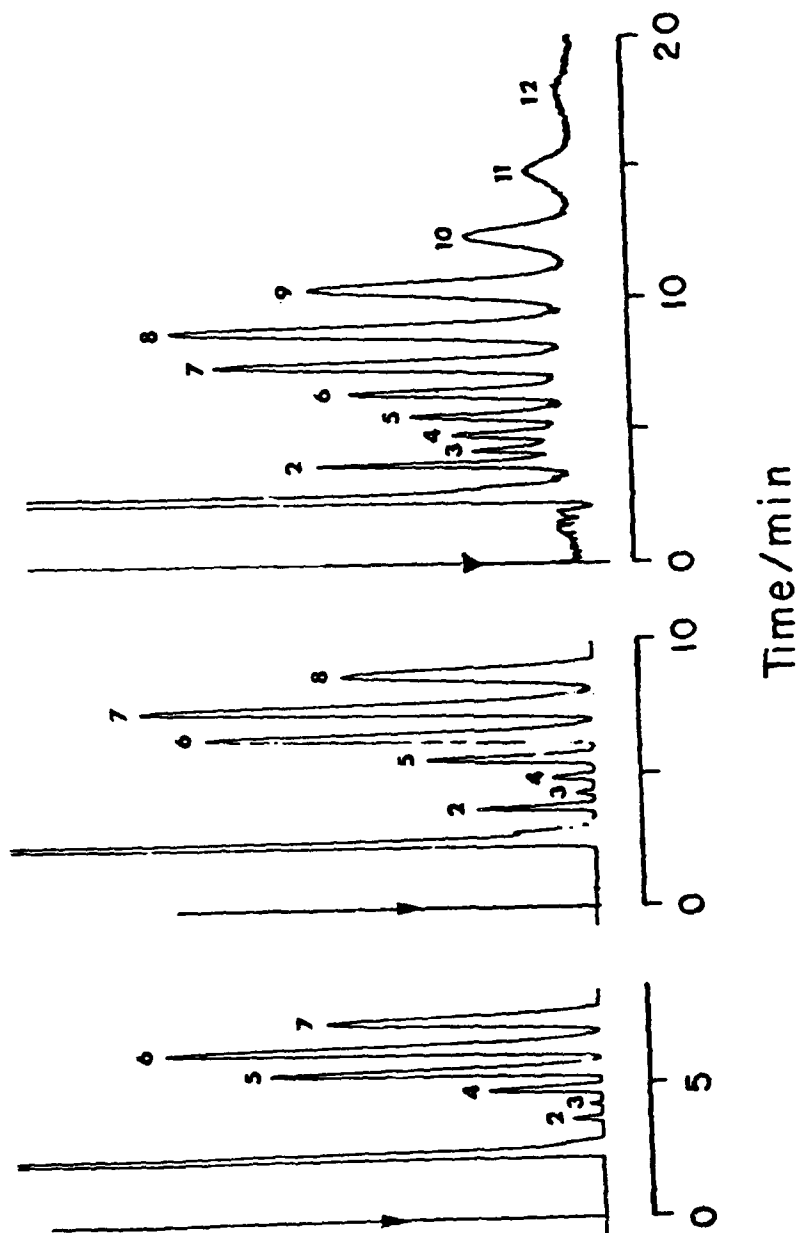


FIGURE 20. Isochratic reverse-phase analytical chromatograms of 580M polystyrene fractions 5-7. Column and conditions as in Figure 18.

Fractionation of 500M Polybutadiene. The first attempt at reverse-phase LC fractionation of this sample (pure MeOH the mobile phase; UV detection at 240 nm) resulted in PBD eluting with THF peak. However, the chromatogram obtained with 10% H₂O/90% MeOH gratifyingly showed three sets of peaks where each set appeared in addition to contain several components. Better separation of the sets of peaks was found with 20% H₂O/80% MeOH, as shown in Figure 21: the first band shows a main peak bracketed by two partially-resolved shoulders, while band no. 2 shows at least 5 peaks. The third band still shows only two peaks (the low broad peaks between set nos. 2 and 3 are spurious, as they could not be repeated). The results found for band nos. 1 and 2 with 30% H₂O/70% MeOH mobile phase were little improved over that shown in Figure 21.

The above results were far from satisfactory insofar as speciation of what were presumed to be polybutadiene homologs was incomplete. That is, further optimization was indicated in order to improve the separations (see below); even so, the chromatograms firmly established that polybutadienes (as with polystyrenes) of low molecular weight interact with (hence could be separated by) reverse-phase LC stationary phases. However, the results also indicated that above some limit of molecular weight the retention mechanism for PBD reverts to one analogous to that found for the polystyrenes, i.e., precipitation/critical solution. Thus, beyond this limit, the LC stationary phase ceases to become of any importance and the packing could just as simply be replaced by one of glass beads with, however, no separation of homologs.

Several chromatograms were run of PBD of 500 Da nominal molecular weight with an optimized gradient elution, where the mobile phase was programmed from 75%MeOH/25% H₂O to 100% MeOH v/v at 1% min⁻¹. Four major bands were clearly visible, the first, second, and fourth being of about equal area, with the third being about one-third the area of the others. Each of the peaks was collected, and each of the fractions was combined with those obtained from subsequent runs and held for further examination by mass spectrometry.

Fractionation of 1000M PBD. It was assumed at the outset that separation of the 1000M sample of PBD would prove somewhat more difficult than that of the 500M polymer. This was indeed confirmed to be the case. Chromatograms obtained for pure THF solvent with pure THF mobile phase for 1000M PBD resulted in no separation of the polymer. Several gradients were then employed, e.g., mobile phase of 85% MeOH/15% H₂O to 100% MeOH at 1% min⁻¹, 80% MeOH/20% H₂O to 100% MeOH at the same gradient rate of change, and so forth. Several shoulders were evident in some of these, however, it was ultimately found that isocratic elution was the best suited for analytical-scale fraction collection, where the optimal mobile phase was 80% MeOH/20% H₂O. A representative chromatogram of the several of those run is shown in Figure 22, where the fractions collected are indicated as before by the solid circles connected with straight lines.

Interestingly enough, the chromatograms of 500M and 1000M PBD were very similar. For example, both exhibited four major bands; cf. Figures 21 and 22. The respective areas under the peaks were also roughly equivalent, even though the average molecular weight of the latter sample was, presumably, double that of the former.

Analytical-Scale Reverse-Phase LC Fractionation of HTPB Homologs. Overall, it had been found at this point that 500M and 1000M PBD could indeed be separated by reverse-phase LC (although the identities of the various fractions had not been established; see Mass Spectrometry Section). Thus, study of the LC separation of molecular-weight homologs of HTPB was undertaken next.

Methanol/Tetrahydrofuran Mobile Phases (RI Detection). The HTPB band in this Laboratory was insoluble in methanol, yet very soluble in THF. Accordingly, the first set of combinations of mobile phases to be evaluated comprised MeOH + THF, proceeding from high concentrations of the latter to high concentrations of the former. Chromato-

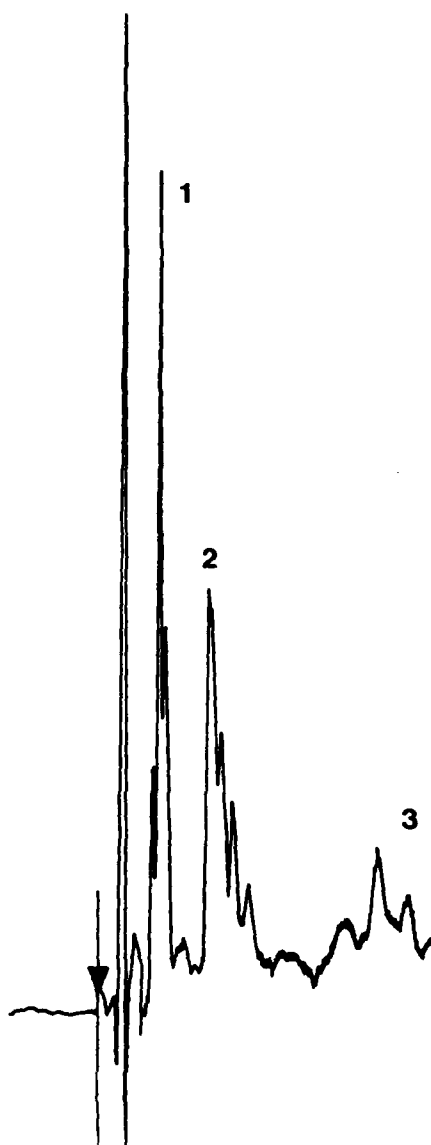


FIGURE 21. Isochratic reverse-phase analytical LC of Goodyear PBD, 500 Da. Column: 25 cm by 4.6-mm i.d. 5- μ m Spherisorb ODS; room temperature; 10- mm^3 injection loop; UV detection at 240 nm; chart speed: 2 min cm^{-1} . Mobile phase: 20% H_2O /80% MeOH at 4 $\text{cm}^3 \text{min}^{-1}$.

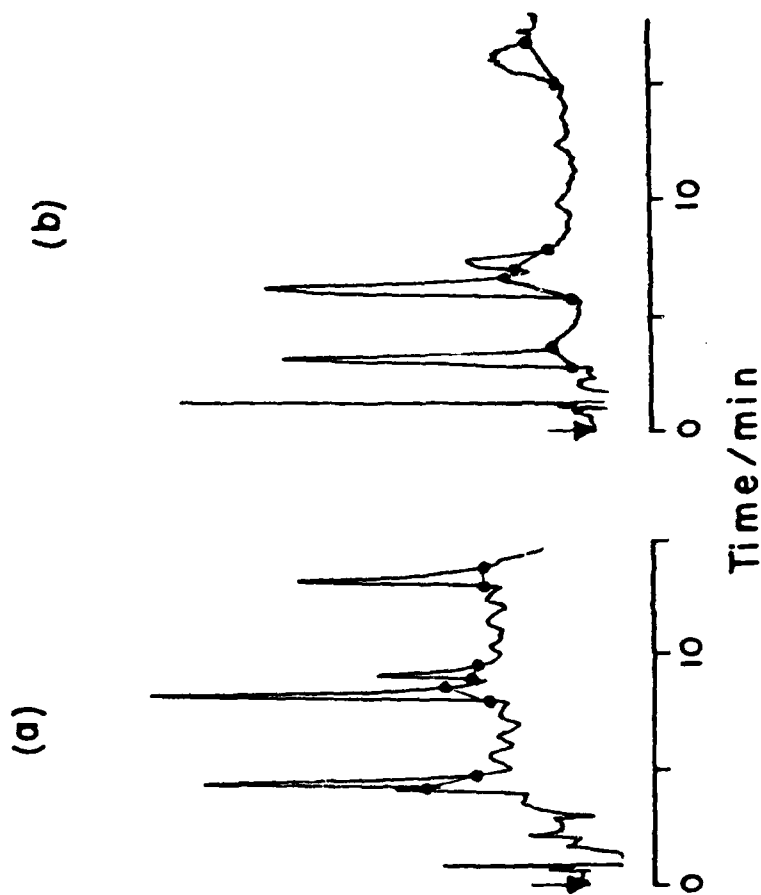


FIGURE 22. Repeat runs of analytical-scale reverse-phase J.C fractionation of 1000M PBD. Column: 25-cm Spherisorb ODS 5- μm ; injector: Rheodyne valve with 10-mm³ loop; detector: UV at 240 nm (0.5 AUPS); chart speed: 2 min cm⁻¹. Mobile phase: 80% MeOH/25% H₂O at 4 cm³ min⁻¹ flow rate. Dots indicate fractions collected.

grams obtained for HTPB with a mobile phase of 1% MeOH/99% THF (v/v) with the refractive index detector, as well as those for pure THF, showed that the HTPB eluted before the THF (solvent) peak. That is, HTPB was less strongly retained by the column than was THF. The MeOH content of the mobile phase was then increased to 5% v/v and the flow rate returned to $4 \text{ cm}^3 \text{ min}^{-1}$. The resultant chromatograms for pure THF, HTPB + THF, and for a diluted aliquot of the HTPB solution again left no doubt that HTPB eluted before THF. The methanol content of the mobile phase was next increased successively to 10%, 20%, 25%, 30%, 50%, and 60% in THF. In each case, there was no movement of the HTPB peak. Moreover, in the latter several runs there was evident the eventual disappearance of what HTPB peak was seen, with the appearance of a tail following the THF solvent peak. That is, beyond 30% MeOH the solvent was so poor that only a small fraction of the HTPB eluted, with the remaining amount staying at the head of the column. This was evident on changing the carrier to pure THF, whereupon the accumulated HTPB was found to elute.

Water/Tetrahydrofuran Mobile Phases (RI Detection). Combinations of water/THF mobile phases were evaluated next. The result for pure THF carrier again indicated saw no movement of the HTPB peak from that corresponding to the column dead volume. The LC run was then repeated at a flow rate of $1 \text{ cm}^3 \text{ min}^{-1}$; the result showed that there might in fact have been at least some separation of the HTPB with pure THF mobile phase, although it was entirely unsatisfactory for separations on a preparative scale. Some water was then added to the THF mobile phase; however, the separations achieved were as poor as before, nor did subsequent runs with increasing amounts of water in the carrier show any improvement.

UV Detection. At this point, UV detection of the LC effluent was employed in order to ensure that the apparent lack of separation was indeed extant. A UV spectrum (Cary 17 spectrophotometer) of HTPB in THF showed a band maximum at 240 nm and so, the Varian variable-wavelength UV/Vis LC detector was used at this wavelength. Even so, the chromatogram of HTPB obtained with a mobile phase of 1% H_2O /99% THF was virtually the same as those found previously, that is, virtually all of the polymer eluted with the THF solvent peak. The UV detector did show, however, that a considerable amount of material eluted as a pronounced tail with various combinations of MeOH/THF mobile phases e.g., 55% MeOH, 65% MeOH, and 75% MeOH/25% THF. Once again no movement of the HTPB peak could be discerned, the only evidence of any HTPB being present at all amounting to the peak tail in excess of that observed for an injection of pure THF.

These results were disappointing insofar as no separation of HTPB was found to be possible with the reverse-phase LC system and mobile phases employed. Two additional experiments were therefore carried out at this point. In the first, the mobile phase was adjusted to 1% H_2O /99% THF, and sufficient silver nitrate added to bring its molar concentration to 1 mM. The column was allowed to equilibrate with this mobile phase by passing a total volume of ca. 200 cm^3 through it. The HTPB solution was then chromatographed. There was no change in the retention of the polymer peak, and it eluted just before the THF solvent peak as before. Thus, and despite the dynamic deposition of AgNO_3 onto the column (intended to interact with the polybutadiene double bonds), no change in retention was seen. This indicated that the stationary phase played no role in the elution (or otherwise) of higher molecular-weight HTPB, and that the characteristics of the mobile phase dominated the retention mechanism entirely. Accordingly, a second experiment was performed: the column was rinsed free of silver nitrate with water eluent, followed by returning to a mobile phase of 1% H_2O /99% THF. Then, 1% v/v acetic acid (HOAc) was added the mobile phase, and the HTPB solution chromatographed once more. As in previous runs, the HTPB peak eluted just prior to the THF solvent peak. That is, making the aqueous component of the mobile phase highly unfavorable failed to alter the solubility of the polymer. (It was therefore concluded inter alia that water by itself represented the limit of "poor" solvents.)

Limitations of Reverse-Phase LC for Fractionation of HTPB Homologs. The failure to resolve crude HTPB by reverse-phase LC was analogous to the failure of separation of PS that exceeded a certain molecular weight (ca. 2000 Da), as mentioned in the initial Sections of this Report. As noted earlier, this is a critical molecular-weight phenomenon where, for mixtures of homologs that exceed M^c , the polymer chains cannot not be resolved with reverse-phase LC systems. This was found to be true even if the mixture contained low molecular-weight homologs that were, by themselves, otherwise separable.

A plausible explanation of the phenomenon is as follows: when high molecular-weight oligomers are present, interchain tangling is such that low molecular-weight chains are incorporated into the bulk. In the case of HTPB, the critical molecular weight is expected to be very low indeed, since short-chain incorporation into bulk polymer is greatly facilitated by hydrogen bonding between hydroxyl groups. (This is the source of the extraordinary tensile strength of nylon polymers.) For example, in situations typical of polystyrenes and polybutadienes, long polymer strands can incorporate shorter strands, the bulk material being held together by van der Waals forces and so, can be expected to disentangle as the temperature is increased. Also, if at a given temperature the forces of attraction of the reverse-phase LC packing for the short strands are less than those holding the short strands to the long, the former will elute from an LC system with the polymer bulk. That is, no separation will be achieved. On the other hand, if the polymer bulk were to be composed of nothing but short chains, each held to the rest by weak van der Waals forces, there is then the possibility that the net attraction will break apart the bulk, resulting in the separation of the individual chains. Thus, with polystyrenes and polybutadienes, low molecular-weight fractions were in fact separable by homolog number. However, mixtures of low- and high-molecular-weight homologs of polystyrenes gave no separation of the low molecular-weight constituents.

In contrast, a number of short chains comprising bulk HTPB are likely held together quite strongly by hydrogen bonds extant between chains. Disentanglement of these would obviously require much higher temperature than discussed above. However, increased temperature may in addition bring about chemical change and so, will most likely not be useful. Also, the separation of individual chains will not occur with C_{18} reverse-phase LC packings, since the forces of attraction of the packing for an individual chain are much less than the strength of the hydrogen bonds holding the chain to bulk polymer. Moreover, this can be expected to be the case even with very short chains of HTPB.

An obvious way to overcome this is silylation of the hydroxyl groups. An efficacious reagent for doing so is hexamethyldisilazane (HMDS), which has been used for these purposes for many years in gas chromatography. Moreover, silylation with HMDS is particularly convenient in that all that is required is refluxing with ca. 5% v/v of the reagent in toluene solvent for ca. 4-8 h. The only by-product is ammonia and, thus, work-up of the desired end-product amounts simply to stripping off the solvent e.g., by rotary evaporation. Accordingly, a portion of low molecular-weight HTPB was silylated. Thus, approximately 1 g of HTPB was taken up in 100 cm³ of a solution containing 5% v/v HMDS in toluene. The mixture was then allowed to reflux for 4 hr in a round-bottom flask equipped with a reflux condenser, which was protected from moisture by attachment of a drying tube containing calcium chloride. The solvent and HMDS were then removed by rotary evaporation, and the sample dried completely by insertion into a vacuum line of 10⁻³ torr. The product was clear and straw-colored.

A representative IR spectrum of underivatized HTPB clearly showed hydrogen-bonded OH groups at ca. 3300-3400 cm⁻¹, while the remainder of the spectrum was as might be expected. There was, however, some small carbonyl content, as indicated by a band at 1650 cm⁻¹. In the IR spectrum of derivatized HTPB, the OH stretch band had nearly disappeared. Also, several new bands appeared. These were due to Si-CH₃ stretching (1250 cm⁻¹); Si-O-R stretching (1090 cm⁻¹); and Si-CH₃ deformations (840-880 cm⁻¹). Thus, the silylation procedure appeared to have been somewhat successful in derivatizing

the majority of available hydroxyl. Even so, the synthesis was repeated at this point with fresh reactants and HTPB, where the solution was allowed to reflux for 24 h.

Reverse-phase liquid chromatography of the apparent derivatized HTPB was taken up at this point. Chromatograms of 500M PBD were taken first to determine the general behavior of this material, where the mobile phase was a gradient of 70% MeOH/30% H₂O to 100% MeOH at 2% min⁻¹. The chromatogram of derivatized HTPB was then taken under the same gradient. There was clearly a very substantial difference between the two patterns: the PBD exhibited the four major bands described earlier; while the HTPB showed only two major peaks with several smaller bands. Also, there was a noticeable broad band that might well have contained several unresolved species.

The results were in any event considered to be suspect, since subsequent infrared spectra showed that derivatization was not complete. Thus, the fully-derivatized material was chromatographed with the reverse-phase system under a slightly less-steep gradient. The chromatogram was obtained with a mobile phase of 50% MeOH/50% H₂O to 100% MeOH at 2% min⁻¹. There were apparent several large bands, including one off-scale peak that contained the majority of the total peak area, with several smaller bands also visible. Moreover, the pattern was roughly the same as that found previously: the first large peak of the partially-derivatized material was resolved into two bands, while the second large peak corresponded to the third peak in the latter. However, the fourth large (off-scale) peak was absent. This might have been due to underivatized material not eluted from the column in the first place. That is, the large peak might have been due to fully-derivatized HTPB, whereas partially-derivatized HTPB remained on the column and was only eluted (but not detected) when it was flushed (as was done routinely between runs) with THF. In any event, derivatization of the HTPB did indeed give a material that presented a unique pattern when chromatographed by reverse-phase LC.

Preparative-Scale Bulk Fractional-Solution Fractionation of HTPB. Because of the inherent difficulties, let alone ambiguities, noted above in the LC fractionation of HTPB, bulk-scale solvent solution was used at this point, as described in the Experimental Section. Thus, 4 g of the low molecular-weight fraction of HTPB was obtained. The material was then examined by GPC and LC.

GPC Characterization of Fractionated HTPB. Gel-permeation chromatograms of crude (i.e., unfractionated) HTPB were taken first with the PL-GEL column. [The solution was made as dilute as possible, which required high (0.1 AUFS) detector sensitivity; thus, the baseline noise was appreciable.] First, there was a very sharp rise on the left side of the peak, which corresponded roughly to the exclusion limit of the column. Secondly, a sharp negative peak was observed on the main-peak tail, which might have been due to stabilizers. This was reproducible, as demonstrated in chromatograms that were run at one-fifth the sensitivity. Taken next for comparison was the GPC trace of polybutadiene (PBD) of 500 Da. The peak exhibited several shoulders, which corresponded to the groups that were fully resolved by reverse-phase LC as described earlier. GPC traces were also obtained for the fractions obtained with 5% THF/95% MeOH, 10% THF/90% MeOH, and 20% THF/80% MeOH fractions; each fraction was chromatographed twice in order to ensure that they were reproducible. The results showed that the solvent-solution fractionation technique was successful in cutting the crude HTPB such that the resultant material ranged in molecular weight roughly from 1000-3000 Da. Also, the GPC traces showed little difference between the overall peak positions and symmetry of the 5%, 10%, and 20% fractions. However, there was a shoulder peak visible in the 5% fraction near the elution point of PBD. This became substantially larger in the 10% fraction, and larger still in the 20% fraction. Samples were in any event collected for further characterization.

Analytical-Scale Reverse-Phase LC Characterization of Fractionated HTPB. Having cut the low molecular-weight portion of the HTPB sample, the separation of homologs

was attempted once more by reverse-phase liquid chromatography. The column was as usual packed with 5- μ m Spherisorb ODS, while the mobile-phase combinations were THF ("good" solvent) + MeOH ("poor" solvent).

Chromatograms were taken initially of the 10% fraction with pure THF mobile phase at detector settings of 1 and 0.5 AUFS. There was no separation from pure THF, since the mobile phase was far too "good" a solvent for the HTPB. That is, some methanol was required in the carrier in order to reduce the solvent "strength". The chromatograms obtained for the 10% fraction with a mobile phase of 45% THF + 55% MeOH v/v with detector settings of 0.5 and 1 AUFS, however, were precisely those that were found for the crude HTPB as described earlier: the samples merely exhibited a tail with little or no separation of the peak maximum from that given by THF. Moreover, the exponential-decay form of peak elution was that expected if the (relatively-short) chains of the fractionated HTPB were hydrogen-bonded to one another.

The strong self-association of the HTPB chains was tested further with a mobile-phase composition of 35% THF/65% MeOH: the peaks exhibited tailing that was more pronounced than that found previously; also, there was the beginning of separation of the main band of HTPB from the peak maximum position of THF. The chromatogram of the 20% fraction material exhibited a slightly better separated peak maximum, but not substantially so over those noted above.

Peak tailing for the 10% and 20% fractions was found to increase as the methanol content of the mobile phase was increased, as for example, with 25% THF/75% MeOH. However, the peak maximum of the latter was once more only slightly better separated from the solvent front than was that of the former.

Finally, the chromatograms of the 20%, 10%, and 5% fractions with 15% THF/85% MeOH showed no differences, other than the peak heights of the two visible bands diminished on passing from the former fraction to the latter. In fact, overall, the only change on passing from pure THF mobile phase to one of only 15% THF was that band-tailing became more pronounced. This was strong evidence for tight inter-chain binding.

Characterization of Polystyrene and HTPB Fractions. The second portion of the work of Task 1 was comprised of characterizing the fractions of polystyrenes and HTPB, collected as described in the preceding Sections. As part of this effort, it was also intended to identify, insofar as was possible, real as well as potential sources of error that might be inherent in the conventional characterization techniques themselves. Thus, polystyrenes fractions collected by GPC were examined by analytical-scale reverse-phase LC; while the polystyrenes collected from the preparative-scale reverse-phase LC system, along with the bulk-scale fractionated HTPB, were characterized by gel-permeation chromatography, vapor-phase osmometry, and viscosity.

Analytical-Scale Reverse-Phase LC Characterization of GPC Fractions of Polystyrenes. It will be recalled that a number of fractions of 680M polystyrene had been collected from the PL-GEL GPC column. These were also shown to correspond (very marginally) to different elution volumes. The fractions were examined in the first part of this portion of the work with the usual analytical reverse-phase Spherisorb ODS LC system in order to assess the utility (or otherwise) of GPC as a suitable technique for the speciation of prepolymers according to molecular weight.

First, for a reference-point, the 680M polystyrene standard was run again with the reverse-phase system, where a mobile phase of 65% THF/H₂O was utilized. The chromatogram (which was reproduced several times) is shown in Figure 23, where each of the isomer peaks have been numbered as 1 through 10. Recall next Figure 6, p. 20, that summarized the GPC fractions collected with THF eluent. Figures 24-28 then present the reverse-phase liquid chromatograms obtained for the GPC fractions C₁ through G₁ (there was not enough left of B₁, B₂, or G₂ to obtain reasonable responses).

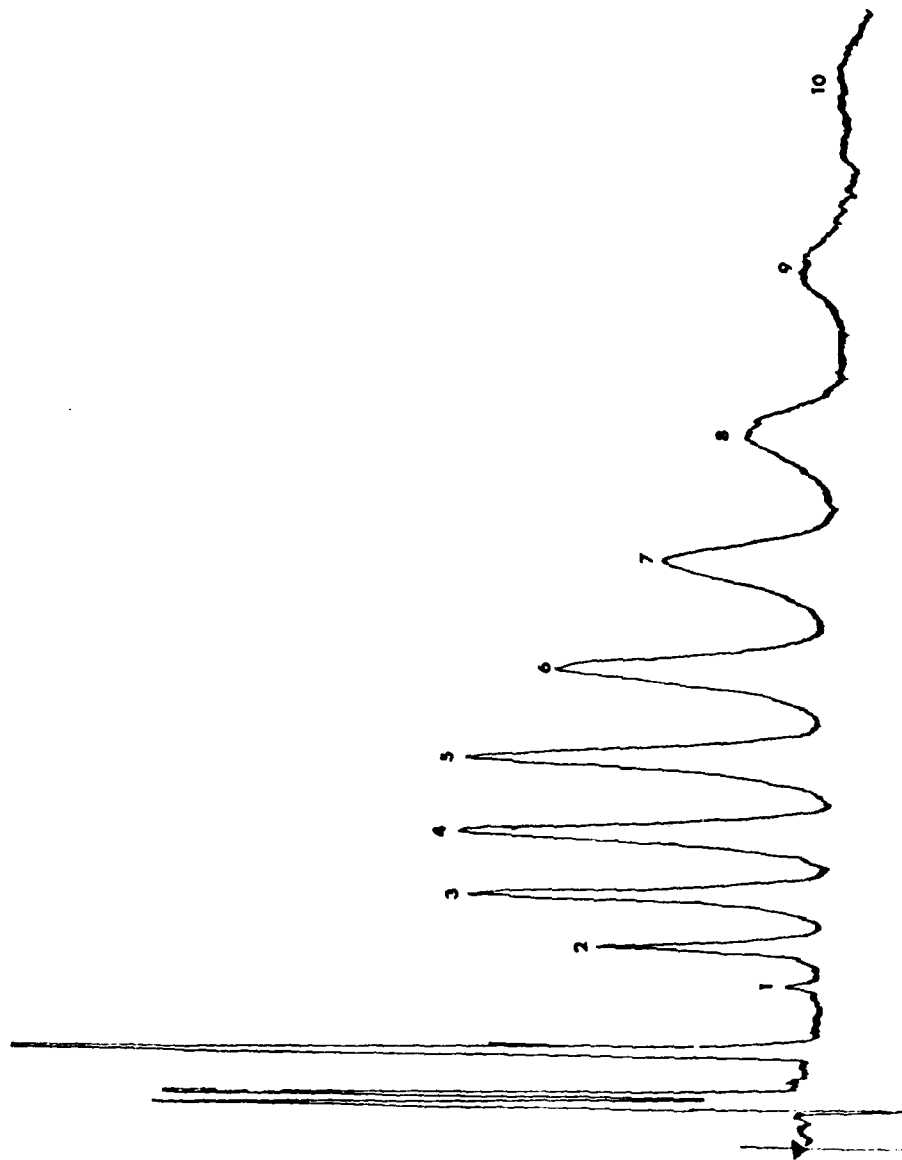


FIGURE 23. Isochratic reverse-phase LC separation of 680M polystyrene. Column: 25-cm Spherisorb C₁₈ 5- μ m; flow rate: 1 cm³ min⁻¹; chart speed: 2 min cm⁻¹; 25°C column temperature; 10-mm³ injection-loop volume. Mobile phase: 65% v/v THF/H₂O.

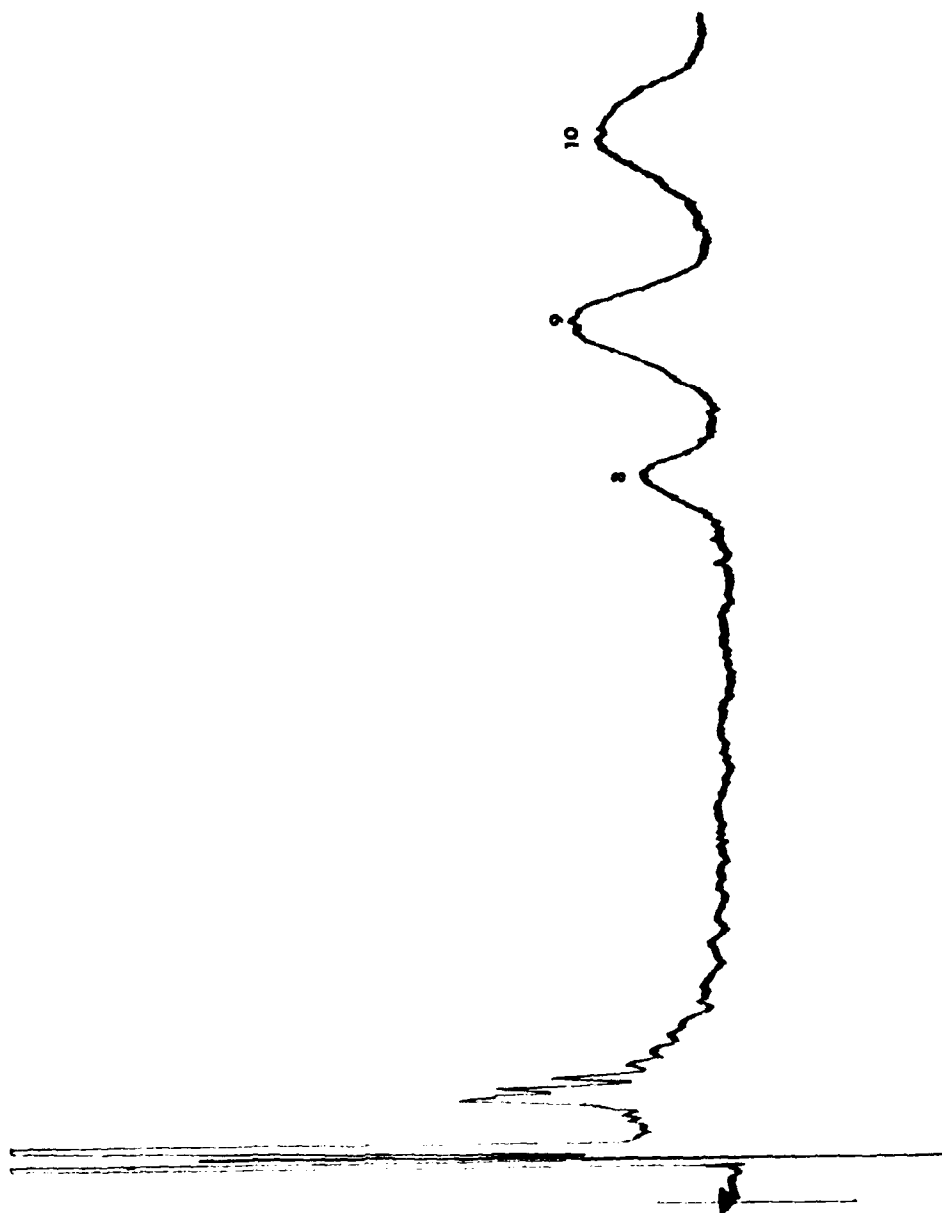


FIGURE 24. As in Figure 23; GPC fraction C₁.

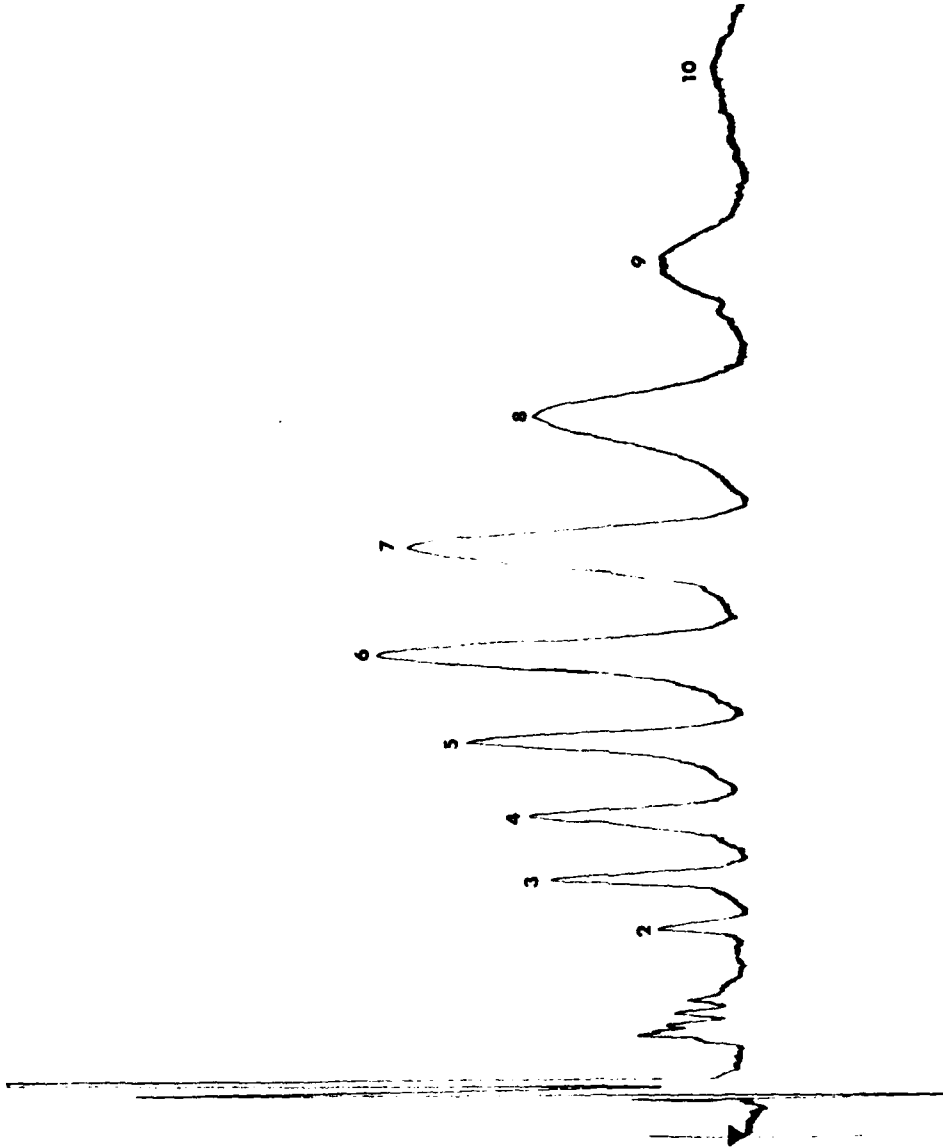


FIGURE 25. As in Figure 23; GPC fraction D₁.

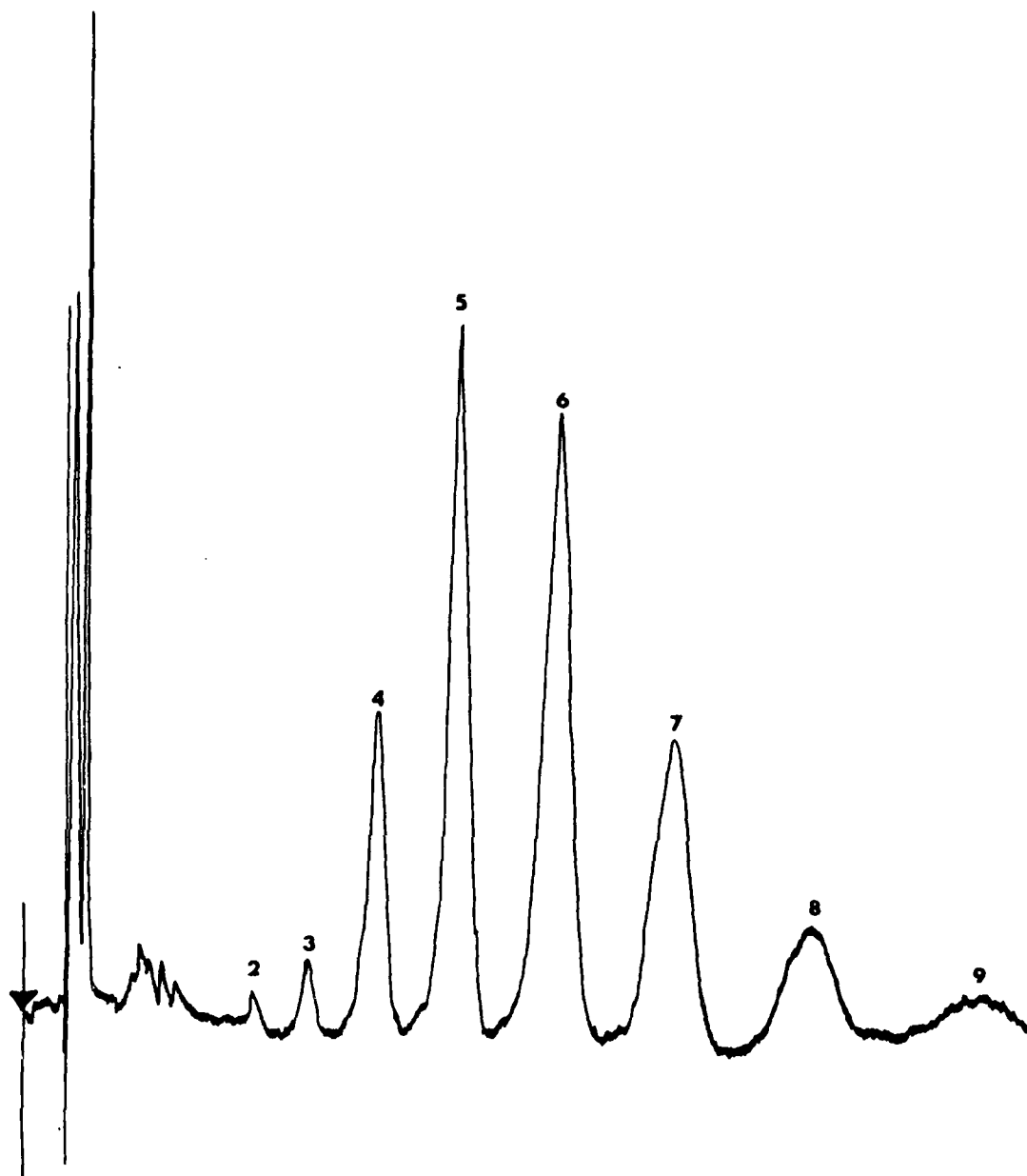


FIGURE 26. As in Figure 23; GPC fraction E₁.

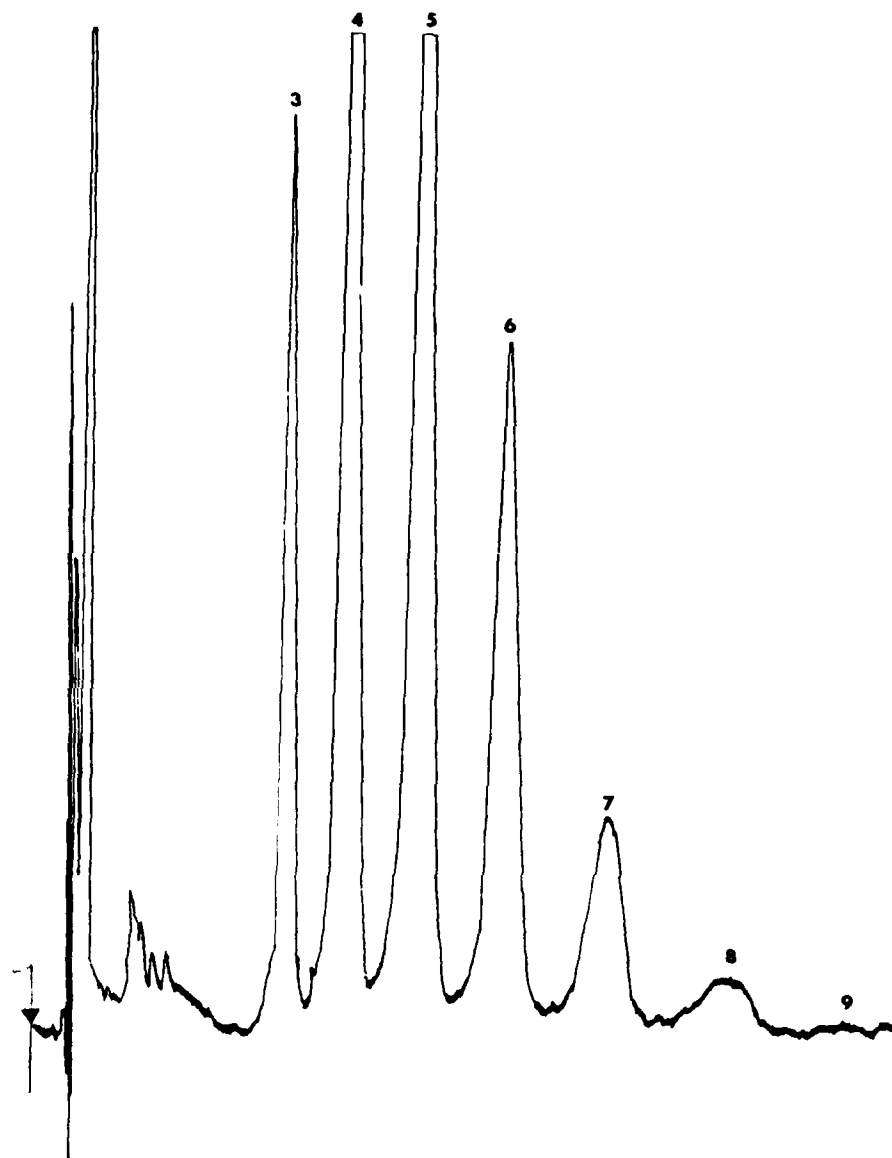


FIGURE 27. As in Figure 23; GPC fraction F_1 .

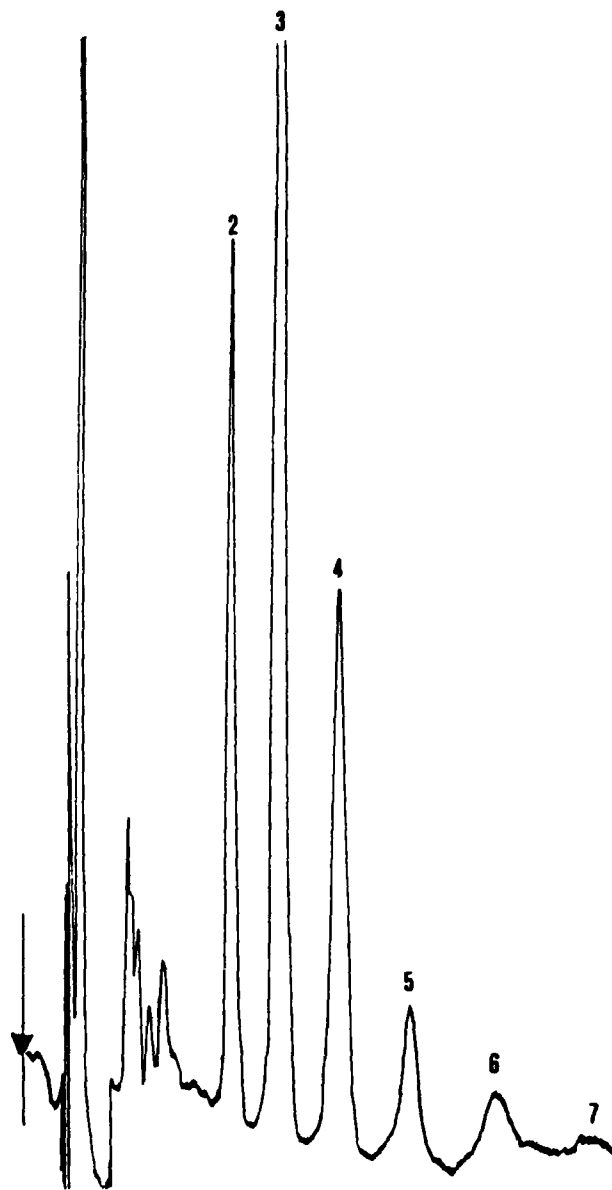


FIGURE 28. As in Figure 23; GPC fraction G_1 .

The results were quite interesting: fraction C₁ was comprised of isomers 8-10 with very little else, while fraction D₁ contained virtually every isomer peak. Moreover, the envelope roughly approximated that found previously for neat 680M. In contrast, fraction E₁ contained mostly isomers 4-9, with very little of 2 and 3, and none of isomer 1. This pattern was repeated with fraction F₁ with, however, a diminution of isomers 8 and 9. Fraction G₁ was perhaps the most interesting: recall that the GPC trace of this group appeared to resemble neat 680M, i.e., it did not appear as if any fractionation had been achieved. In complete contrast, the reverse-phase LC trace showed that, in fact, only isomers 2-4 were present in any great abundance in this fraction.

These results confirmed the supposition inferred earlier, that GPC does not appear to be appropriate for the speciation (let alone collection) of low molecular-weight homologs of polystyrenes.

GPC Characterization of Reverse-Phase LC Fractions of Polystyrenes. In a further evaluation of the utility of gel-permeation chromatography, several of the 526M polystyrene fractions collected by reverse-phase LC were injected into the PL-GEL GPC column in order to ascertain whether the latter technique was capable of speciating the (LC) homologs according to molecular weight. If this were in fact the case, then each of the LC fractions would be expected to elute at different times from the GPC column. Moreover, this test of the GPC system was not a severe one, insofar as the molecular weights of the homologs ranged only up to ca. 1600 Da, and since the PL unit exhibited high efficiency (ca. 40,000 plates) for lower molecular-weight materials.

Recall that the semi-preparative-scale reverse-phase LC trace of the low molecular-weight (526M) polystyrene standard described and discussed earlier gave seven peaks, which were combined into six fractions corresponding, respectively, to chromatogram-regions 1+2, 3+4, 5-7, 8-10, 12+13, and 16+17. The gel-permeation chromatogram of fraction 1+2 was then obtained. Although very small (i.e., sample diluted too much), the main peak was seen to correspond to an elution time of seven chart divisions (ca. 14 cm³ retention volume). The GPC trace of fraction 3+4 next showed a large main band corresponding also to ca. seven chart divisions, which was accompanied in addition by a base of several other (and very much smaller; probably residual THF) peaks. The GPC of fraction 5-7 showed a main band that eluted as before at seven chart divisions. Finally, the GPC of fraction 8-10 gave a main band that had virtually exactly the same retention volume as those run previously. Thus, overall, there was virtual coincidence of the gel-permeation chromatographic traces of the (very-well-separated) LC peaks. That is, while it was expected that GPC would provide at least some separation of the lower homologs, this was not in fact observed to be the case for the system at hand.

VPO Characterization of Reverse-Phase LC Fractions of Polystyrenes and HTPB. The Knauer vapor-phase osmometer (VPO) received from AFAL was put to use as part of Phase I, Task 1, for the measurement of M_n of several of the bulk (unfractionated) and fractionated polystyrenes and HTPB. "HPLC"-grade chloroform was the solvent throughout, while benzil (1,2-diphenyl-1,2-ethanedione) (highest purity; UIC, Inc.) was the standard. Readings were taken 4 min from the time of drop placement.

Zero Displacement. The instrument was first evaluated from the standpoint of reproducibility of the zero setting with drops of pure solvent on each thermocouple. The instrument drifted so badly on an attenuation of 1 that an attenuation setting of 8 had to be used. (This was also in accordance with the advice obtained from the staff chemist at UIC regarding appropriate attenuation settings.) The results with two operators at this attenuation level are given below in Tables 4-9. Each "measurement set number" corresponds to the average of four individual measurements by each operator. For example, there were 32 measurements made in all for Table 4.

These data indicate a net positive bias between the sample and reference thermocouples (Tables 5,6), which may have been a result of one of them having been

damaged slightly at AFAL (shaft clearly pinched with a pair of needle-nose pliers; plier marks evident on thermocouple shaft). Moreover, the results were reproducible. It was also clear that zeroing the instrument after each measurement very substantially reduced the zero error, as shown in Tables 7-9.

Calibration with Benzil. The reproducibility of VPO measurements was evaluated next with the recommended standard compound benzil. The results are reported below in Tables 10(i) and (ii). Also studied during this portion of the work was the effect that drop size had on the VPO measurements. The results are reported in Table 11, and are grouped in terms of the trends exhibited.

TABLE 4. VPO Zero Displacement Measurements Obtained by Two Operators for Identical Drop Sizes of Pure Chloroform Solvent on Each Thermocouple: Drops Changed on Both Sample and Reference Sides for Each Set of Four Measurements; Instrument Zero Not Changed Until Completion of All Measurements. Attenuation of 8 Throughout.

<u>Measurement Set No.</u>	<u>VPO Reading/mV</u>	
	<u>Operator 1</u>	<u>Operator 2</u>
1	-6.4	-16.8
2	-2.9	-13.3
3	-4.9	-15.3
4	9.2	-1.2
	Ave: -6.45	

TABLE 5. VPO Zero Displacement Measurements Obtained by Two Operators for Identical Drop Sizes of Pure Chloroform Solvent on Each Thermocouple: Drops Changed Only on Sample Side for Each Set of Measurements; Instrument Zero Not Changed Until Completion of All Measurements. Attenuation of 8 Throughout

<u>Measurement Set No.</u>	<u>VPO Reading/mV</u>	
	<u>Operator 1</u>	<u>Operator 2</u>
1	-8.6	1.3
2	-10.6	-0.7
3	-12.9	-3.0
4	-16.9	-7.0
	Ave: -7.30	

TABLE 6. VPO Zero Displacement Measurements Obtained by Two Operators for Identical Drop Sizes of Pure Chloroform Solvent on Each Thermocouple: Drops Changed Only on Reference Side for Each Set of Measurements; Instrument Zero Not Changed Until Completion of All Measurements. Attenuation of 8 Throughout

<u>Measurement Set No.</u>	<u>VPO Reading/mV</u>	
	<u>Operator 1</u>	<u>Operator 2</u>
1	5.0	3.2
2	5.3	3.5
3	6.2	4.4
4	4.2	2.4

Ave: 4.28

Table 7. VPO Zero Displacement Measurements Obtained by Single Operator for Identical Drop Sizes of Pure Chloroform Solvent on Each Thermocouple: Drops Changed on Both Sample and Reference Sides for Each Set of Measurements; Instrument Rezeroed After Completion of Each Measurement. Attenuation of 8 Throughout

<u>Measurement Set No.</u>	<u>VPO Reading/mV</u>
1	-8.2
2	0.8
3	-1.2
4	-2.7

Ave: -2.83

TABLE 8. VPO Zero Displacement Measurements Obtained by Single Operator for Identical Drop Sizes of Pure Chloroform Solvent on Each Thermocouple: Drops Changed Only on Sample Side for Each Set of Measurements; Instrument Rezeroed After Completion of Each Measurement. Attenuation of 8 Throughout

<u>Measurement Set No.</u>	<u>VPO Reading/mV</u>
1	0.0
2	0.4
3	0.5
4	1.3

Ave: 0.55

TABLE 9. VPO Zero Displacement Measurements Obtained by Single Operator for Identical Drop Sizes of Pure Chloroform Solvent on Each Thermocouple; Drops Changed Only on Reference Side for Each Set of Measurements; Instrument Rezeroed After Completion of Each Measurement. Attenuation of 8 Throughout

<u>Measurement Set No.</u>	<u>VPO Reading/mV</u>
1	-0.4
2	4.9
3	0.0
4	0.8
5	0.5
	Ave: 1.16

TABLE 10(I). Raw VPO Measurements Obtained for Indicated Concentrations (g kg^{-1}) of Benzil by Single Operator. Identical Drop Sizes; Pure Chloroform Reference Solvent Changed after Each Set of Measurements; Instrument Rezeroed After Completion of Each Set of Measurements; Attenuation Settings of 8 Through 64 Used as Required

	<u>VPO Reading/Absolute mV for Benzil Concentrations (g kg^{-1}) of:</u>				
<u>Measurement Set No.</u>	<u>5.33</u>	<u>14.92</u>	<u>27.15</u>	<u>37.91</u>	<u>Zero</u>
1	1060	2666	4778	6573	97.6
2	1016	2749	4694	6566	-26.4
3	1048	2754	4739	6618	152
4	1042	2672	4672	6624	46.4
Ave.	1041	2710	4721	6592	

TABLE 10(II). Repeat of Measurements Described in Table 10(I)

	<u>VPO Reading/Absolute mV for Benzil Concentrations (g kg^{-1}) of:</u>				
<u>Measurement Set No.</u>	<u>6.17</u>	<u>15.13</u>	<u>27.04</u>	<u>35.33</u>	<u>Zero</u>
1	1190	2830	4602	6253	147
2	1146	2734	4512	6086	97.6
3	1086	2664	4515	6083	43.2
4	1066	2648	4643	6032	-44.8
Ave.	1122	2719	4568	6114	

TABLE 11. Zero-Corrected VPO Measurements Obtained for Indicated Concentrations (g kg⁻¹) of Benzil by Single Operator. Drop Sizes as Indicated; Pure Chloroform Reference Solvent; Instrument Zeroed After Completion of Each Set of Measurements; Attenuation Settings of 8 Through 64 Used as Required.

	<u>VPO Reading/Absolute mV for Benzil Concentrations (g kg⁻¹) of:</u>			
	<u>5.33</u>	<u>14.92</u>	<u>27.15</u>	<u>37.91</u>
A. Small Drop Size Both for Reference and Sample; Solvent Drop Not Changed Until All Measurements Completed	918	2678	4522	6576
B. Large Drop Size Both for Reference and Sample; Solvent Drop Not Changed Until All Measurements Completed	953	2569	4739	7012
C. Larger Drop Size Both for Reference and Sample; Solvent Drop Not Changed Until All Measurements Completed	971	2754	4913	7443
D. Small Drop Size Both for Reference and Sample; Solvent Drop Changed After Each Measurement	1120	2852	4960	7379
E. Large Drop Size Both for Reference and Sample; Solvent Drop Changed After Each Measurement	1033	2660	4654	7108
F. Larger Drop Size Both for Reference and Sample; Solvent Drop Changed After Each Measurement	926	2666	4738	7353
G. Very Small Drop for Sample Side; Drop Twice as Big for Reference Side		2754		
H. Sample and Reference Drops Roughly Equal		2752		
I. Sample Drop Noticeably Larger than Reference Drop		2756		
J. Sample Drop Very Much Larger than Reference Drop		2758		

The above results were quite revealing regarding the reproducibility of the VPO technique. Clearly, changing the reference drop played a major role: the best results were obtained when the reference drop was changed after each measurement. It also appeared that the relative size of the drops was insignificant, as indicated by the data shown in Table 11.G-J. Thus, it made no difference whether one drop was much bigger or much smaller than the other, so long as the reference was changed after each measurement. In any event, the overall assessment of the VPO technique with the instrument at hand was that the precision that could be expected was no better than $\pm 20\%$, which was in approximate accord with the findings of others (e.g., R. D. Law, JANNAF Round-Robin Report on VPO, 1975).

Number-Average Molecular Weights of Bulk Polystyrenes and HTPB. Despite the seeming imprecision of the VPO technique, the number-average molecular weights were measured of the bulk polystyrenes PL 580M, PL 1240M, (cleaned) Goodyear 1800M, and PL 2470M; as well as AFAL-supplied HTPB. The results are presented graphically in Figures 29 (polystyrenes) and 30 (HTPB). The combined data reduction procedures gave values for the PS of 424, 939, 1423, and 1940 Da; and 1512 Da for the HTPB.

Number-Average Molecular Weights of Reverse-Phase LC Fractions of Polystyrenes. Despite the continuing imprecision of the VPO technique due to drift of the instrument zero, the number-average molecular weights were nevertheless measured of PS 580M fractions 2, 4, and 6. "HPLC"-grade chloroform was the solvent throughout, while benzil was again the standard. Readings were taken after 4 min elapsed time of drop placement on the thermocouples as before. The results are presented graphically in Figure 31; the data reduction procedures (averages of four determinations each) gave values of M_n of 345 for fraction 2; 522 for fraction 4; and 624 for fraction 6.

A Priori Calculation of Number-Average Molecular Weights of Bulk and Fractionated Polystyrenes. The plots were initially quite encouraging since the bulk polymer line fell between fractions 2 and 4, i.e., the value of M_n of bulk 580M appeared to be a composite of a weighted average of the fractions comprising it. This was tested as follows. First, the peak areas found for each of the homologs in fractions 2, 4, and 6 were measured (see the chromatograms in Figures 19 and 20, pp. 40 and 41). Also, the same data were measured for bulk 580M from two other chromatograms that were run especially for this purpose. Since a UV detector was used, the raw areas next required correction for the molar absorptivities a of the solute homologs. The absorptivities were taken to be additive, which seems reasonable since the chromophores (benzene rings) are isolated from one another in polystyrene (i.e., not conjugated). Also, the absorptivity of the first homolog was considered to approximate that of toluene, ca. $7,000 \text{ cm}^2 \text{ mol}^{-1}$. Thus, the absorptivity for homolog $n = 2$ was taken as 14,000; 21,000 for $n = 3$, and so forth. A corrected area was next calculated for each solute by dividing the raw area by the absorptivity, followed by calculation of the relative percent of each species. (Accordingly, the result should be directly proportional to the concentration, hence number of moles, of each homolog present.) Summation of the products of the relative percentages and known molecular weights of the homologs then yielded a predicted M for each mixture. The results (VPO values in parentheses) are provided in Table 12.

First, the data in D and E show gratifyingly good internal agreement ($\pm 3\%$) given that the height and area measurements were made simply with a ruler. However, the discrepancies between the LC and VPO molecular weights increase with increasing M , and approach 16% at 745 Da, indicative of a systematic error in the technique.

Systematic Error Inherent in VPO. In addition to random instrument errors, there exists also a systematic error inherent in the VPO technique, namely, deviations from unity of the solvent activity coefficient in the solute-solvent mixture. Now, the recommended operating procedure is to remain below solute concentrations of ca. 50 g kg^{-1} , hence, the activity coefficient of the solvent should approach its limiting value,

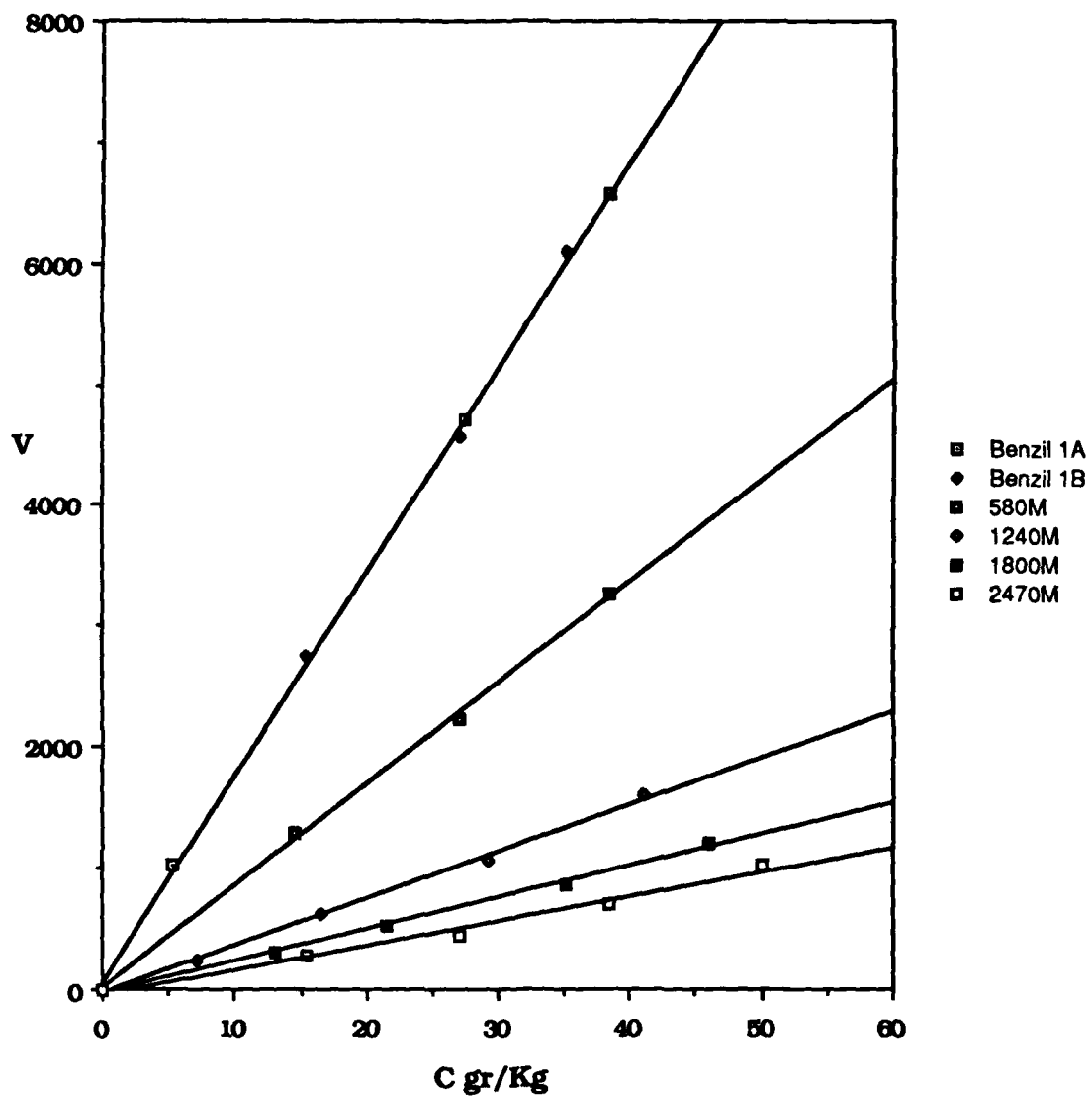


FIGURE 29. Plots of VPO data for benzil and indicated polystyrenes.

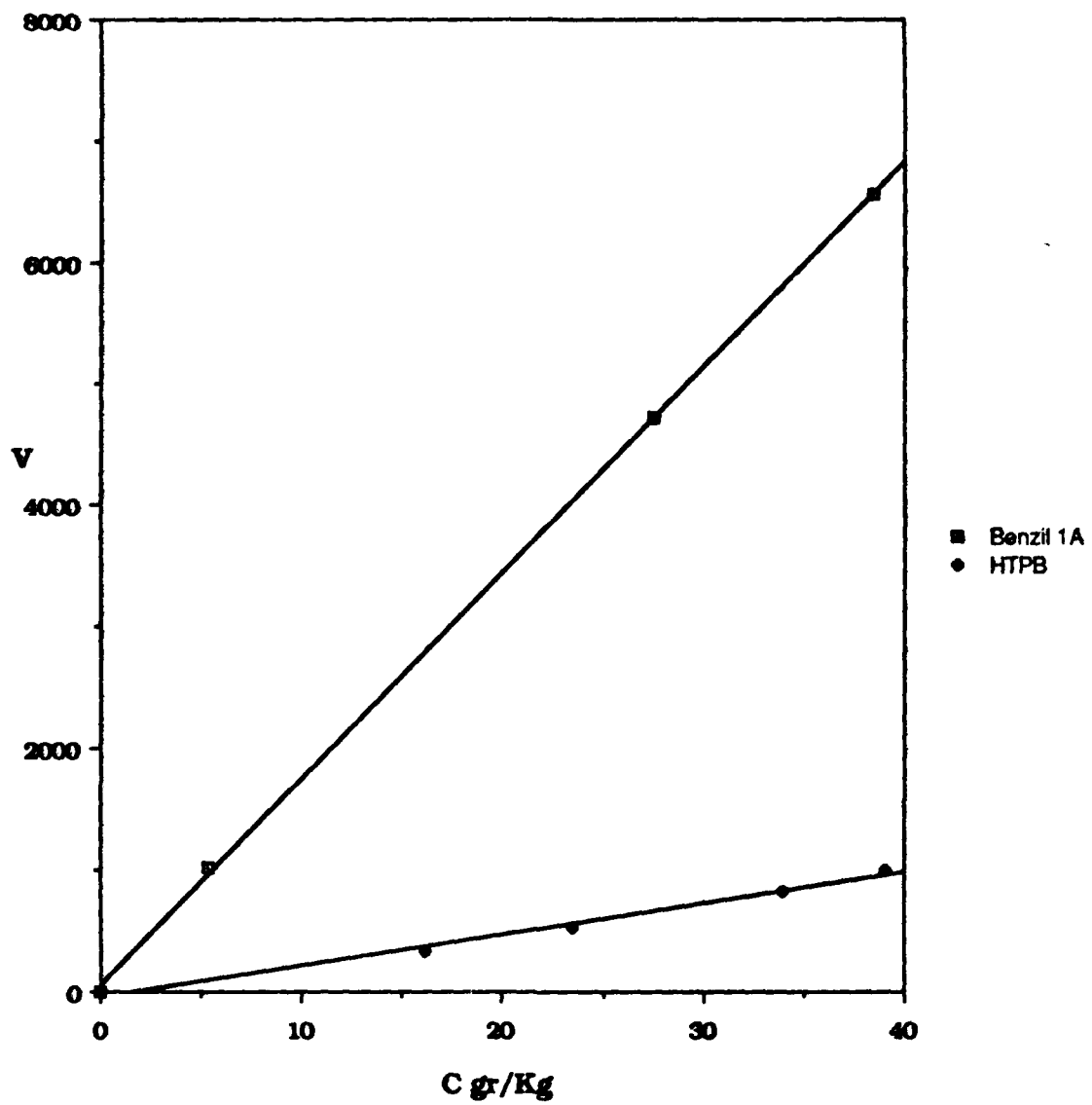


FIGURE 30. Plots of VPO data for benzil and HTPB.

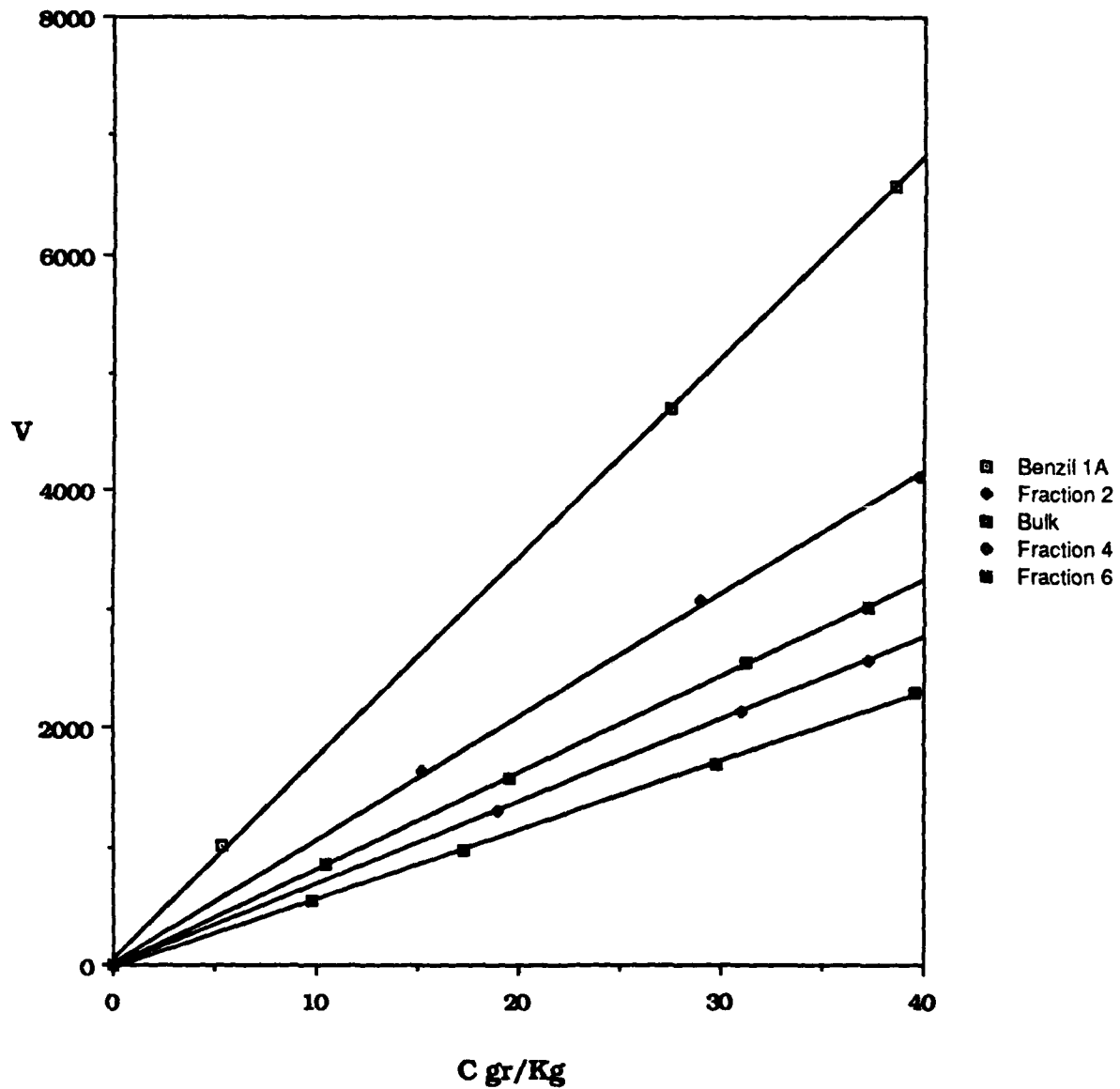


FIGURE 31. VPO data plots for benzil (standard; chloroform solvent); polystyrene 580M fractions 2, 4, and 6; and bulk 580M polystyrene.

TABLE 12. Raw and Corrected Areas and Area Percentages for Indicated Polystyrene Blends

Peak No.	M/Da	$a/cm^2 mol^{-1}$	h/cm	w/cm	A/cm^2	10^4 Cor. A/cm mol	Rel. %
A. Fraction 2							
2	266	14,000	13.4	0.10	1.426	1.0186	43.39
3	370	21,000	16.4	0.10	1.745	0.8310	35.40
4	474	28,000	13.1	0.10	1.394	0.4979	21.21

M = 347 (345 ± 35) Da

B. Fraction 4							
3	370	21,000	4.1	0.10	0.4362	0.2077	11.41
4	474	28,000	11.0	0.10	1.1704	0.4180	22.97
5	578	35,000	15.1	0.14	2.2493	0.6427	35.30
6	682	42,000	12.1	0.18	2.3174	0.5518	30.32

M = 562 (522 ± 52) Da

C. Fraction 6							
3	370	21,000	0.33	0.10	0.0351	0.0167	1.79
4	474	28,000	0.77	0.10	0.0819	0.0293	2.89
5	578	35,000	3.00	0.12	0.3830	0.1094	10.80
6	682	42,000	7.18	0.16	1.2220	0.2910	28.71
7	786	49,000	8.32	0.19	1.6820	0.3433	33.87
8	890	56,000	4.53	0.26	1.2532	0.2238	21.94

M = 740 (624 ± 63) Da

D. Bulk 580M							
1	162	7,000	1.5	0.07	0.1117	0.1596	4.19
2	266	14,000	8.4	0.10	0.8938	0.6384	16.74
3	370	21,000	14.9	0.10	1.5854	0.7549	19.80
4	474	28,000	16.5	0.10	1.7556	0.6270	16.44
5	578	35,000	15.1	0.12	1.9280	0.5509	14.45
6	682	42,000	11.2	0.16	1.9069	0.4540	11.91
7	786	49,000	7.2	0.19	1.4556	0.2971	7.79
8	890	56,000	3.9	0.25	1.0374	0.1853	4.86
9	994	63,000	1.7	0.31	0.5607	0.0890	2.33
10	1098	70,000	0.7	0.38	0.2830	0.0404	1.06
11	1202	77,000	0.25	0.49	0.1303	0.0169	0.43

M = 512 (444 ± 44) Da

TABLE 12 (Continued)

E. Bulk 580M (Repeat)

1	162	7,000	0.90	0.07	0.0670	0.0958	3.36
2	266	14,000	5.5	0.09	0.5267	0.3762	13.18
3	370	21,000	9.4	0.11	1.1002	0.5239	18.33
4	474	28,000	10.3	0.12	1.315	0.4696	16.43
5	578	35,000	9.5	0.17	1.718	0.4909	17.18
6	682	42,000	7.2	0.19	1.456	0.3467	12.13
7	786	49,000	4.6	0.22	1.077	0.2198	7.69
8	890	56,000	2.6	0.28	0.7750	0.1384	4.84
9	994	63,000	1.6	0.35	0.5960	0.0946	3.31
10	1098	70,000	0.9	0.46	0.4405	0.0629	2.20
11	1202	77,000	0.5	0.56	0.2979	0.0387	1.35

$$M = 545 (444 \pm 45) \text{ Da}$$

$$\text{Ave. of Runs D and E: } M = 529 \pm 16 \text{ Da } (\pm 3\%)$$

that is, unity. However, this may or may not be so depending upon the magnitudes of the Raoult's-law activity coefficients both of the solute and the solvent. It is in fact conceivable that for systems wherein heat is absorbed on dilution (i.e., those for which the activity coefficients deviate strongly positively, e.g., CS_2 + hexane) the VPO plots could well be sloped negatively. This in turn would result in a negative molecular weight. Thus, it appears that calibration of VPO apparatus must be carried out with the same polymer that is to be measured, namely, polystyrene calibration for polystyrenes; HTPB standard for HTPB polymers, and so forth. Rather large errors can otherwise be anticipated. (The situation thus is analogous to calibrating GPC columns with polymer standards that have much different hydrodynamic volumes than the polymers of interest.) The only way to avoid this error is to use solutions of true infinite dilution, that is, such that the sample-drop solution is so dilute that the solvent activity coefficient really does approach unity. Unfortunately, however, it was impossible to do so with the Knauer VPO instrument because of the zero-drift noted above. The matter is beyond the scope of this contract but, self-evidently, merits further study and investigation since VPO is a standard method of characterization utilized throughout the polymer industry.

The means of checking at least for systematic errors were to hand, since the 580M fractions were of known molecular weight. Accordingly, Figure 32 shows the data points for the fractions (with appropriate error bars; that for the VPO being taken optimistically as $\pm 10\%$) (average bulk 580M datum in parentheses; dashed line) plotted in the form of relative error of the VPO against the true sample molecular weight. Even allowing for considerable errors in peak areas and over- or underestimation of the solute absorptivities, it is clear that the points fall below the abscissa in each case and that, despite having only three data, the error increases as the molecular weight of the solute blends increases. As a result, it was concluded that the LC/calculational method developed in this portion of the work provides molecular-weight data that are at least as accurate as those arising from VPO; and that, given the particular simplicity of the chromatographic technique, there appears to be considerable practical advantage to it as well.

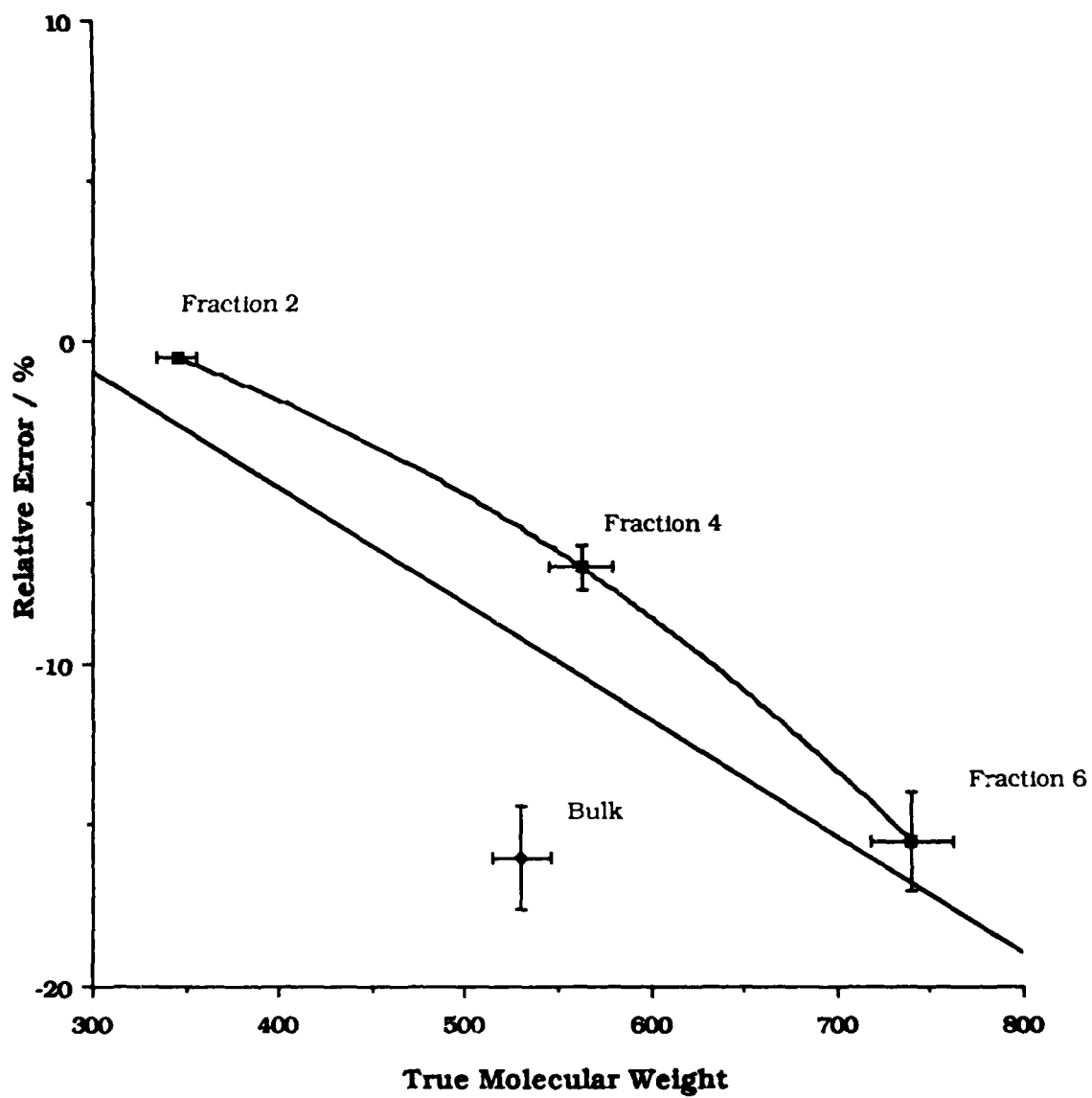


FIGURE 32. Plot of relative error, $10^2(\text{VPO} - \text{true})/\text{true}$, against true molecular weight for indicated polystyrene blends. Error bars represent $\pm 3\%$ on molecular weight, $\pm 10\%$ on VPO data. Solid curve: three datum points; dashed line: four datum points.

Viscosity Characterization. The various kinds of viscosities are defined below:

Commonly Used Viscometry Terms

Common name	Recommended name (IUPAC)	Definition	Symbol
Relative viscosity	Viscosity ratio	η/η_0	η_{rel}
Specific viscosity	—	$\eta/\eta_0 - 1$ or $\eta - \eta_0/\eta_0$ or $\eta_r - 1$	η_{sp}
Reduced viscosity	Viscosity number	η_{sp}/c	η_{red} or η_{sp}/c
Inherent viscosity	Logarithmic viscosity number	$\ln \eta_r/c$	η_{inh} or $\ln \eta_r/c$
Intrinsic viscosity	Limiting viscosity number	$\lim(\eta_{sp}/c)_{c \rightarrow 0}$ or $\lim(\ln \eta_r/c)_{c \rightarrow 0}$	$[\eta]$ or LVN

Thus, the relative viscosity η_{rel} is simply the ratio of the viscosity of the polymer solution η to that of the solvent η_0 . This value minus 1 is then called the specific viscosity, η_{sp} . The reduced viscosity η_{red} is found by dividing the specific viscosity by the polymer concentration, while the intrinsic viscosity $[\eta]$ is given by extrapolation of η_{red} to zero concentration. The intrinsic viscosity is purportedly related to the polymer molecular weight by the Mark-Houwink equation,

$$[\eta] = K M^a$$

where the K and a terms must be determined empirically. Many texts offer reviews of the technique, as well as the models by Debye, Kirkwood, Flory, and others.

In practice, the viscosity (more properly, the coefficient of viscosity) is defined by Poiseuille's law:

$$\frac{dV}{dt} = \frac{nr^4(p_1 - p_2)}{8nL}$$

where dV/dt represents a volume flow rate through an empty tube of radius r and length L , and where $(p_1 - p_2)$ is the pressure gradient across the tube. In making use of an Ubbelohde viscometry tube the relation is cast in the form:

$$\frac{\eta}{r} = Bt - \frac{V}{8nLt}$$

where the pressure difference has been replaced by the solution density (to which it is directly related), and where the right-hand term amounts to a kinetic-energy correction that is usually neglected. Thus, the measurement of solution viscosity requires that the viscometer tube be calibrated to determine the value of B which, in turn, requires knowledge of the densities of the polymer solutions as well as that of the solvent itself.

Densities and Viscosities of Solvents. It is common in the initial use of viscometer tubes that one first assesses the constant B with distilled degassed water. The viscosity of water over the ranges 0-20°C and 20-100°C is given by the following respective equations:

0 to 20°C:

$$\log n = \frac{1301}{998.333 + 8.1855(t - 20) + 0.00585(t - 20)^2} - 3.30233$$

20 to 100°C:

$$\log \frac{n_t}{n_{20}} = \frac{1.3272(20 - t) - 0.001053(t - 20)^2}{t + 105}$$

The density of water at various temperatures is provided in many reference works. The values at from 10 to 50°C are reproduced below.

$r/g \text{ cm}^{-3}$								
<u>10°C</u>	<u>15°C</u>	<u>20°C</u>	<u>25°C</u>	<u>30°C</u>	<u>35°C</u>	<u>40°C</u>	<u>45°C</u>	<u>50°C</u>
0.99973	0.99913	0.99823	0.99708	0.99568	0.99406	0.99225	0.99024	0.98807

The densities and viscosities of CHCl_3 , a popular solvent for the study of HTPB, are provided in Table 13. The densities were calculated from those provided in "The International Critical Tables" Series and from the relation:

$$r = r_s + 10^{-3}At + 10^{-6}Bt^2 + 10^{-9}Vt^3$$

where $r_s = 1.52643 \text{ g cm}^{-3}$; $A = -1.8563 \text{ g cm}^{-3} \text{ deg}^{-1}$; $B = -0.5309 \text{ g cm}^{-3} \text{ deg}^{-2}$; $V = -8.81 \text{ g cm}^{-3} \text{ deg}^{-3}$; and where t is in degrees Centigrade. (These are slightly discrepant with those calculated from the law of rectilinear diameters,

$$r = a + bt$$

where $a = 1.49652 \text{ g cm}^{-3}$, and where $b = -0.00062$ as reported by Dreisbach in "Physical Properties of Chemical Compounds", ACS Advances in Chemistry Series, Vol. II.) The viscosities were taken from "The Handbook of Chemistry and Physics" and, as with the density data, are slightly discrepant from the kinematic viscosities n_k (ratio of viscosity to density) reported by Dreisbach:

$$\log n_k / \text{cS} = -1.57472 + \frac{B}{T}$$

where T is in degrees Kelvin, and where n_k has units of centistokes ($\text{dm}^2 \text{ sec}^{-1}$). For the sake of consistency as well as wide availability, the "Handbook" sets of data are employed throughout in what follows.

Several solutions of HTPB in CHCl_3 were next made up, and their densities determined with the Mettler-Parr density meter. These are reported below in Table 14. The data are also shown plotted as a function of weight percent in Figure 33. The linearity was indicative of quite substantial mixing volumes since, in the absence of excess volumes of mixing, density is linear only in volume percent (or fraction) and not in weight percent (or fraction):

$$r = \phi_A r_A^0 + \phi_S r_S^0$$

where ϕ_i ($i = A$ or S) are volume fractions, and where r_i^0 are the densities of the pure substances i . Further, volume fractions are related to weight fractions w_i by the expression:

$$w_A = \frac{\phi_A}{(r_S^0/r_A^0) + \phi_A[1 - (r_S^0/r_A^0)]}$$

Thus, density is linear in weight fraction only if $r_S^0 = r_A^0$, which is certainly not the case here, the density of chloroform being ca. 1.4 g cm^{-3} while the density of HTPB presumably is something less than unity. This was tested by measurement of the density of bulk HTPB as well as the 10% fraction of HTPB described earlier. The results are provided in Table 15, while the plots of density against temperature are shown in Figure 34.

TABLE 13. Densities and Viscosities of Chloroform at Indicated Temperatures

$t/^\circ\text{C}$	$r/\text{g cm}^{-3}$	n/cS
15	1.4963	0.596
20	1.4868	0.580
25	1.4774	0.542
30	1.4680	0.514
40	1.4489	0.485

TABLE 14. Densities of Chloroform Solutions of Bulk HTPB at Indicated Temperatures

$\text{Conc./g 100 cm}^{-3}$	$r/\text{g cm}^{-3}$				
	15°C	20°C	25°C	30°C	40°C
1.5314	1.4819	1.4723	1.4627	1.4530	1.4337
3.6020	1.4688	1.4594	1.4497	1.4400	1.4217
7.6570	1.4429	1.4339	1.4250	1.4161	1.3984
10.2040	1.4274	1.4185	1.4098	1.4009	1.3834
15.3140	1.3930	1.3839	1.3748	1.3676	1.3517

TABLE 15. Densities of Chloroform, Bulk HTPB, and 10% Fraction HTPB at Indicated Temperatures

$t/^\circ\text{C}$	CHCl_3	Bulk HTPB	Fract. HTPB
15	1.4963	0.9065	0.9208
20	1.4868	0.9032	0.9173
25	1.4774	0.9000	0.9139
30	1.4680	0.8968	0.9108
35	1.4585	0.8936	0.9073
40	1.4489	0.8908	0.9037

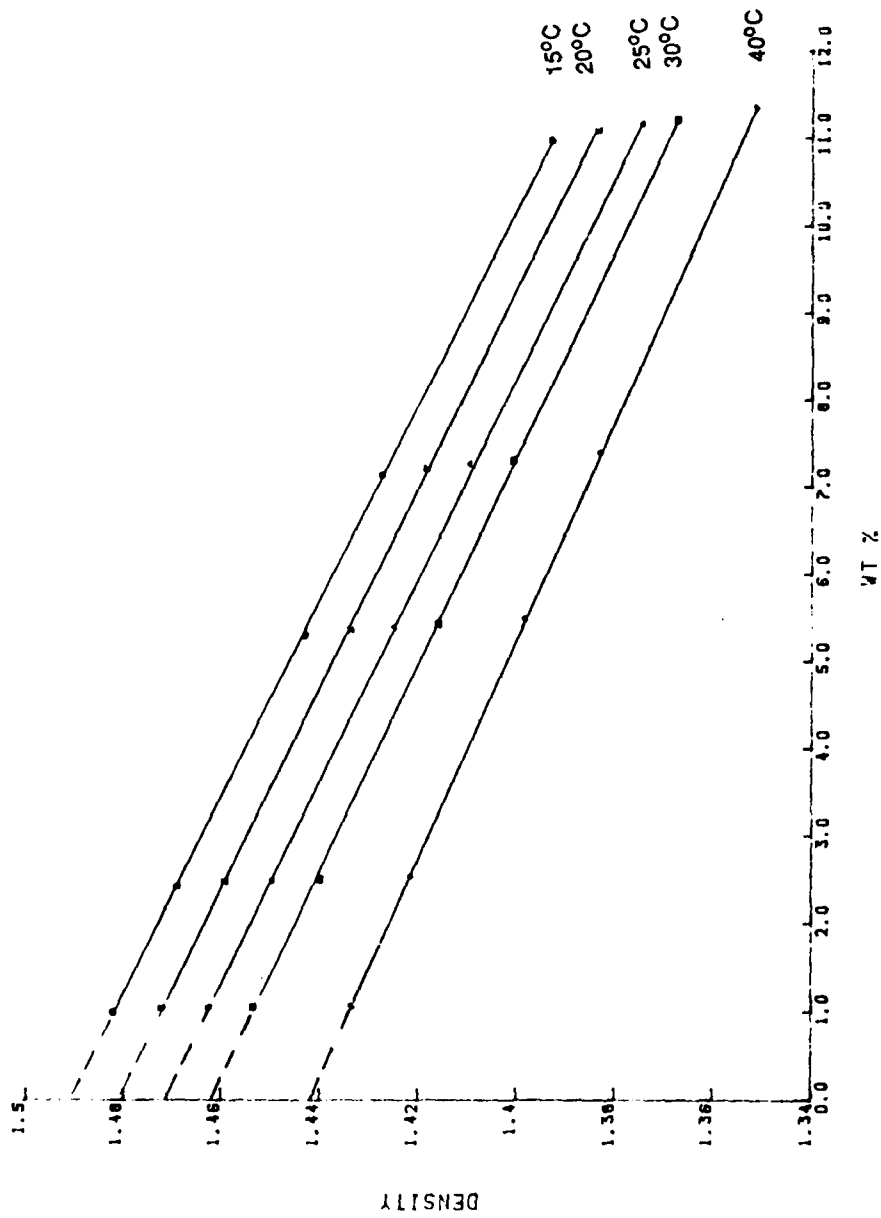


FIGURE 33. Plots of density against weight percent of solutions of Table 14.

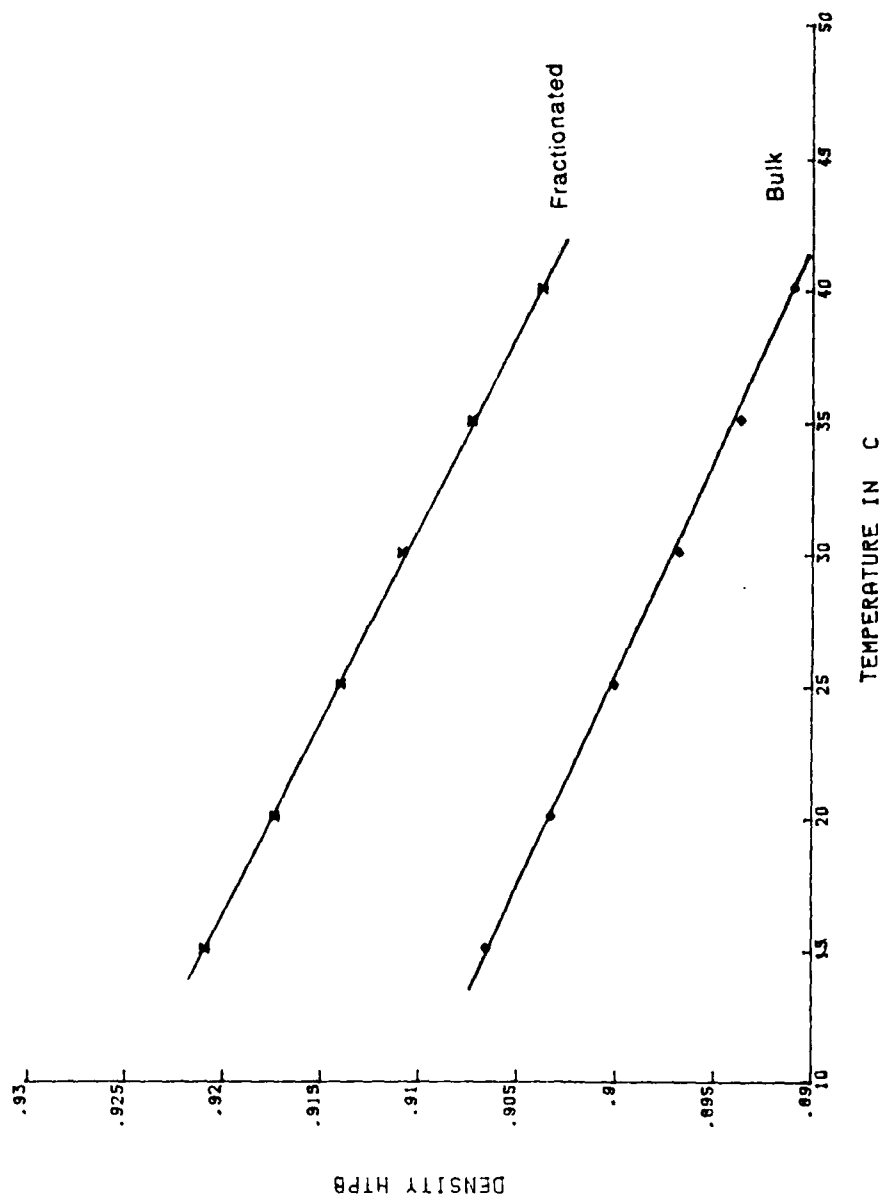


FIGURE 34. Plots of density against temperature $t/^{\circ}\text{C}$ for Bulk and Fractionated HTPB.

Parenthetically, the density of the fractionated HTPB was appreciably greater than the crude material (recall that the density data are accurate to 2 parts in 10,000). This conforms with what would be predicted, since the lower molecular weight material consists of shorter polymer chains that can pack more tightly in solution. That is, there is volume contraction on lowering the molecular weight, which was reflected as an increase in the density.

The densities of the HTPB solutions are next shown plotted as a function of temperature in Figure 35, the concentrations being as indicated. These varied linearly as expected. The plots show that density measurements can be used to determine concentrations of HTPB quite easily as in, for example, process streams. In addition, it is interesting to speculate that six-place density measurements (as with, for example, a Mettler-Paar DMA-60) carried out in different solvents (e.g., trifluoroacetic acid, which should disrupt interchain hydrogen bonding) should enable the determination of molecular weight as well as hydroxyl-group content.

Characterization of Bulk and Fractionated HTPB. At this point, the apparent solution viscosities were measured. All were curved, irrespective of the form of data reduction. Extrapolation to obtain the inherent viscosity was therefore impossible. The reason for this was that the solutions were too concentrated, and the fall times were much too rapid. Two separate viscometer tubes were then acquired, for which the fall times of chloroform solvent exceeded 200 sec at 15°C.

Phase I, Task 2. Mass Spectral Determination of Fraction Molecular Weights

Calibration to 2000 Da. As part of an effort at characterizing prepolymer materials, the high-resolution double-focussing MS 902 was routinely used to derive molecular-weight information up to 1000 Da. However, it was not known initially whether the instrument could be calibrated successfully at masses covering up to 2000 Da, nor whether appropriate standards were available with which to do so. However, an interesting aspect of the computer system attached to the instrument was taken advantage of, which did permit such calibration. First, the accelerating potential used normally was 8000 V. If this were cut in half to 4000 V, ions of twice the mass would be passed through the electrostatic and magnetic sectors, thence would be detected. Moreover, the factor of 2 increase in mass was linear, that is, ions of exact mass 400 appeared to the computer system to be ions of exact mass 200; ions of exact mass 800 appeared to be ions of exact mass 400, and so on. Thus, it turned out that calibration of the system up to 2000 Da could be done simply by determining the exact ratio of the accelerating potentials when 4000 V was selected instead of 8000 V. This was done with perfluorokerosine (PFK). The system was first calibrated normally with PFK; then, 4000 V was selected and several of the PFK peaks (the mass of each being known to 6 decimal places) were examined to determine what the computer system thought the masses were. The ratio for each peak examined turned out to be 2.001485. Moreover, this will not change with time, so long as the power supply does not change. As it happens, the Wallis (U.K.) power supply for the accelerating potential is stable to 5 ppm. Thus, the ratio was valid for months at a time. Upon entering this "correction" factor into the computer, it then corrected (by this factor) what masses it saw. Following calibration to 1000 Da, and upon telling the computer to apply the correction factor to the PFK peaks, the instrument was thereby calibrated automatically up to 2000 Da.

Characterization of Reverse-Phase LC Fractions of Polystyrenes. The first prepolymer materials to be characterized by mass spectrometry were those comprised of polystyrene fractions 3+4; 5-7; and 8-10 that were recovered by semi-preparative-scale reverse-phase LC as described earlier. A typical mass spectrum of the first is given in Figure 36. This shows that each of the polystyrene homologs amounts to a molecular-weight difference of the styrene unit, 104 Da, coupled with an n-butyl end-group.

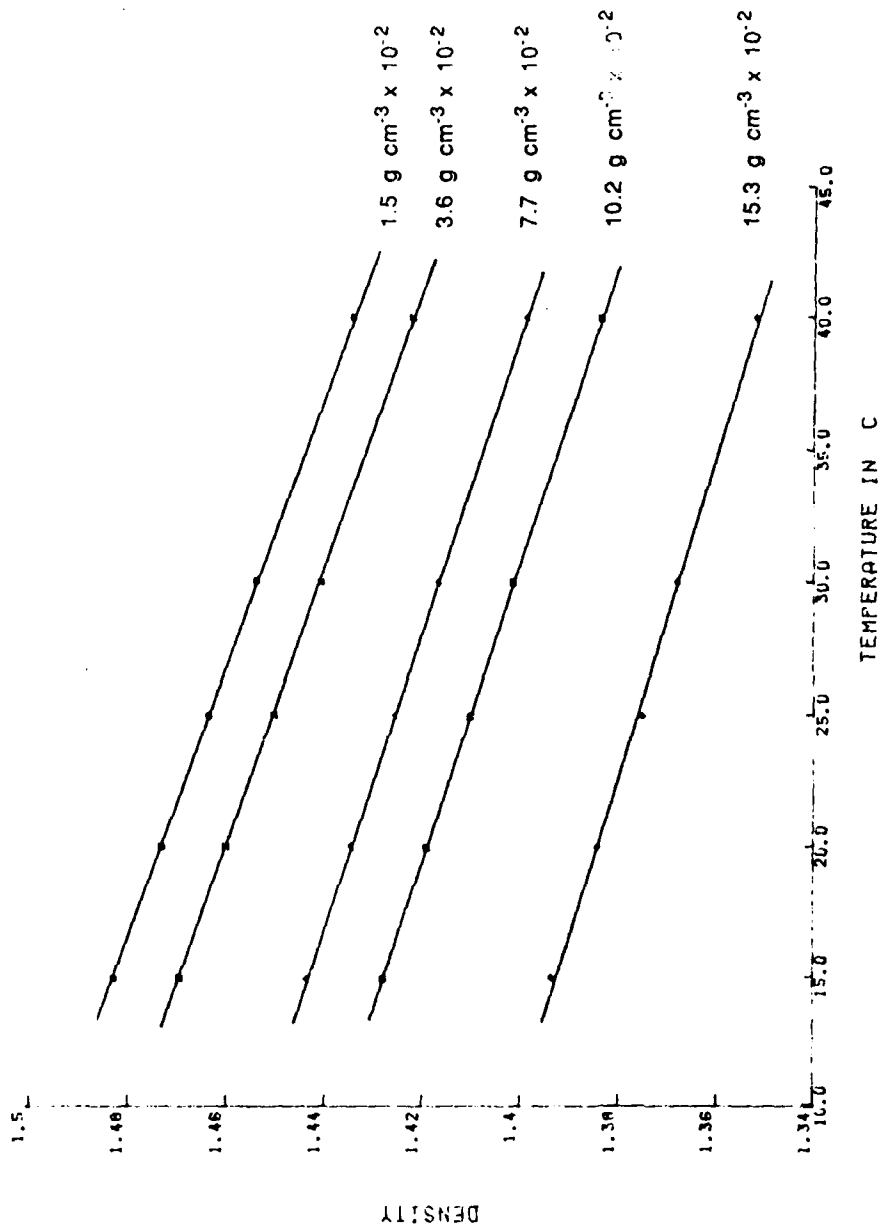


FIGURE 35. Plots of density against temperature for indicated concentrations of HTPB in chloroform.

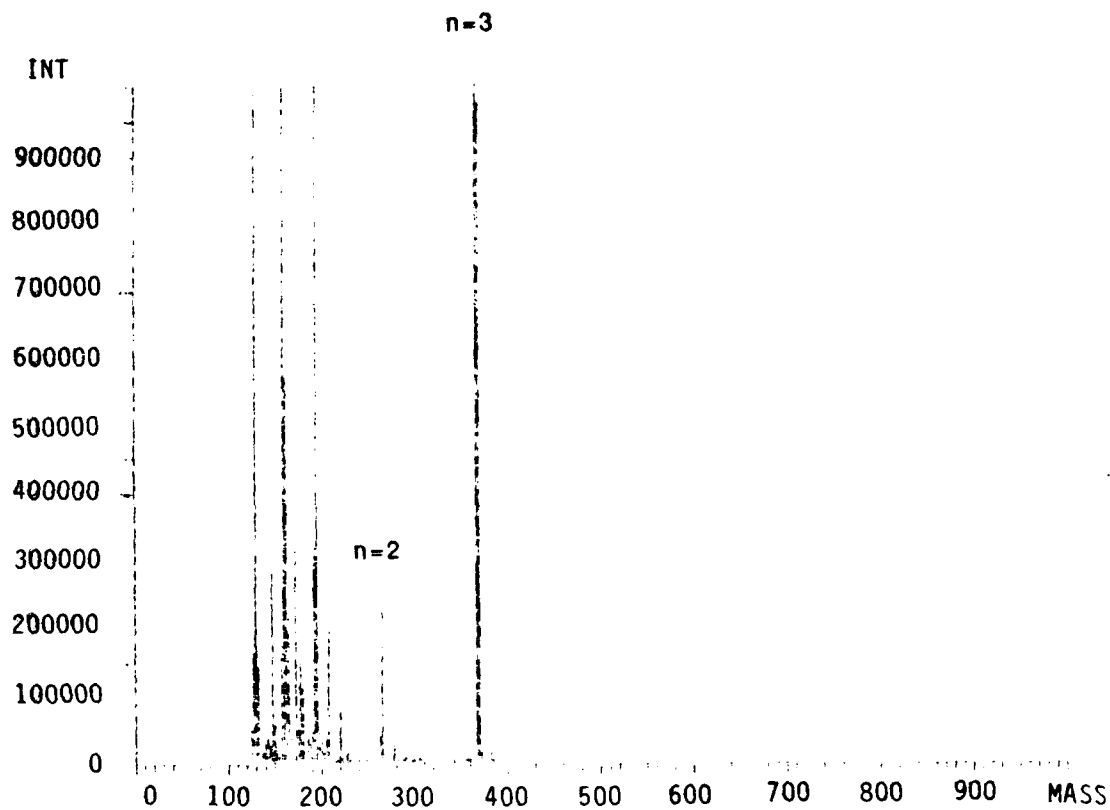
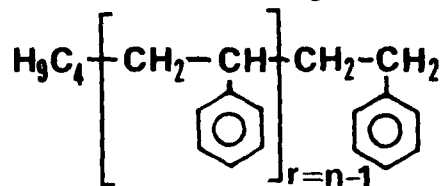


FIGURE 36. Mass spectrum of polystyrene fractions 3+4. AEI MS-902 double-focussing mass spectrometer; 70 eV electron impact ionization; 8kV accelerating potential.

The masses therefore correspond to what would be expected on the basis that the homologs were comprised of the addition or subtraction of styrene units (and not, as had been tentatively postulated at one time, of positional isomers).

The masses and molecular formulae of the first fifteen polystyrene isomers are given below, these corresponding to the general formula: $C_{8n+4}H_{8n+10}$.

TABLE 16. Molecular Formulas and Weights of Polystyrene Homologs^{a,b}



<u>n</u>	<u>M/Da</u>	<u>Formula^c</u>
0	58	C_4H_{10}
1	162	$C_{12}H_{18}$
2	266	$C_{20}H_{26}$
3	370	$C_{28}H_{34}$
4	474	$C_{36}H_{42}$
5	578	$C_{44}H_{50}$
6	682	$C_{52}H_{58}$
7	786	$C_{60}H_{66}$
8	890	$C_{68}H_{74}$
9	994	$C_{76}H_{82}$
10	1098	$C_{84}H_{90}$
11	1202	$C_{92}H_{98}$
12	1306	$C_{100}H_{106}$
13	1410	$C_{108}H_{114}$
14	1514	$C_{116}H_{122}$
15	1618	$C_{124}H_{130}$

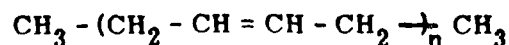
^a n corresponds also to the LC peak numbers in Figure 10, p. 35. ^b n-C₄H₉-terminated. ^c $C_{8n+4}H_{8n+10}$

The mass spectra of the preparative-scale reverse-phase LC fractions, nos. 1 through 6 were also taken. As with the semi-preparative-scale LC fractions, and with the exception of preparative fraction no. 1, these were also comprised of molecular-weight homologs. (Fraction no. 1 was clearly a very complex mixture.) Thus, for example, fraction no. 2 showed peaks for n = 2, n = 3, and n = 4; however, the former two might

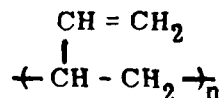
have been due to loss of a styrene unit from the back end of the molecule and so, without further spectral interpretation, it was not possible to specify quantitatively the isomer make-up of this fraction.

Characterization of Reverse-Phase LC Fractions of Polybutadienes. This portion of the mass spectrometry work was carried out at 22 eV (300 uA trap current; rhenium filament at ca. 4 A), as it was discovered early on with PBD that 70 eV resulted in very considerable fragmentation with, however, no information regarding the molecular ions. Also, the sensitivity of the instrument was considerably higher at 22 eV than at 20 eV. (The scan speed was 10 sec decade⁻¹, and the range scanned was from 950 to 100 Da.) It was found in addition that the lower molecular-weight homologs flashed off of the solid inlet system probe if the ion block was preheated. As a result, the ion block was set initially at 120°C, then gradually increased so as to reach 190°C by the end of a set of runs. In doing so, homologs of ca. 500 Da (see below) could be detected, whereas higher molecular-weight materials condensed on the source. When this was heated, they would then volatilize and be detected also. A kind of non-pyrolytic thermal analysis of the polymers was thereby implemented.

In setting out to interpret the mass spectra, the molecular ions could be explained by postulating the following structure:



i.e., methyl-terminated polybutadiene. However, due to the complexity of the fragmentation pattern below mass 400 (even at 22 eV), the possibility of branched structures resulting from 1,2-addition could not be ruled out, viz.,



In any event, and based upon the postulated structure, the molecular-weight homologs correspond to:

<u>n</u>	<u>M/Da</u>
0	30
1	84
2	138
3	192
4	246
5	300
6	354
7	408
8	462
9	516
10	570
11	624
12	678
13	732
14	786

Bulk PBD. A crude (i.e., unfractionated) sample of 500M PBD was examined first. The resultant mass spectra showed that homologs of $n = 8$ and $n = 9$ (molecular ions, respectively, of 462 and 516 Da) were quite prominent, while there were also small amounts of $n = 10$ and $n = 11$ present (570 and 624 Da). Upon heating the ion source somewhat, homologs of $n = 12$ (678 Da) and $n = 13$ (732 Da) also appeared, although the amounts were very small compared to those of $n = 9-11$. Homologs of $n = 11-13$ were evident, with the highest homolog found in the sample, $n = 14$, also being observed. (No detectable amounts of homologs higher than this were found in the material.)

Fractionated PBD. The mass spectra of each of the fractions of PBD was very puzzling. The fragmentation pattern was certainly reminiscent of PBD; however, the two major peaks corresponded to masses of 377 (100%) and 362 Da (70%), i.e., not any of the homologs listed above.

Characterization of HTPB. The low-mass spectrum of the 10% fraction HTPB showed that the polymer molecule fragmented extremely easily. Thus, the spectrum obtained at 70 eV resembled very strongly that of a mixture of alkanes. Accordingly, the electron beam was reduced to 22 eV, which, however, still gave extensive fragmentation. Even so, there were many peaks visible at greater than mass 500.

Liquid Chromatography/Mass Spectrometry. Unfortunately, the current consensus regarding LC/EI-MS is that it does not appear to be feasible on a routine basis. The difficulty is that, even though a large turbomolecular pump on the ion source can remove LC solvent of as much as $20 \text{ mm}^3 \text{ min}^{-1}$ flow rate, severe electrical arcing occurs due to the high source pressure. Thus, the only viable LC/MS interface at the present time is the moving-belt technique, wherein the solvent is removed prior to the sample entering the source chamber. However, there are so many difficulties inherent in this method (e.g., matrix effects) that it is not useful for the MS 902 mass spectrometer. Off-line LC/MS is an alternative. That is, samples collected from LC columns are introduced into the mass spectrometer via the solids-probe inlet system, which was done during the course of the work of this Phase. The sample is placed in a quartz-glass cup. The solvent is allowed to evaporate, and the probe is then inserted directly into the ion source. The technique is clearly more time-consuming than direct-inlet LC/MS; however, fractions taken off-line can be stored indefinitely. In any event, near-continuous LC/MS could thereby be effected.

There has been one major advance in the area: nebulization of liquid samples has been of major concern in atomic absorption spectroscopy for many years. One such individual, Browner, has described what he refers to as a "MAGIC" interface for LC/EI-MS. The device consists of concentric cones that are pumped differentially, such that the vacuum strips the solvent/solute solution of solvent. Also, the hollow-point cones serve to define a beam of solute (i.e., act like circular slits) such that, by the time the particle beam reaches the ion source, it is coherent as well as virtually free of solvent. The advance is a welcomed one, and the interface does in fact appear to offer the promise of direct coupling of EI as well as CI and FAB mass spectrometers with liquid chromatographs. (The device has since been made available through Hewlett-Packard.)

Phase II, Task 1. Ultra-High Resolution Reverse-Phase Microbore-Column Liquid Chromatography

It was intended in the initial portion of the work of Phase II to characterize polystyrene fractions by microbore-column liquid chromatography. Following this, the resultant optimized reverse-phase LC system(s) would then be employed for the further fractionation of R-45M, under the presumption that any separation of peaks would be due to differences in the types of branching. However, microbore-column LC even of polystyrenes proved to be less efficient with the equipment at hand than was HPLC with columns of conventional dimensions. As a result, bulk-scale fractional solution of R-45M

was resorted to, with considerable success. Very many fractions both of silylated as well as unsilylated materials were collected in this way; and each was further characterized by vapor-phase osmometry, gel-permeation chromatography, viscosity, and Fourier-transform infrared spectroscopy. Relative chain-branching functions, as well as cis-, trans-, and vinyl contents, were derived also.

Microbore-Column LC Fractionation of Polystyrenes. As described and discussed above, polystyrenes of modest molecular weight were found to be easily separable with reverse-phase LC systems. (Recall that the fan-shaped distribution of peaks corresponds to molecular-weight homologs.) However, chromatograms obtained in this portion of the work for 580M polystyrene with the microbore-column system and a mobile phase of 100% MeOH proved to be somewhat less than satisfactory. For example, the separation was worse than that achieved with conventional HPLC apparatus. Moreover, while the usual fan-like distribution of peaks was observed, the resolution between each homolog was far from baseline.

The flow rate used to generate the chromatogram was $200 \text{ mm}^3 \text{ min}^{-1}$ and, conceivably, it might be argued that this was well beyond the van Deemter optimum for microbore systems. Indeed, the optimum flow rate generally quoted for such columns is on the order of $5\text{-}10 \text{ mm}^3 \text{ min}^{-1}$. Accordingly, the flow rate was changed to $100 \text{ mm}^3 \text{ min}^{-1}$, the slowest of which the Varian LC is capable. The resolution improved somewhat over that found previously, although at the sacrifice of a considerable increase in analysis time. Moreover, neither of the two microbore-column separations was anywhere as good as that achieved for the more difficult separation with the conventional LC system. Thus, in order to realize any advantage with microbores for the analysis at hand, the flow rate would have to be reduced to that mentioned above; however, elution times on the order of hours, if not days, would then have to be endured. These requirements are clearly impractical from the standpoint of substitution of the method by polymer laboratories for those techniques being utilized currently. Bulk-scale fractional-solution fractionation was therefore resorted to at this point.

Fractional-Solution Fractionation of Untreated R-45M. Both analytical- as well as preparative-scale fractional-solution fractionation of untreated R-45M was carried out in this portion of the work as a substitute for reverse-phase liquid chromatography. However, other than the system efficiency, no great sacrifice of results arose in doing so, since solvent extraction is in principle identical to reverse-phase LC. That is, solutes are eluted in order of decreasing solubility in the mobile phase (extractant solvent) and, thus, the most-soluble solutes elute (are extracted) first. Further, and in order that homologs be eluted at roughly constant intervals, a gradient elution program can be used to alter the solvent polarity during a run (similar to temperature-programming in gas chromatography) while, in the case of discontinuous batch-wise solvent extraction, the analogous technique is changing stepwise the composition of the extractant liquid.

Analytical-Scale Fractionation. Several interesting features were immediately apparent from the results obtained for the analytical-scale solvent fractionation utilizing IPA + benzene (35°C) [as recommended by Ramey (10), and by Blanks, Shephard, and Stephens (11)]. First, the total amount obtained for fraction 1 was very large, and comprised very nearly 15% w/w of the total sample. However, this might be a result of the extraction of water, peroxides, stabilizers, and so forth; i.e., some of what was obtained could well be comprised of compounds other than R-45M. Also, there was a step-like decrease of the amounts obtained for each fraction on passing from IPA extractant through ca. 15% v/v benzene + IPA. Thereafter, the amounts obtained increased as the amount of benzene in the extractant solvent was increased until, at 40% benzene, nearly 20% of the total weight of R-45M was removed (fraction 9). The next fraction, 10, was that obtained with 50% benzene, in which all of the remaining R-45M was soluble.

Most of the fractions were obtained after standing for 18 h; however, some were allowed $\frac{1}{2}$ days for phase separation. No trends in the relative amounts obtained could be discerned, that is, the amounts recovered appeared to reach a constant value after 18 h. In a repeat of this work, each fraction was allowed at least 1 week for phase separation; the results differed little from those found in which 18-h standing times were used.

Preparative-Scale Fractionation. The work was next repeated on the preparative-scale, where the amounts used were scaled up by an order of magnitude. Thus, the starting amount of R-45M was 0.5 kg; and the total volume of extractant solvent, per fraction, was 1 dm³. The results are shown in Figure 37, and compare very favorably (certainly to within 10%) with those found in the analytical-scale experiments. For example, the total amount of analytical-scale fraction 1 was 15.0% w/w; while the preparative-scale procedure yielded 15.5%. Similarly, analytical-scale fraction 9 yielded 18.9%, while its preparative-scale counterpart comprised 18.0%.

Fractional-Solution Fractionation of Silylated R-45M. Silylation with hexamethyldisilazane (HMDS), followed by preparative-scale fractional-solution fractionation (benzene + IPA; 35°C) (as well as viscosity measurements; see later) were also carried out as part of the characterization of chain-branching.

Silylation of R-45M. Silylated R-45M was straw-to-orange colored, which was consistent with what was observed previously for this material. Also, the viscosity decreased notably upon treatment with HMDS (see later). However, FT-IR spectra of untreated and silylated materials were not as different (i.e., informative) as might otherwise be thought despite the evident disappearance of the hydroxyl band at ca. 3500 cm⁻¹.

Fractionation of Silylated R-45M. The results obtained for the amounts of HMDS-treated R-45M extracted with IPA + benzene were roughly in accord with those shown in Figure 37. The decrease in the amounts extracted as the quantity of benzene was increased from zero to 10% v/v was not nearly so dramatic as that found previously with untreated R-45M; also, the amounts extracted increased exponentially beginning with 15% v/v benzene (fraction 5). All of the fractions were orange-brown in color, viz., reminiscent of the polybutadiene standards obtained from Goodyear.

Gel-Permeation Chromatography of Fractionated R-45M. Gel-permeation chromatography of all fractions was carried out immediately following completion of the fractionation of a particular material. Also, the results were of interest from more than just the standpoint of molecular weight insofar as others have claimed that such fractions are comprised of increasing hydroxyl equivalent weight rather than molecular weight.

Plots of log M against GPC raw retention volume V_R given by the polybutadiene standards available in this laboratory (straight-line portion parallel to that of the polystyrenes standards) were constructed without incident; and the usual type of nomographic curves were obtained. The resultant peak-maximum GPC molecular weights of the untreated as well as silylated R-45M fractions are summarized in Table 17.

No unusual peak shapes or distortions were observed in the gel-permeation chromatograms of the R-45M fractions. However, differences between the GPC calibration curves for the PS and PBD standards, while not appearing to amount to much, in fact resulted in a doubling of the apparent molecular weights of the R-45M fractions. For example, fraction no. 11A had an apparent molecular weight of 50,120 when calculated from the PS standards data, yet 22,390 when the PBD standards were employed for calibration. (This emphasizes once again that appropriate standards must be employed to calibrate GPC columns if meaningful data are to be derived from the technique.)

Vapor-Phase Osmometry. It will be recalled that systematic errors were identified as inherent in vapor-phase osmometry. Nevertheless, the technique was used to measure M_n of at least modest accuracy for some of the R-45M fractions.

FRACTIONATED R-45 M

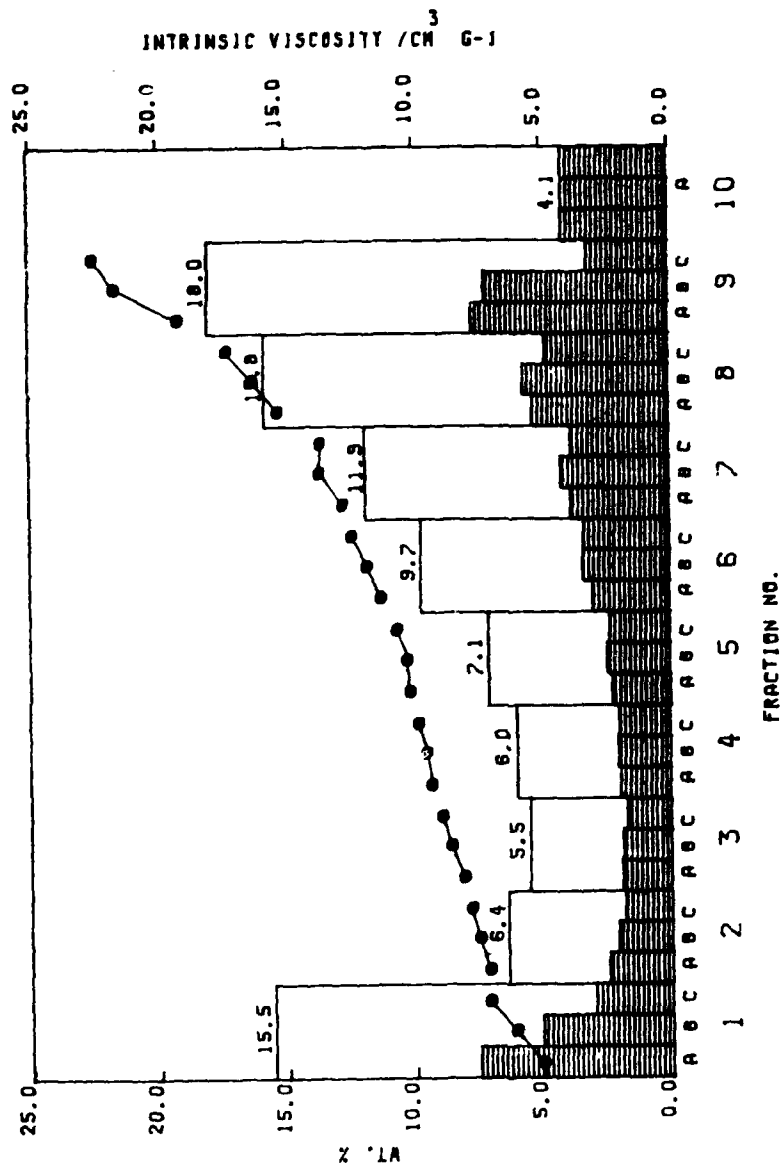


FIGURE 37. Summary bar-graph of the preparative-scale amounts (% w/w) obtained for each extraction of R-45M. Solvents: IPA, fraction 1, + 5% (v/v) increments of benzene (subsequent fractions). Intrinsic viscosities (right-hand ordinate: THF, 30°C) superposed as connected dots (see later).

TABLE 17. Summary of Preparative-Scale Amounts/% (wt/wt) and GPC Peak-Maximum Molecular Weights/Da for Indicated HMDS-Treated and Untreated Fractions of R-45M

HMDS-Treated R-45M			Untreated R-45M		
Fraction No.	M/Da	% wt/wt	Fraction No.	M/Da	% wt/wt
1A	1,060	2.72	1A	1,440	7.49
1B	1,310	2.74	1B	1,620	5.08
1C	1,625	1.95	1C	1,785	2.97
2A	1,730	1.62	2A	2,050	2.46
2B	1,955	1.75	2B	2,355	2.08
2C	1,955	1.56	2C	2,500	1.83
3A	2,220	1.55	3A	2,600	1.90
3B	2,455	1.53	3B	2,550	1.88
3C	2,300	1.47	3C	2,645	1.71
4A	2,400	1.62	4A	3,045	1.95
4B	2,485	1.78	4B	3,180	2.04
4C	2,665	1.62	4C	3,345	1.98
5A	3,040	1.77	5A	3,665	2.27
5B	3,105	1.90	5B	3,575	2.45
5C	3,200	1.94	5C	3,645	2.37
6A	3,625	2.32	6A	4,045	2.99
6B	3,820	2.46	6B	4,110	3.39
6C	4,045	2.57	6C	4,560	3.35
7A	4,470	2.60	7A	4,745	3.83
7B	4,720	3.39	7B	5,205	4.22
7C	4,965	3.11	7C	5,360	3.82
8A	5,880	3.75	8A	6,415	5.33
8B	6,070	3.79	8B	7,430	5.67
8C	6,625	3.80	8C	8,505	4.82
9A	7,140	5.25	9A	10,230	7.66
9B	8,470	6.89	9B	11,630	7.17
9C	9,950	6.19	9C	13,010	3.15
10A	12,810	10.20	10A	28,355	4.14
10B	18,115	10.19			
10C	30,640	3.15			
11A	30,247	2.80			

Densities of Standard Solutions of Benzil. One of the most convenient means of making up standard solutions of benzil for calibration of the VPO is weighing a known amount of the (solid) standard into a tared 5- or 10-cm³ volumetric flask and then diluting to the mark with the solvent of choice. (Volume dilution is in any event much more accurate as well as convenient than dilution by weight when volatile solvents are employed.) Then, in order to make up subsequent dilutions of the stock, a known volume would be added to a second volumetric flask, diluting again to the mark; and so on. However, the relevant form of data reduction in VPO is a plot of the instrument reading (mV) against the solution molality m/g kg⁻¹ solvent. Further, diluting a solution of some molality with an equal volume of pure solvent will not result in a 50:50 decrease in m unless the densities of the pure solvent and the solution are identical. For highly dilute solutions the error will be minimal; even so, and in order to attempt to account for all possible sources of error in the VPO technique, the densities of benzil solutions were measured as functions of concentration and temperature. The data are presented in Table 18. The extremum values, 1.4872 and 1.4613 g cm⁻³, in fact differ by 1.8%. Differences in solvent and solution densities were therefore taken into account in calculating the molalities of all solutions in what follows.

TABLE 18. Densities of Listed Chloroform Solutions of Benzil at Indicated Temperatures

m/g kg ⁻¹	r/g cm ⁻³					
	15°C	20°C	25°C	30°C	35°C	40°C
0.	1.4872 ₂	1.4831 ₆	1.4798 ₅	1.4765 ₀	1.4748 ₂	1.4717 ₂
9.984	1.4827 ₂	1.4786 ₆	1.4757 ₅	1.4724 ₀	1.4712 ₂	1.4681 ₂
15.100	1.4807	1.4769	1.4741	1.4713	1.4701	1.4674
22.667	1.4781	1.4744	1.4718	1.4689	1.4679	1.4654
30.180	1.4760	1.4722	1.4697	1.4669	1.4665	1.4638
34.850	1.4737	1.4706	1.4683	1.4658	1.4654	1.4630
40.958	1.4713	1.4682	1.4662	1.4637	1.4635	1.4613

Calibration Plots with Chloroform and THF Solvents. Having established that the VPO was functioning satisfactorily, and having also learned to correct for solution densities in making up standards, the instrument was calibrated with benzil dissolved in chloroform and THF solvents. The raw data for chloroform solutions at 35.0° and at 37.5°C gave a line of slope 170.8 mV/m. Moreover, the points at 35.0°C established that the instrument constant was relatively insensitive to small (ca. 2-4°) temperature changes. However, the constant was at considerable variance from that obtained by AFAL personnel for THF and 1,2-dichloroethane solvents and so, as an additional check on the instrument, the benzil standard was rerun in THF. The resultant slope was 92.2 mV/m, in good agreement with that found by AFAL.

VPO of Polystyrenes Fractions. All of the polystyrene fractions collected by preparative LC were run next. The results gave excellent straight lines for all fractions. Moreover, the nominal number-average molecular weights determined from these runs were in very good agreement with those measured previously. Thus, the results of this evaluation (instrument working well; excellent return to zero) turned out to be nearly identical to those obtained more than a year prior (random variation of instrument zero). That is, the VPO technique was confirmed to be accurate to no better than ± 15% for the determination of number-average molecular weights, and the method was therefore abandoned.

Viscosity. The measurement of viscosity was explored in very great detail, as such data, together with GPC peak-maximum molecular weights, are required for calculation of relative chain-branching functions. Accordingly, the precision and accuracy of the data arising at each step in making viscosity measurements were carefully evaluated. Several major sources of error were thereby identified.

Independent Calibration of the Viscometer Tube. The viscometer-tube calibration constant B supplied by Cannon was first verified. (Chloroform solvent was used at this stage.) In order to check it, the viscosities of chloroform were required over the temperature range of interest, here, 15-40°C. These were obtained from the equation provided by Dreisbach ("Physical Properties of Chemical Compounds", Vol. II, p. 196):

$$\log \eta/cS = -1.57472 + 338.5/T$$

where T is in K. Comparison of the values calculated from this relation with those determined experimentally gave excellent agreement. An indication of the goodness of fit of the calculated data was that the worst discrepancy amounted only to 0.3% at 20°C. This level of variation is negligible in comparison with the level of impurities that are normally encountered in reagent-grade solvents. [No special precautions (e.g., drying over molecular sieves) were taken with the chloroform used in this portion of the work. For highest accuracy, "HPLC-" or "Spectro-grade" solvents should be used.]

Next, having ascertained the viscosities of chloroform as a function of temperature, the apparent constants (labeled as B') of the viscometer tube were determined over the temperature-range 15-40°C, as described in the Experimental Section. The raw fall times were in all cases less than 200 sec. Thus, and in accordance with ASTM Procedure D-445, each required that the kinetic-energy correction be applied. This takes the form:

$$\eta/cS = Bt - E/t^2$$

where the E-term is given by:

$$E = \frac{1.66V^{3/2}}{L(Bd)^{1/2}}$$

where V, L, and d are the volume of bulb C (cm³), the length of the working capillary tube H (cm), and the diameter of the working capillary (cm), respectively. These dimensions are provided in ASTM D-446 and are, for the Ubbelohde OC tube, 2.0 ± 0.1 cm³, 9.0 ± 0.1 cm, and 0.036 ± 0.007 cm. Putting these value into the above relation then gives:

$$E = \frac{2.74954}{B^{1/2}}$$

The resultant B values obtained in this portion of the work gave a standard deviation of the average of ± 0.000001 cS sec⁻¹; while the confidence interval at the 95% level (Student t value of 2.57 for 5 degrees of freedom) was ± 0.000002 cS sec⁻¹. Thus, the confidence interval of the average ranged from 0.002843 to 0.002839 cS sec⁻¹. This was clearly outside that stated on the Calibration Certificate, viz., 0.002832 cS sec⁻¹, the discrepancy amounting to ± 0.15%. This might have been due to several factors. First, the gravitational constant in Pennsylvania is 980.1 cm sec⁻², whereas it is 979.5 cm sec⁻² in San Diego (32.43° N latitude). The correction for this is found by multiplying the Calibration value of B by the ratio of the gravitational constants, here, (0.002832)(979.5/980.1) = 0.002830 cS sec⁻¹. Thus, taking into account the acceleration due to gravity makes the discrepancy worse by roughly 0.01%. A potentially larger source of error arises from the possibility of variations in the dimensions of the tube in the calculations used to derive the above relation. Also, the reagent-grade chloroform used in the work may have a significantly-different viscosity from that utilized to derive

the first of the above relations. In any event, a value of $0.002841 \text{ cS sec}^{-1}$ for the (temperature-independent) constant B was used in all subsequent studies.

Importance of Viscometer Cleaning. Having found at this point that the apparatus and procedures gave results that agreed at least to within $\pm 0.15\%$ of the Cannon calibration, the extent that the cleanliness of the tube affected fall times was tested. To do so, a solution of 27.3054 m (molal; g solute per kg solvent) of bulk 580M polystyrene in chloroform was used. It was degassed, and was then transferred to the viscometer tube and allowed to come to thermal equilibrium as described in the Experimental Section. (It was later determined that degassing had no measurable effect on fall times.) Next, a series of runs was carried out without cleaning the tube between each run. That is, solution was taken up into the capillary arm; allowed to fall; taken up again; and so on. The extraordinary results are provided below in Table 19.

TABLE 19. Successive Raw Fall Times and Resultant Calculated Viscosities n/cS of 27.3054 m Solution of 580M Polystyrene in Chloroform at 15°C (Tube Not Cleaned Between Runs; B constant of $0.002842 \text{ cS sec}^{-1}$)

<u>Run No.</u>	<u>Fall Time/sec</u>	<u>n/cS</u>
1	171.36	0.4870
2	195.60	0.5559
3	196.92	0.5596
4	211.62	0.6014
5	211.62	0.6014
6	225.48	0.6408
7	215.34	0.6120
8	226.56	0.6439
9	228.00	0.6480
10	229.50	0.6522
11	229.20	0.6513
12	242.58	0.6894
13	251.94	0.7160
14	246.24	0.6998
15	259.56	0.7377

Thus, the apparent viscosity nearly doubled over the course of the 15 runs. Contamination of the viscometer-tube capillary walls was in fact found to be the major source of error throughout this work. The error is understandable in terms of the widely-used dynamic coating technique of fabrication of open-tubular GC columns, wherein a dilute solution of stationary phase is pumped slowly through a capillary tube. This leaves behind a thin film of the phase on the column walls, which can approach as much as 2 μm in thickness depending upon its concentration in the coating solution.

Also tried in this portion of the work was rinsing with various combinations of chloroform, methylene chloride, and acetone, none of which gave results that were any better than those shown above. Accordingly, viscosity measurements must be carried out in conjunction with thorough cleaning of the tube between each run with fresh hot chromic acid; data acquired in work for which this is not the case must otherwise be considered highly suspect.

Measurement of Viscosity of Bulk R-45M. Having identified the major sources of error, as well as error limits, of the apparatus and procedures at hand in this laboratory,

measurement of the viscosity of the bulk R-45M provided by AFAL was next undertaken. Also, and in order to permit comparisons with the data of others, THF solvent was employed. This had the added advantage of being a "good" solvent, i.e., for which intrinsic viscosities are temperature-independent. The measurements were therefore confined to 30°C. In addition, data reduction was simplified by plotting $(1/c)(t - t_0)/t_0$ against c ; where $c/g\text{ cm}^{-3}$ is a weight-based concentration, t is the fall time of the solution, and t_0 is the fall time of the solvent. Extrapolation to $c = 0$ then yielded $[\eta]$ as the ordinate intercept. Note that this method is precisely equivalent to the use of viscosity-converted data; however, the conversion factor (the B constant of the viscometer tube) cancels out. Further, the densities of the (highly-dilute) solutions were found to differ from that of neat solvent by less than 0.5% and so, errors incurred on account of different solution specific gravities were minimal. (This was not true for chloroform solvent, density of 1.5 g cm^{-3} , since that for R-45M is ca. 0.9 g cm^{-3} .)

The results revealed several interesting trends. First, there was no question of the linearity of the data at values of c greater than 0.02 g cm^{-3} . However, the regression curved downward at concentrations less than this. That is, the function $(1/c)(t - t_0)/t_0$ went to zero as c went to zero. This is as it should be, since $(t - t_0)/t_0$ goes to zero despite $1/c$ going to infinity. The data thus demonstrated that concentrations of greater than ca. 0.03 g cm^{-3} must be used in order to define the linear portion of the plot. Also, the way in which the measurements were carried out involved making up the solution of interest in a volumetric flask, and then transferring 15.00 cm^3 of the liquid (following thermostating for at least 20 min at the temperature of interest) to the viscometer tube with a volumetric pipet. Thus, at least 25 cm^3 of solution was required, which in turn meant that at least 0.75 g of prepolymer was needed to start with in order to be able to make up the most dilute solution that could be run with confidence. Assuming that 0.1 g cm^{-3} is the upper limit of concentration that should be run in defining the linear portion of the plot, 2.5 g of prepolymer is then required for this solution. Altogether, then, ca. 5 g of material is needed for the measurement of viscosity of an adequate number of solutions covering a range of concentrations.

The amount of prepolymer required can be reduced somewhat by first making up the most concentrated solution, and then diluting it in turn down to the lower limit of ca. 0.03 g cm^{-3} . However, the fall times of diluted solutions were irreproducible, because the volumetric flask as well as the vial required cleaning with fresh hot cleaning solution; failure to do so caused to the irreproducibility mentioned above. This was surprising because the surface area of such flasks is small, and it is difficult to imagine that contaminants left on the walls could affect the measurements to the extent observed. Nevertheless, reproducible data were obtained only after these additional cleaning steps were incorporated into the procedures.

Comparison of Results with Viscosity Data of Carver. Carver (2) reported the intrinsic viscosities of several lots of R-45M (source not given) in THF (30°C). The average for all batches was $20.49\text{ cm}^3\text{ g}^{-1}$; the low being $18.93\text{ cm}^3\text{ g}^{-1}$, with a high of $22.02\text{ cm}^3\text{ g}^{-1}$. The result of this work was $15.70\text{ cm}^3\text{ g}^{-1}$, which is of course appreciably different from Carver's work. Both sets of data may in fact be correct, although such a substantial discrepancy might otherwise be considered to be somewhat unusual. (It may be relevant that Carver employed a Cannon-Ubbelohde No. 25 viscometer tube; however, the viscosity limit of this device is 0.5-2 cS, which is close to that of the Ubbelohde No. 0C tube employed in this work, 0.6-3 cS. Also, each device operates in the same manner in that both are distinguished by the lower meniscus of falling fluid being "suspended" immediately below the working capillary. According to ASTM D-446, this then ensures a uniform driving head of liquid that is independent of the quantity of sample placed in the viscometer and, thus, the viscometer constant is independent of temperature. Also, by making the diameter of the lower meniscus approximately equal to the average diameter of the upper meniscus, the kinetic-energy correction is greatly reduced.)

Measurement of Viscosity of Fractionated R-45M. The fall times of solutions of the fractions of fractionated R-45M were taken in THF as described above over the temperature-range 15-40°C. Data reduction was performed by plotting $(1/c)(t - t_0)/t_0$ against c . The results for fraction no. 10A are presented in Figure 38 as a typical example.

First, there was no question of the temperature-independence of the data. That is, THF is a "good" solvent for fractions of R-45M since, otherwise, the plot would have been curved concave to the abscissa (an indication of a "poor" solvent becoming a "good" solvent as the temperature was increased). Accordingly, the intrinsic viscosity of R-45M need henceforth be determined only at 30°C. In addition, the Mark-Houwink data-reduction treatment (see later) was applied without the worry that K and a would be temperature-dependent.

Interestingly enough, the value obtained for fraction no. 10A, $21.2 \pm 0.3 \text{ cm}^3 \text{ g}^{-1}$, corresponded precisely to the average value of the intrinsic viscosities of several lots of R-45M reported several years ago by Carver.

Measurement of Viscosity of Fractionated HMDS-Treated R-45M. The intrinsic viscosities of the fractions of silylated R-45M were also determined as described above; the results are shown in Table 20. They can be summarized by saying that there was not much difference between the two sets. That is, it was originally supposed that the hydroxyl content of R-45M might be determined simply by measuring the viscosity difference between silylated and untreated materials. However, the average hydroxyl content is apparently too small to result in viscosity differences of greater than ca. 10%.

Mark-Houwink Constants. The Mark-Houwink constants for PBD were determined first. In order to do so, the intrinsic viscosities of each standard were measured. The results for 500, 1000, and 22,000 Da were 2.0356, 3.4423, and $39.1161 \text{ cm}^3 \text{ g}^{-1}$, respectively (THF; 30°C). These data then gave Mark-Houwink values of: $a = 0.7811$ and $K = 0.0159$. For example, the molecular weight of the 1000M PBD standard is calculated to be 980 Da using these values and the usual relation: $[\eta] = K M^a$. Several iterations with different fractions of untreated R-45M next yielded the best-fit Mark-Houwink constants: $K = 0.0490$ and $a = 0.6510$. Also, the constants for silylated R-45M were found to be: $K = 0.0510$ and $a = 0.6440$. The goodness of fit of these values is illustrated in Table 21, where the GPC molecular weights observed experimentally are compared with those calculated from the intrinsic viscosity data and the above K and a constants. Clearly, the Mark-Houwink constants do in fact permit reasonably accurate calculation of M .

Branching. The method outlined by Coleman and Fuller (20) was used to derive the branching parameter n for the silylated fractions. However, the values did not vary in a consistent manner, which has also been found to be the case by others. Thus, fraction 1C gave 1×10^{-4} ; fraction 2C gave 2×10^{-4} ; fraction 9A gave 1×10^{-5} , and so on. Overall, the values averaged ca. 5×10^{-5} .

Plots of $[\eta]$ vs. molecular weight are frequently said to describe inverted parabolas, that is, the extent of branching passes through a maximum as the prepolymer M increases. However, it has also been noted that $[\eta]$ is in fact essentially constant below ca. 10,000 Da, which corresponds roughly to the results observed in this work.

Type and Extent of Unsaturation. As an ancillary part of studies relating to chain-branching, a critical examination of the ARCO method for determination of the cis-, trans-, and vinyl-contents of the silylated fractions were carried out. Essentially, the technique makes use of IR bands at certain wavelengths (cis isomer: 13.8 μm ; vinyl isomer: 11.0 μm ; trans isomer: 10.38 μm), corrected for the respective molar absorptivities. The ARCO method also recommends CS_2 as the solvent. It was found, first, that the absorption spectrum of the silylated fractions was strongly solvent-dependent; that is, use of a different solvent gave entirely different results. An alternative technique known as attenuated total reflectance (ATR) was therefore examined, where neat sample

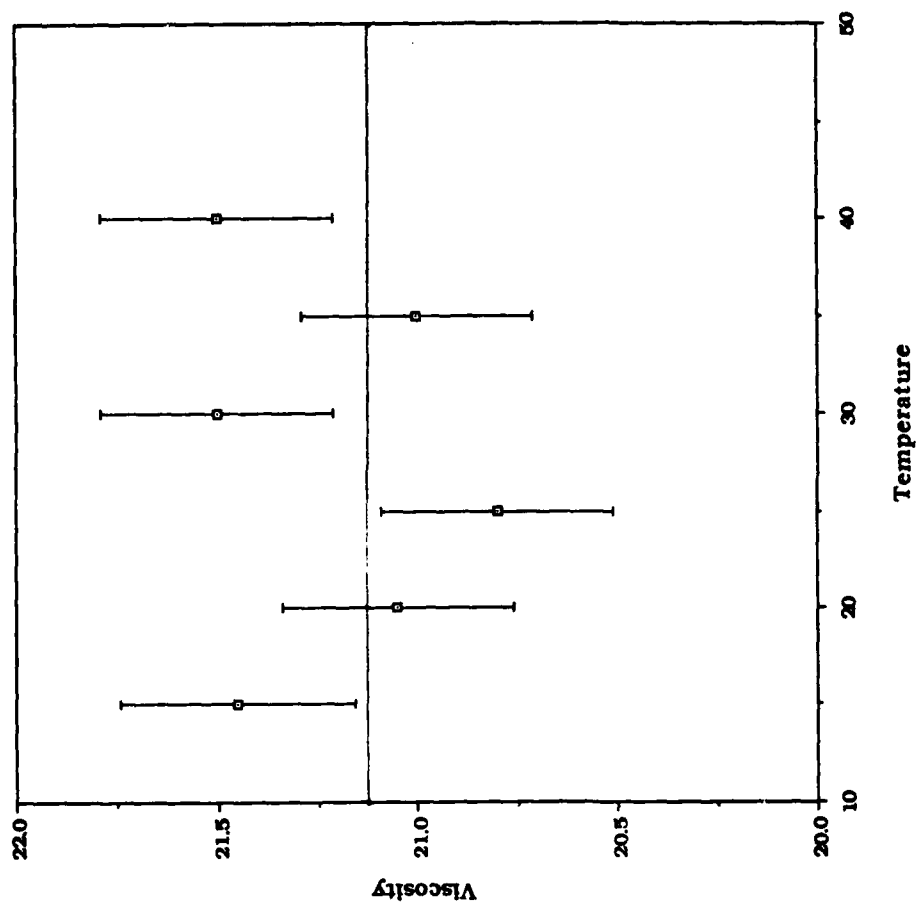


FIGURE 38. Intrinsic viscosities of fraction 10A of R-45M at indicated temperatures.

TABLE 20. Comparison of Intrinsic Viscosity Data $[\eta]/\text{cm}^3 \text{g}^{-1}$ at 30°C for Indicated HMDS-Treated and Untreated Fractions of R-45M Obtained at 35°C with Mixtures of IPA + Benzene

HMDS-Treated R-45M		Untreated R-45M	
Fraction No.	$[\eta]/\text{cm}^3 \text{g}^{-1}$	Fraction No.	$[\eta]/\text{cm}^3 \text{g}^{-1}$
1A	5.703	1A	5.047
1B	5.177	1B	6.083
1C	5.844	1C	7.068
2A	6.026	2A	6.056
2B	6.666	2B	7.420
2C	7.301	2C	7.755
3A	7.761	3A	8.027
3B	7.688	3B	8.538
3C	7.600	3C	8.887
4A	8.414	4A	9.278
4B	8.870	4B	9.50
4C	8.715	4C	9.810
5A	9.178	5A	10.17
5B	9.068	5B	10.25
5C	9.561	5C	10.57
6A	10.21	6A	11.26
6B	10.22	6B	11.82
6C	10.45	6C	12.40
7A	10.57	7A	12.72
7B	11.89	7B	13.66
7C	12.73	7C	13.60
8A	12.37	8A	15.27
8B	13.50	8B	16.25
8C	13.45	8C	17.26
9A	14.71	9A	19.11
9B	15.81	9B	21.63
9C	16.67	9C	22.47
10A	20.85	10A	38.22
10B	22.82		
10C	24.55		
11A	40.32		

TABLE 21. Comparison of GPC Molecular Weights (M/Da) with Those Calculated from Best-Fit Mark-Houwink Constants (M-H) for Indicated R-45M Fractions

HMDS-Treated R-45M			Untreated R-45M		
Fraction No.	M/Da		Fraction No.	M/Da	
	GPC	M-H		GPC	M-H
1A	1,060	1,510	1A	1,440	1,235
1B	1,310	1,305	1B	1,620	1,645
1C	1,625	1,575	1C	1,785	2,075
2A	1,730	1,650	2A	2,050	1,635
2B	1,955	1,930	2B	2,355	2,235
2C	1,955	2,225	2C	2,500	2,390
3A	2,220	2,450	3A	2,600	2,520
3B	2,455	2,410	3B	2,550	2,770
3C	2,300	2,370	3C	2,645	2,950
4A	2,400	2,775	4A	3,045	3,150
4B	2,485	3,010	4B	3,180	3,265
4C	2,665	2,930	4C	3,345	3,430
5A	3,040	3,175	5A	3,665	3,625
5B	3,105	3,115	5B	3,575	3,670
5C	3,200	3,380	5C	3,645	3,850
6A	3,625	3,750	6A	4,045	4,240
6B	3,820	3,755	6B	4,110	4,570
6C	4,045	3,885	6C	4,560	4,915
7A	4,470	3,955	7A	4,745	5,110
7B	4,720	4,750	7B	5,205	5,705
7C	4,965	5,280	7C	5,360	5,665
8A	5,880	5,050	8A	6,415	6,770
8B	6,070	5,780	8B	7,430	7,450
8C	6,625	5,750	8C	8,505	8,170
9A	7,140	6,605	9A	10,230	9,555
9B	8,470	7,390	9B	11,630	11,555
9C	9,950	8,020	9C	13,010	12,250
10A	12,810	11,355	10A	28,355	27,705
10B	18,115	13,065			
10C	30,640	14,635			
11A	30,247	31,620			

wherein neat sample is coated onto the faces of a transmitting crystal. The IR beam is then reflected internally in a zig-zag path through the crystal, where reflections take place just beyond the crystal-sample interface. Thus, the IR beam is attenuated by whatever extent the thin film of sample absorbs the radiation. The technique has the advantage that no solvent is required whatsoever, so long as the sample can be held against the crystal faces.

ATR was found to be ideal for bulk untreated as well as silylated R-45M fractions, which are tacky fluids and which were found to wet the ATR crystal very well. Also, no special care or precautions were required in coating the crystal faces (disposable wooden spatulas were used in this portion of the work to do so). This was so because the internally-reflected ATR beam passes beyond the face of the crystal by a certain amount each pass, no matter what is coated onto the crystal surface. Thus, a uniform path length is obtained irrespective of the thickness of the sample film, so long as the thickness exceeds the distance the IR beam travels beyond the crystal interface. In the present instance, although the number is difficult to estimate, the distance is much less than a micron. That is, the sample thickness need be only a micron to ensure an adequate coating of the crystal. There was the added advantage of the ATR technique as well, that when a spectrum had been taken, the cell was cleaned simply by washing the crystal face with chloroform. The situation could hardly be more favorable for taking IR spectra of tacky prepolymers such as R-45M, particularly since the results are solvent-independent. The spectra of neat silylated fraction 1A obtained by ATR FT-IR is presented as an example in Figure 39.

It was found that the trans/vinyl ratios were approximately constant. Also, the cis band was about the same height on passing from the first to the tenth fraction. (However, there were a large number of other differences in the spectra.) In any event, presented below in Table 22 are the cis-, trans-, and vinyl contents of each of the silylated R-45M fractions found by the ATR technique. Those with the carbon disulfide methodology are presented for comparison.

The cis-, trans-, and vinyl-contents of the Thiokol lots of R-45M were also measured by the ATR FT-IR technique. Interestingly, the spectra failed to reveal any differences in the materials. The respective types of unsaturation were calculated to be 32.6, 33.6, and 33.9% (cis-content; lots 1A-200, 1B-108, and 2A-404, respectively); 24.6, 24.1, and 24.2% (vinyl-content); and 42.8, 42.3, and 41.9% (trans-content). These compare very favorably with the averages of the values found for the fractionated HMDS-treated R-45M, viz., $35.4 \pm 1.9_5$ (\pm standard deviation), $23.4 \pm 0.6_6$, and $41.2 \pm 1.5_4$ % for the cis-, vinyl-, and trans-contents, respectively. That is, silylation appeared to have had no effect on the type and extent of unsaturation when assessed by FT-IR.

It might be argued at this point that the results could depend upon the thickness of the prepolymer layer coated onto the flat-plate crystal (KRS-5: thallium bromide-iodide). Accordingly, an alternative cell system was evaluated that was comprised of an optical rod of ZnSe placed parallel to the long axis of a cylindrical boat. The technique is known as cylindrical internal reflectance (CIRCLE), and has the advantage that when the boat is filled with liquid sample (ca. 1 cm³) the surface of the rod is in intimate contact with a uniform layer of material. However, in principle, the technique is identical to ATR for neat samples. Further, bulk liquid beyond the interfacial boundary layer is not seen at all either by ATR or by CIRCLE. This was verified insofar as the ATR and CIRCLE cells gave the same results for identical samples of neat prepolymer.

Phase II, Task 2. Liquid Chromatography/Mass Spectrometry

It was intended in this portion of Phase II that the lower molecular-weight fractions of polystyrene and R-45M would be used in conjunction with reverse-phase microbore-column liquid chromatography/mass spectrometry to characterize further chain branching in the latter prepolymer. However, as noted earlier, microbore-column LC was not as efficient as conventional-bore HPLC. Also, and in contrast with the polystyrenes fractions obtained in the last interim period, polybutadiene and hydroxy-terminated polybutadiene prepolymers even of low molecular weight failed to give useful mass spectra of any kind, as discussed below. An alternative technique, inverse gas chromatography, was therefore developed for this portion of the Contract.

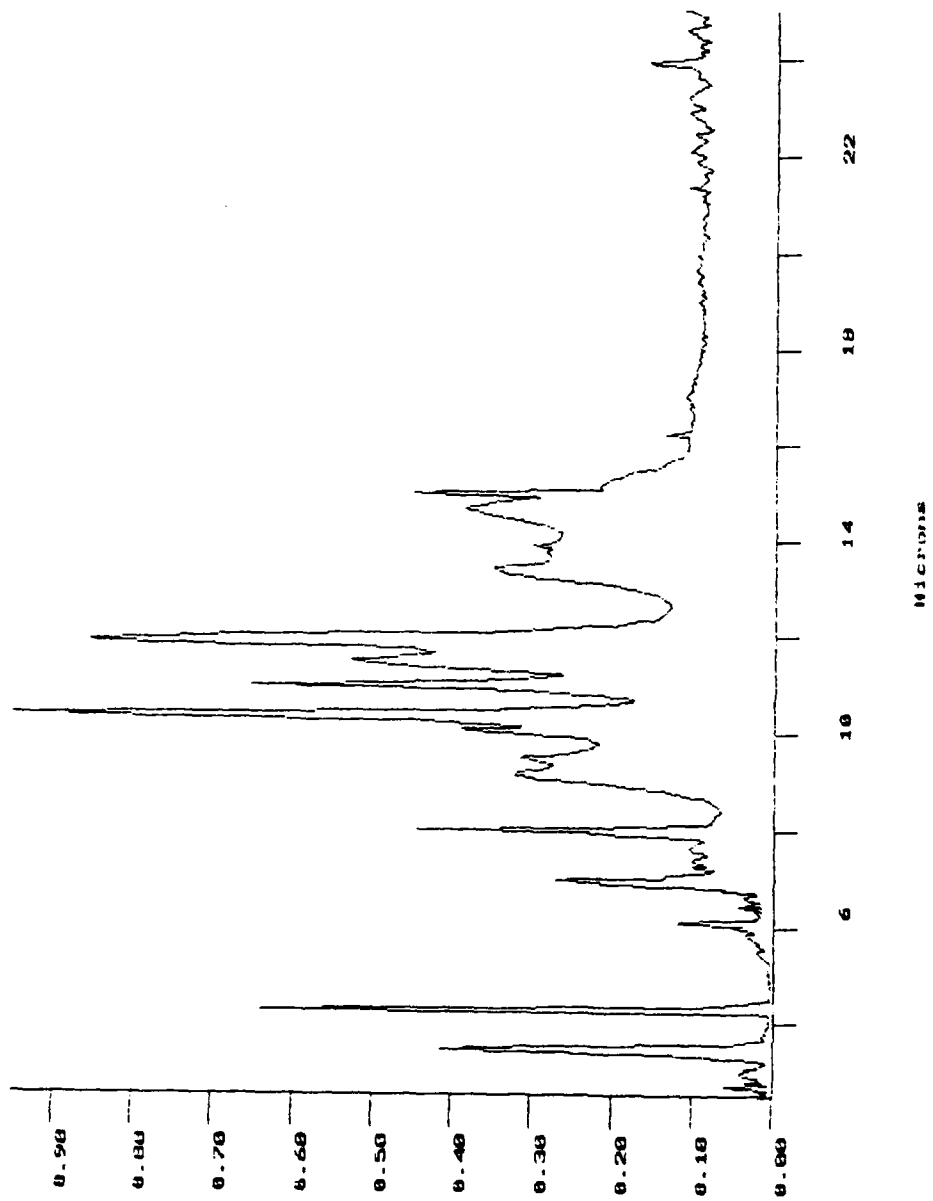


FIGURE 39. ATR FT-IR spectrum of fraction 1A.

TABLE 22. Cis-, Trans-, and Vinyl-Contents of Silylated R-45M Fractions Obtained by ATR FT-IR

Fraction No.	Cis/%	Trans/%	Vinyl/%	Fraction No.	Cis/%	Trans/%	Vinyl/%
1A	40.8 [#]	37.7 [#]	21.5 [#]	6A	35.1	41.2	23.7
	70.0 [#]	18.0 [#]	12.0 [#]	6B	37.6	39.3	23.1
	56.0 [#]	24.8 [#]	19.2 [#]	6C	32.9	43.8	23.3
1B	36.4	41.0	22.6				
1C	36.6	39.9	23.5				
2A	37.1	39.0	23.9	7A	33.6	42.2	24.2
2B	36.7	39.1	24.2	7B	34.7	41.8	23.5
2C	35.5	40.8	23.7	7C	34.6	41.6	23.8
3A	37.3	40.3	22.4	8A	34.0	42.3	23.7
3B	34.2	42.3	23.5	8B	33.3	42.7	24.0
3C	35.2	41.5	23.3	8C	33.2	43.2	23.6
4A	34.5	41.8	23.6	9A	39.8	38.0	22.2
4B	34.5	42.0	23.5	9B	32.8	43.4	23.8
4C	34.9	41.4	23.7	9C	33.2	43.3	23.5
5A	34.5	41.8	23.7	10A	34.7	41.9	23.4
5B	34.6	41.7	24.7	10B	34.8 [*]	41.8 [*]	23.4 [*]
5C	34.6	41.5	23.9		23.6 [*]	51.4 [*]	25.0 [*]
				10C	38.4	39.2	22.4
				11A	36.3	41.0	22.7

* CS₂ solvent. # Acetone solvent.

Mass Spectrometry of R-45M Fractions. In seeking to establish chain-branching in fractional-solution fractions of R-45M, the efficacy of electron-impact (EI) mass spectrometry was evaluated. It proved to be of little use, since very extensive fragmentation patterns were found even at 20 eV. A Fourier-transform ion-cyclotron-resonance (FT-ICR) mass spectrometer equipped with a fast-atom bombardment (FAB) source was therefore examined. This method of ionization is one of the "softest" (i.e., least-energetic) that is currently available, and usually gives enhanced molecular ions with little or no fragmentation. However, even the lowest molecular-weight fraction of silylated R-45M failed to produce useful spectra. Accordingly, a FAB gun (Ar gas) from Frazer Scientific (marketed through Vacuumetrics) was fitted to the MS902. (The advantage of this particular unit is that the sample is contained on a probe tip, and the entire apparatus goes into the MS directly through the solids-probe inlet port, i.e., no new or specialized ion sources are required other than the existing ion source.) The result obtained with the FT-ICR MS was repeated, namely, that the sample could be sputtered off of the probe. Unfortunately, however, no meaningful fragments either of derivatized or of underivatized R-45M could be distinguished.

Inverse Gas Chromatography. Historically, and with very few exceptions, inverse gas chromatography has been limited to the study of the gross morphology of individual polymers: this or that material is employed as a GC stationary phase, and discontinuities in plots of log(probe-solute relative retentions) (usually n-alkanes) against reciprocal temperature are used to determine the degree of crystallinity, glass transitions, and so forth (30). However, the inverse GC technique is remarkably sensitive as well to small changes in the physicochemical properties (viscosity, functionality, molecular weight,

etc.) of the liquid phase. Moreover, **high-precision** gas chromatographic instrumentation is capable of detection of differences in partition coefficients and, more pertinent to polymer studies, specific retention volumes $V_g^0 (= 273 K_R / r_s T_c)$, where r_s is the density of the stationary phase at the column temperature T_c) of probe-solutes at the level of $\pm 1\%$. Thus, the averaged molecular weight, chain-branching, and functionality content of this or that material can in principle be determined simply by fabricating a GC packing from it and then measuring the retentions of appropriate probe-solutes. For example, partition coefficients vary inversely as the stationary-liquid molecular weight and so, the retentions of n-alkanes offer a measure of M irrespective of the nature of the prepolymer. Also, alcohol and ketone solutes are presumably sensitive to the hydroxyl content of species such as R-45M and so, would be the appropriate probe-solutes for gauging this property of this prepolymer. In addition, simulated aging can be carried out by passing air of a given humidity through the column at some appropriate temperature and then re-chromatographing the probe-solutes; where differences in the retentions measured before and after aging reflect the kinds and magnitudes of changes that have taken place.

Accordingly, and because of the attendant advantages of simplicity, precision, ease, and accuracy of the technique, the potential utility of the inverse GC method was evaluated in this portion of the work as an alternate method of characterizing Defense-related prepolymer materials in general, and R-45M in particular. In the course of doing so, the specific retention volumes of a bank of 23 solutes, comprised of normal- and branched aliphatic, aromatic, alicyclic, heterocyclic, and heterofunctional hydrocarbons, were determined over the temperature-span 30-80°C with four batches of R-45M.

Reproducibility of the GC Technique. Despite the very many studies over the years that have confirmed the reproducibility of the GC technique (20,27), an investigation of the precision with which probe-solute specific retention volumes with R-45M could be measured with the instrumentation to hand in this laboratory was nevertheless carried out. Also, it was not known in advance whether this prepolymer was suitable for use as a stationary phase, that is, whether its volatility was sufficiently low (ca. 0.01 torr) at upwards of 100°C; and whether the material was stable at least over the duration of the use of the columns (ca. 3 days each).

It was found, first, that R-45M (as well as PBD of 1000 and 2500 Da) was ideally suited as a stationary phase insofar as no column bleed was observed at the maximum temperature (90°C) of the system thermostat and at maximum sensitivity of the thermal conductivity detector. In addition, repeated cycling of the temperature, coupled with reinjection of several of the solutes, demonstrated that the properties of the stationary packings remained invariant over the course of individual experiments.

Specific Retention Volumes of Probe-Solutes. The fully-corrected specific retention volumes $V_g^0 / \text{cm}^3 \text{g}^{-1}$ were next determined for all probe-solutes (minimum of three replicate injections of each) with four lots of R-45M at 30-80°C (60/80-mesh AW/DMCS-treated Chromosorb G support). The smoothed V_g^0 data are provided in the following tables, together with the slopes, intercepts, and least-squares correlation coefficients for the van't Hoff regressions ($\ln V_g^0$ against T^{-1}). The probe-solute specific retention volumes were also determined for several other lots of R-45M, as well as for a number of the fractions obtained by solvent precipitation. Illustrated below in Figure 40 are the variations of retentions of several solutes with fractions 1A and 10A and bulk AFAL R-45M. The figure clearly shows that the probe-solute GLC technique offers much promise in the characterization of bulk as well as fractionated R-45M. (This work is being continued under a separate Contract.)

TABLE 23. Smoothed (van't Hoff) Specific Retention Volumes $V_g^0 / \text{cm}^3 \text{g}^{-1}$ for Listed Probe Solutes at Indicated Temperatures with Lot AFAL of R-45M

	$V_g^0 / \text{cm}^3 \text{g}^{-1}$					
	30°C	40°C	50°C	60°C	70°C	80°C
n-Pentane	53.03	38.62	28.68	21.69	16.67	13.00
n-Hexane	157.3	107.8	75.64	54.21	39.61	29.46
n-Heptane	456.3	295.0	196.0	133.4	92.89	66.01
n-Octane	1314.	800.4	502.8	324.8	215.2	146.0
3-Methylpentane	127.6	88.95	63.42	46.14	34.20	25.78
2,3-Dimethyl-pentane	322.3	214.2	146.0	101.8	72.51	52.64
3-Methylhexane	344.1	226.4	152.9	105.7	74.68	53.81
3-Methylheptane	953.3	592.5	379.2	249.3	167.9	115.7
1-Hexene	156.4	107.7	75.85	54.58	40.03	29.88
1-Heptene	450.7	292.8	195.4	133.6	93.37	66.60
1-Octene	1289.	788.7	497.7	322.8	214.7	146.2
Benzene	487.8	328.1	226.2	159.4	114.7	84.05
Toluene	1492.	941.3	611.2	407.2	277.8	193.7
Ethylbenzene	3625.	2192.	1367.	877.4	577.8	389.6
o-Xylene	5406.	3219.	1980.	1253.	814.9	542.9
p-Xylene	4175.	2507.	1554.	991.3	649.1	435.3
Cyclohexane	364.7	245.8	169.8	119.9	86.38	63.41
Methylcyclohexane	655.3	428.7	287.9	198.0	139.2	99.84
Tetrahydrofuran	417.7	277.7	189.3	132.1	94.10	68.34
Thiophene	596.1	397.6	271.9	190.3	135.9	98.97
Acetone	91.77	65.63	47.92	35.65	26.99	20.75
Methyl Ethyl Ketone	261.2	176.7	122.4	86.74	62.69	46.15
Methyl Propyl Ketone	659.6	424.1	280.2	189.8	131.5	93.06
Methyl Butyl Ketone	1889.	1149.	720.2	464.4	307.2	208.0
Acetylacetone	1764.	1109.	718.2	477.3	324.8	225.9
Methylene Chloride	123.0	91.52	66.34	49.03	36.88	28.19
Chloroform	359.0	240.8	165.6	116.4	83.58	61.13
1-Chloropentane	1020.	646.0	420.7	281.1	192.3	134.4
n-Butyronitrile	539.3	355.8	240.9	167.0	118.2	85.37
n-Valeronitrile	1555.	972.0	625.6	413.4	279.8	193.7

TABLE 24. Slopes m , Intercepts b , and Correlation Coefficients r for van't Hoff Plots of $\ln V_g^0$ of Listed Probe-Solutes Against $10^3 T^{-1}$ with Lot AFAL of R-45M

<u>Probe Solute</u>	<u>m</u>	<u>- b</u>	<u>r</u>
n-Pentane	3.0097	5.9574	0.9999 ₈
n-Hexane	3.5866	6.7728	0.9999 ₈
n-Heptane	4.1393	7.5311	0.9999 ₈
n-Octane	4.7047	8.3386	0.9999 ₈
3-Methylpentane	3.4238	6.4454	0.9999 ₇
2,3-Dimethylpentane	3.8795	7.0219	0.9998 ₈
3-Methylhexane	3.9726	7.2637	0.9999 ₇
3-Methylheptane	4.5154	8.0351	0.9999 ₈
1-Hexene	3.5433	6.6362	0.9998 ₇
1-Heptene	4.0941	7.3943	0.9999 ₈
1-Octene	4.6601	8.2108	0.9999 ₈
Benzene	3.7650	6.2298	0.9999 ₂
Toluene	4.3708	7.1103	0.9999 ₇
Ethylbenzene	4.7759	7.5586	0.9999 ₇
o-Xylene	4.8409	7.6381	0.9999 ₃
p-Xylene	4.9212	7.6318	0.9999 ₃
Cyclohexane	3.7460	6.4579	0.9999 ₉
Methylcyclohexane	4.0286	6.8040	0.9999 ₉
Tetrahydrofuran	3.8759	6.7507	0.9999 ₈
Thiophene	3.8447	6.2921	0.9999 ₄
Acetone	3.1829	5.9800	0.9998 ₈
Methyl Ethyl Ketone	3.7113	6.6772	0.9999 ₃
Methyl Propyl Ketone	4.1932	7.3406	0.9999 ₆
Methyl Butyl Ketone	4.7239	8.0387	0.9999 ₈
Acetylacetone	4.4004	7.0404	0.9997 ₃
Methylene Chloride	3.2555	5.8794	0.9998 ₅
Chloroform	3.7905	6.6203	0.9997 ₁
1-Chloropentane	4.3398	7.3877	0.9999 ₁
n-Butyronitrile	3.9465	6.7283	0.9998 ₀
n-Valeronitrile	4.4601	7.3632	0.9998 ₈

TABLE 25. Smoothed (van't Hoff) Specific Retention Volumes $v^{\circ}/\text{cm}^3 \text{g}^{-1}$ for Listed Probe Solutes at Indicated Temperatures with Lot 1A-200 of R-45M

	$v^{\circ}/\text{cm}^3 \text{g}^{-1}$					
	30°C	40°C	50°C	60°C	70°C	80°C
n-Pentane	52.89	38.91	29.18	22.26	17.25	13.56
n-Hexane	157.7	109.2	77.41	56.01	41.29	30.97
n-Heptane	461.3	301.1	201.8	138.5	97.22	69.60
n-Octane	1325.	816.3	518.3	338.1	226.1	154.7
3-Methylpentane	128.3	90.47	65.19	47.91	35.84	27.26
2,3-Dimethylpentane	323.9	217.7	150.0	105.7	76.02	55.70
3-Methylhexane	346.1	230.8	157.9	110.5	78.92	57.47
3-Methylheptane	969.6	609.1	393.8	261.4	177.7	123.4
1-Hexene	156.6	109.0	77.61	56.40	41.76	31.45
1-Heptene	455.0	298.3	200.7	138.3	97.38	69.95
1-Octene	1298.	803.1	512.0	335.3	225.1	154.5
Benzene	492.3	331.6	228.9	161.5	116.4	85.38
Toluene	1516.	958.9	623.8	416.4	284.6	198.7
Ethylbenzene	3691.	2242.	1404.	904.8	598.1	404.7
o-Xylene	5534.	3302.	2037.	1290.	840.3	560.7
p-Xylene	4238.	2556.	1591.	1018.	669.2	450.3
Cyclohexane	362.9	247.7	173.2	123.7	90.06	66.78
Methylcyclohexane	660.7	436.3	295.7	205.1	145.3	105.0
Tetrahydrofuran	434.0	288.7	197.0	137.5	98.05	71.26
Thiophene	602.3	402.2	275.4	192.9	138.0	100.6
Acetone	94.30	67.21	48.92	36.29	27.39	21.01
Methyl Ethyl Ketone	270.4	182.3	125.9	88.88	64.05	47.02
Methyl Propyl Ketone	683.4	438.2	288.8	195.2	135.0	95.30
Methyl Butyl Ketone	1958.	1189.	744.2	479.2	316.6	214.1
Acetylacetone	1819.	1134.	727.3	479.2	323.5	223.3
Methylene Chloride	128.0	91.21	66.39	49.25	37.18	28.52
Chloroform	356.2	240.2	165.9	117.2	84.52	62.07
1-Chloropentane	1027.	654.5	429.0	288.5	198.5	139.5
n-Butyronitrile	552.4	363.3	245.3	169.5	119.7	86.22
n-Valeronitrile	1604.	997.0	638.2	419.6	282.7	194.8

TABLE 26. Slopes m , Intercepts b , and Linear Regression Correlation Coefficients r for van't Hoff Plots of $\ln V_g^0$ of Listed Probe-Solutes Against $10^3 T^{-1}$ with Lot 1A-200 of R-45M

<u>Probe Solute</u>	<u>m</u>	<u>$-b$</u>	<u>r</u>
n-Pentane	2.9137	5.6431	0.9998 ₇
n-Hexane	3.4845	6.4338	0.9999 ₀
n-Heptane	4.0493	7.2233	0.9999 ₃
n-Octane	4.5980	7.9781	0.9998 ₉
3-Methylpentane	3.3165	6.0856	0.9999 ₀
2,3-Dimethylpentane	3.7690	6.6525	0.9998 ₅
3-Methylhexane	3.8442	6.8341	0.9999 ₅
3-Methylheptane	4.4134	7.6816	0.9999 ₂
1-Hexene	3.4366	6.2831	0.9998 ₈
1-Heptene	4.0092	7.1050	0.9999 ₂
1-Octene	4.5564	7.8616	0.9999 ₂
Benzene	3.7510	6.1744	0.9999 ₆
Toluene	4.3512	7.0291	0.9999 ₇
Ethylbenzene	4.7330	7.3990	0.9999 ₉
o-Xylene	4.9021	7.5520	0.9999 ₆
p-Xylene	4.8001	7.4822	0.9999 ₇
Cyclohexane	3.6244	6.0616	0.9999 ₆
Methylcyclohexane	3.9384	6.4984	0.9999 ₄
Tetrahydrofuran	3.8684	6.6876	0.9998 ₉
Thiophene	3.8327	6.2420	0.9999 ₆
Acetone	3.2148	6.0582	0.9999 ₈
Methyl Ethyl Ketone	3.7459	6.7565	0.9999 ₈
Methyl Propyl Ketone	4.2182	7.3876	0.9999 ₈
Methyl Butyl Ketone	4.7388	8.0522	0.9999 ₉
Acetylacetone	4.4913	7.3090	0.9999 ₉
Methylene Chloride	3.2144	5.7515	0.9998 ₄
Chloroform	3.7406	6.4639	0.9999 ₀
1-Chloropentane	4.2733	7.1623	0.9999 ₆
n-Butyronitrile	3.9767	6.8038	0.9999 ₄
n-Valeronitrile	4.5138	7.5095	0.9999 ₈

TABLE 27. Smoothed (van't Hoff) Specific Retention Volumes $v^{\circ}/\text{cm}^3 \text{g}^{-1}$ for Listed Probe Solutes at Indicated Temperatures with Lot 1B-108 of R-45M^g

	$v^{\circ}/\text{cm}^3 \text{g}^{-1}$					
	30°C	40°C	50°C	60°C	70°C	80°C
n-Pentane	55.13	40.26	29.97	22.71	17.49	13.67
n-Hexane	164.2	112.9	79.49	57.14	41.88	31.23
n-Heptane	471.0	306.8	205.2	140.6	98.51	70.41
n-Octane	1369.	837.0	527.6	342.0	227.3	154.6
3-Methylpentane	134.0	93.66	66.94	48.82	36.26	27.40
2,3-Dimethylpentane	336.0	224.4	153.6	107.6	76.93	56.07
3-Methylhexane	358.9	237.3	160.9	111.7	79.23	57.29
3-Methylheptane	997.3	622.2	399.6	263.6	178.2	123.1
1-Hexene	163.1	112.5	79.38	57.20	42.01	31.40
1-Heptene	469.1	305.5	204.3	140.0	98.03	70.05
1-Octene	1337.	821.9	520.9	339.3	226.6	154.8
Benzene	503.0	336.7	231.0	162.1	116.2	84.80
Toluene	1526.	961.8	623.7	415.0	282.8	197.0
Ethylbenzene	3803.	2286.	1418.	905.3	593.2	398.1
p-Xylene	5675.	3354.	2048.	1288.	832.4	551.4
o-Xylene	4373.	2609.	1607.	1019.	663.8	442.9
Cyclohexane	380.0	256.8	177.8	125.9	90.90	66.87
Methylcyclohexane	680.1	446.6	301.1	207.8	146.6	105.4
Tetrahydrofuran	452.9	298.3	201.6	139.5	98.65	71.13
Thiophene	617.7	409.0	277.8	193.2	137.2	99.32
Acetone	93.51	66.24	47.93	35.37	26.56	20.28
Methyl Ethyl Ketone	270.6	181.2	124.4	87.30	62.57	45.70
Methyl Propyl Ketone	686.0	437.1	286.4	192.5	132.4	93.00
Methyl Butyl Ketone	1976.	1190.	739.1	472.5	310.1	208.4
Acetylacetone	1868.	1148.	727.3	473.5	316.1	215.9

TABLE 28. Slopes m , Intercepts b , and Linear Regression Correlation Coefficients r for van't Hoff Plots of $\ln V_g^0$ of Listed Probe-Solutes Against $10^3/T^{-1}$ with Lot 1B-108 of R-45M

<u>Probe Solute</u>	<u>m</u>	<u>$-b$</u>	<u>r</u>
n-Pentane	2.9853	5.8378	0.9999 ₄
n-Hexane	3.5533	6.6201	0.9999 ₅
n-Heptane	4.0689	7.2675	0.9999 ₄
n-Octane	4.6691	8.1804	0.9999 ₆
3-Methylpentane	3.3988	6.3139	0.9999 ₄
2,3-Dimethylpentane	3.8339	6.8297	0.9999 ₉
3-Methylhexane	3.9286	7.0762	0.9999 ₈
3-Methylheptane	4.4795	7.8713	0.9999 ₈
1-Hexene	3.5277	6.5425	0.9999 ₃
1-Heptene	4.0713	7.2794	0.9999 ₇
1-Octene	4.6157	8.0279	0.9999 ₉
Benzene	3.8118	6.3535	0.9999 ₉
Toluene	4.3841	7.1311	0.9999 ₉
Ethylbenzene	4.8323	7.6965	0.9999 ₉
p-Xylene	4.9029	7.7900	0.9999 ₈
o-Xylene	4.9920	7.8232	0.9999 ₉
Cyclohexane	3.7203	6.3317	0.9999 ₈
Methylcyclohexane	3.9914	6.6442	0.9999 ₉
Tetrahydrofuran	3.9636	6.9590	0.9999 ₁
Thiophene	3.9132	6.4825	0.9999 ₉
Acetone	3.2732	6.2592	0.9999 ₃
Methyl Ethyl Ketone	3.8078	6.9603	0.9999 ₉
Methyl Propyl Ketone	4.2788	7.5834	0.9999 ₉
Methyl Butyl Ketone	4.8162	8.2985	0.9999 ₉
Acetylacetone	4.6202	7.7081	0.9999 ₉

TABLE 29. Smoothed (van't Hoff) Specific Retention Volumes $v_g^0/\text{cm}^3 \text{g}^{-1}$ for Listed Probe Solutes at Indicated Temperatures with Lot 2A-404 of R-45M

	$v_g^0/\text{cm}^3 \text{g}^{-1}$					
	30°C	40°C	50°C	60°C	70°C	80°C
n-Pentane	55.76	40.76	30.38	23.04	17.76	13.90
n-Hexane	164.4	113.3	79.94	57.58	42.28	31.60
n-Heptane	468.0	306.0	205.4	141.2	99.21	71.12
n-Octane	1353.	831.2	526.1	342.2	228.3	155.8
3-Methylpentane	134.7	94.43	67.65	49.45	36.81	27.87
2,3-Dimethyl- pentane	336.3	225.2	154.6	108.6	77.83	56.85
3-Methylhexane	358.3	237.7	161.8	112.6	80.11	58.09
3-Methylheptane	985.8	617.7	398.5	263.9	179.0	124.1
1-Hexene	162.2	112.4	79.71	57.70	42.56	31.94
1-Heptene	467.4	305.1	204.5	140.4	98.56	70.57
1-Octene	1325.	817.4	519.5	339.3	227.1	155.6
Benzene	500.7	336.1	231.2	162.7	116.8	85.48
Toluene	1521.	961.0	624.6	416.6	284.5	198.5
Ethylbenzene	3774.	2276.	1417.	907.1	596.1	401.2
o-Xylene	5601.	3324.	2037.	1286.	833.5	553.8
p-Xylene	4344.	2597.	1603.	1018.	664.3	444.0
Cyclohexane	379.3	257.2	178.7	126.8	91.86	67.75
Methylcyclo- hexane	680.6	447.6	302.1	208.8	147.4	106.1
Tetrahydrofuran	442.0	292.4	198.5	137.9	97.85	70.80
Thiophene	608.5	405.3	276.9	193.5	138.1	100.4
Acetone	94.75	67.29	48.81	36.09	27.16	20.77
Methyl Ethyl Ketone	272.0	182.6	125.6	88.41	63.50	46.47
Methyl Propyl Ketone	686.4	438.7	288.3	194.3	134.0	94.36
Methyl Butyl Ketone	1981.	1196.	744.3	476.8	313.4	211.0
Acetylacetone	1825.	1132.	723.6	474.9	319.5	219.8

TABLE 30. Slopes m , Intercepts b , and Linear Regression Correlation Coefficients r for van't Hoff Plots of $\ln V_g^0$ of Listed Probe-Solutes Against $10^3 T^{-1}$ with Lot 2A-404 of R-45M

Probe Solute	m	$-b$	r
n-Pentane	2.9750	5.7926	0.9999 ₈
n-Hexane	3.5308	6.5451	0.9999 ₃
n-Heptane	4.0341	7.1588	0.9999 ₀
n-Octane	4.6286	8.0581	0.9999 ₃
3-Methylpentane	3.3740	6.2264	0.9999 ₃
2,3-Dimethylpentane	3.8060	6.7368	0.9999 ₈
3-Methylhexane	3.8958	6.9697	0.9999 ₂
3-Methylheptane	4.4367	7.7418	0.9999 ₂
1-Hexene	3.4790	6.3874	0.9999 ₄
1-Heptene	4.0478	7.2055	0.9999 ₃
1-Octene	4.5869	7.9416	0.9999 ₅
Benzene	3.7848	6.2689	0.9999 ₆
Toluene	4.3598	7.0545	0.9999 ₆
Ethylbenzene	4.7991	7.5950	0.9999 ₄
o-Xylene	4.9544	7.7124	0.9999 ₇
p-Xylene	4.8837	7.7333	0.9999 ₀
Cyclohexane	3.6883	6.2282	0.9999 ₆
Methylcyclohexane	3.9787	6.6016	0.9999 ₅
Tetrahydrofuran	3.9214	6.8443	0.9999 ₄
Thiophene	3.8572	6.3128	0.9999 ₆
Acetone	3.2495	6.1677	0.9999 ₆
Methyl Ethyl Ketone	3.7833	6.8742	0.9999 ₉
Methyl Propyl Ketone	4.2486	7.4836	0.9999 ₉
Methyl Butyl Ketone	4.7956	8.2276	0.9999 ₈
Acetylacetone	4.5323	7.4411	0.9999 ₈

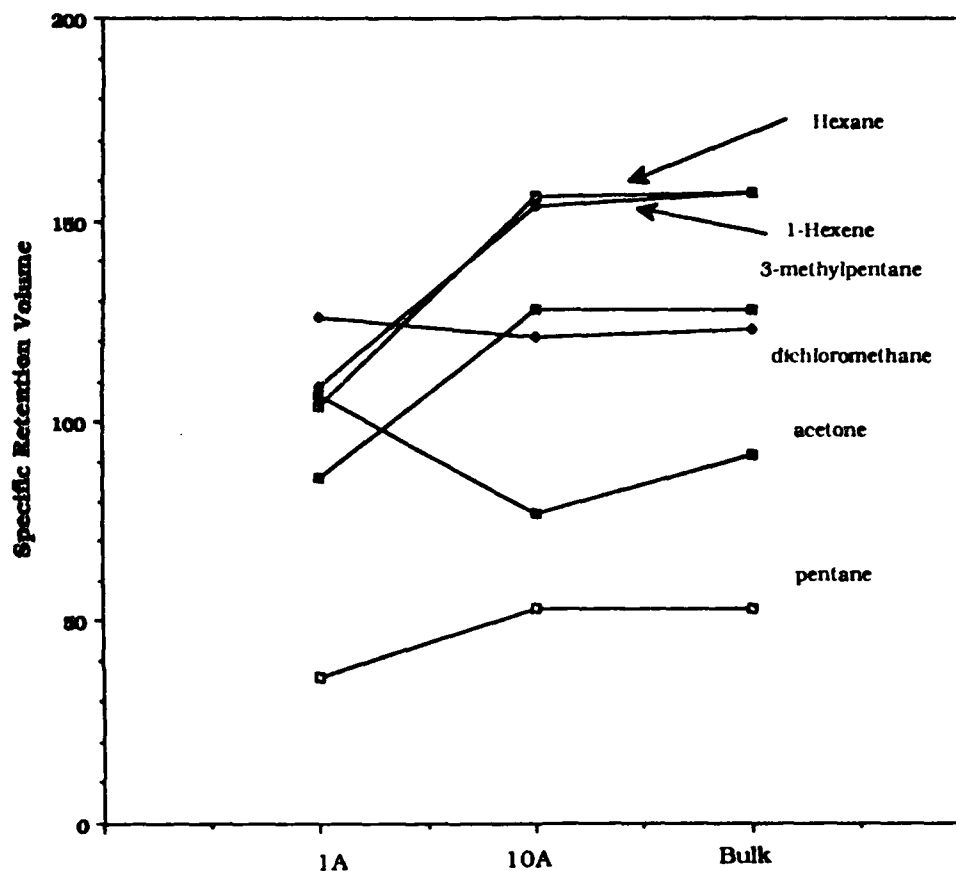


FIGURE 40. Plots of the specific retention volumes $V^0/\text{cm}^3 \text{g}^{-1}$ obtained for the indicated probe-solutes n-pentane ($n\text{-C}_5$), acetone (MMK), dichloromethane (DCM), 3-methylpentane (3MC_5), 1-hexene (1-C_6), and n-hexane ($n\text{-C}_6$) with fractions 1A and 10A and bulk R-45M.

Phase III, Task 1. Hydroxyl Content

Direct Measurement of Hydroxyl Content by FT-IR. The calibration plot of the absorbance of 6-undecanol at 3628 cm^{-1} against millimolar concentration of OH with the Mattson Alpha Centauri instrument (see Experimental Section) is shown in Figure 41. (That obtained with a Perkin-Elmer FT-IR was curved, and this instrument was not used further in this work.) The line is dead straight over the second through the sixth points, which cover the concentration range $20\text{--}100\text{ meq dm}^{-3}$. The equation of the line is as shown, $Y = 0.001482 X + 0.01768$, where the linear least-squares correlation coefficient is 0.9999_3 . (The ordinal intercept is indicative of the level of noise.)

The absorption spectra were next taken for three concentrations of R-45M fraction 1A; the results gave an average hydroxyl content of 2.088 meq g^{-1} , roughly what would be expected, since its molecular weight is only 1440 Da. (By way of comparison, the most recent data sheets issued by ARCO list an hydroxyl content of 1.73 meq g^{-1} for their standard, Poly bd X-10LM, which is listed as having a number-average molecular weight M_n of 1040 Da.) The hydroxyl content of the remaining R-45M fractions were then taken in the same way; the results are presented below in Table 31 and are shown plotted in Figure 42.

The data were roughly what would be expected insofar as there was an exponential decrease in OH content with increasing molecular weight. The equation of the solid curve in Figure 42 was in fact found to be:

$$C_{\text{OH}} = 4.04 e^{-7.47 \times 10^{-4} M} + 0.473$$

The goodness of fit of this relation is illustrated in Table 31, where the C_{OH} calculated with it agree with those determined experimentally on average to no worse than $\pm 10\%$. For example, the lowest molecular-weight fraction exhibited 1.87 meq g^{-1} OH, while the calculated value was 1.85 meq g^{-1} . Also, a similar resin from ARCO, Poly bd X-10LM (number-average molecular weight M_n of 1040 Da), yielded 1.73 meq g^{-1} .

Having obtained the exponential-decay data, we next attempted to refine the form of data representation as follows. First, $1/C_{\text{OH}}$ was regressed against M . However, the data are clearly concave to the abscissa. $-\log C_{\text{OH}}$ was next plotted against M , the result being a curve that was concave to the abscissa. Finally, the data regressed as $\log C_{\text{OH}}$ against $\log M$ were weakly convex to the abscissa. Thus, there does not appear to be a simpler form of the functionality distribution than that given by the above (exponential) relation.

FT-IR of Derivatized R-45M. It was originally intended to verify the hydroxyl data obtained by FT-IR by selective derivatization of R-45M fractions then, quantitation of the derivatization group (thence the hydroxyl content) by NMR. However, in previous work completed with hexamethyldisilazane (HMDS) derivatization, it was found that the reaction was far from complete, i.e., that HMDS was surprisingly ineffective in forming trimethylsilyl ethers. Accordingly, several alternative derivatizing reagents and procedures were investigated, where the effectiveness of each was gauged by the disappearance of the FT-IR hydroxyl band at ca. 3500 cm^{-1} . Ultimately it was found that formic acid is a very powerful derivatizing agent for prepolymer hydroxyls, and appears to be the most useful as an alternative means of quantitating R-45M functionality.

As an example of this portion of the work, Figure 43 presents an FT-IR spectrum of underivatized bulk R-45M, where the broad hydroxyl band at ca. 3500 cm^{-1} is clearly visible. Next, Figure 44 provides the spectrum following derivatization with HCOOH: the OH band has disappeared entirely; while several new bands (asterisks) have appeared that are due to formate esters. However, given the limits of accuracy of the FT-IR technique in general, it can only be said that derivatization is complete to within $\pm 1\text{--}2\%$.

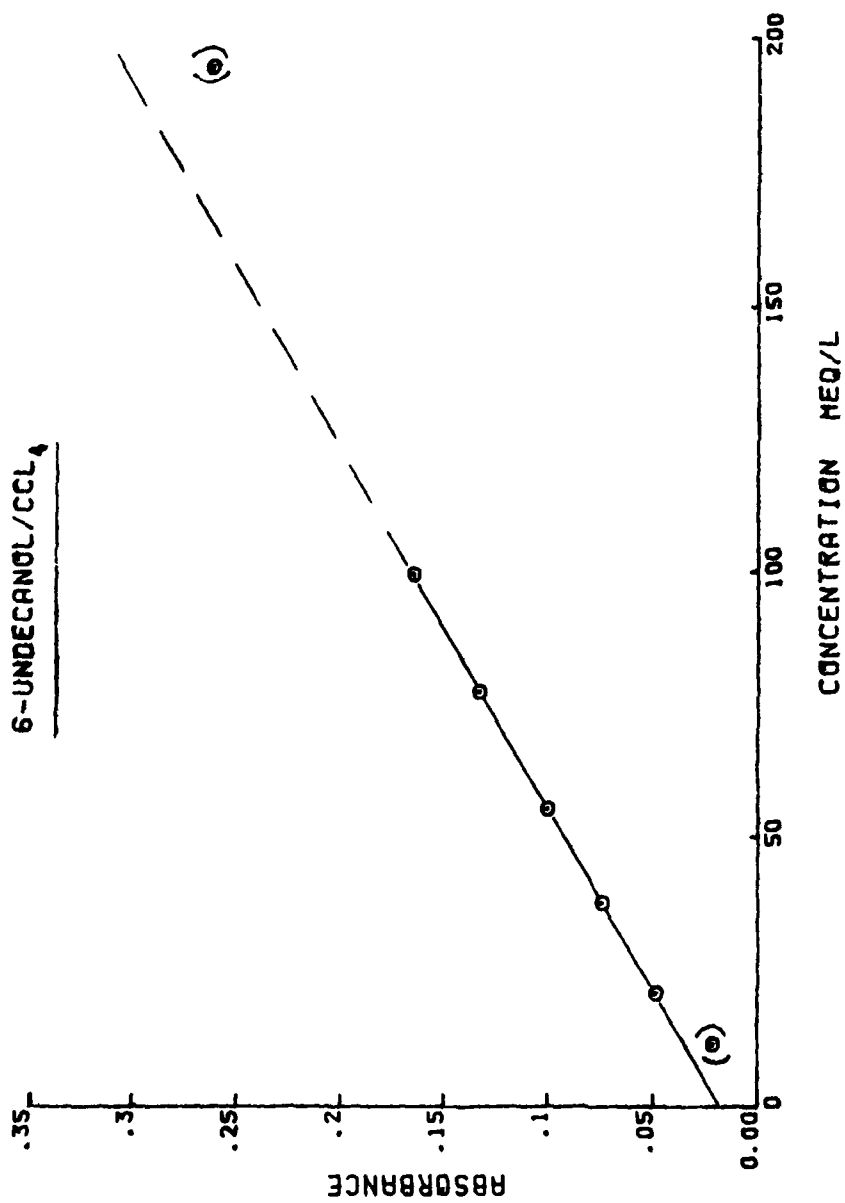


FIGURE 41. FT-IR Beer's-law plot for 6-undecanol in CCl₄.

TABLE 31. Experimental and Calculated Hydroxyl Contents of Indicated Fractions of R-45M and ARCO Hydroxy-Terminated Polybutadiene Resins

Fraction No.	OH/meq g ⁻¹	
	Exptl	Calc
1A	1.87	1.85
1B	1.79	1.68
1C	1.45	1.54
2A	1.30	1.35
2B	1.17	1.16
2C	1.21	1.10
3A	1.08	1.05
3B	0.99	1.07
3C	0.90	1.03
4A	0.81	0.89
4B	0.85	0.85
4C	0.78	0.81
5A	0.76	0.73
5B	0.71	0.75
5C	0.79	0.74
6A	0.71	0.67
6B	0.71	0.66
6C	0.68	0.61
7A	0.65	0.59
7B	0.59	0.56
7C	0.60	0.55
8A	0.56	0.51
8B	0.57	0.49
8C	0.48	0.48
9A	0.45	-
9B	0.45	-
9C	0.40	-
10A	0.30	-
bulk	0.82	-
10LM	1.73	-
20LM	1.40	-
25LM	1.18	-
R-45M	0.72	-
120HM	0.59	-

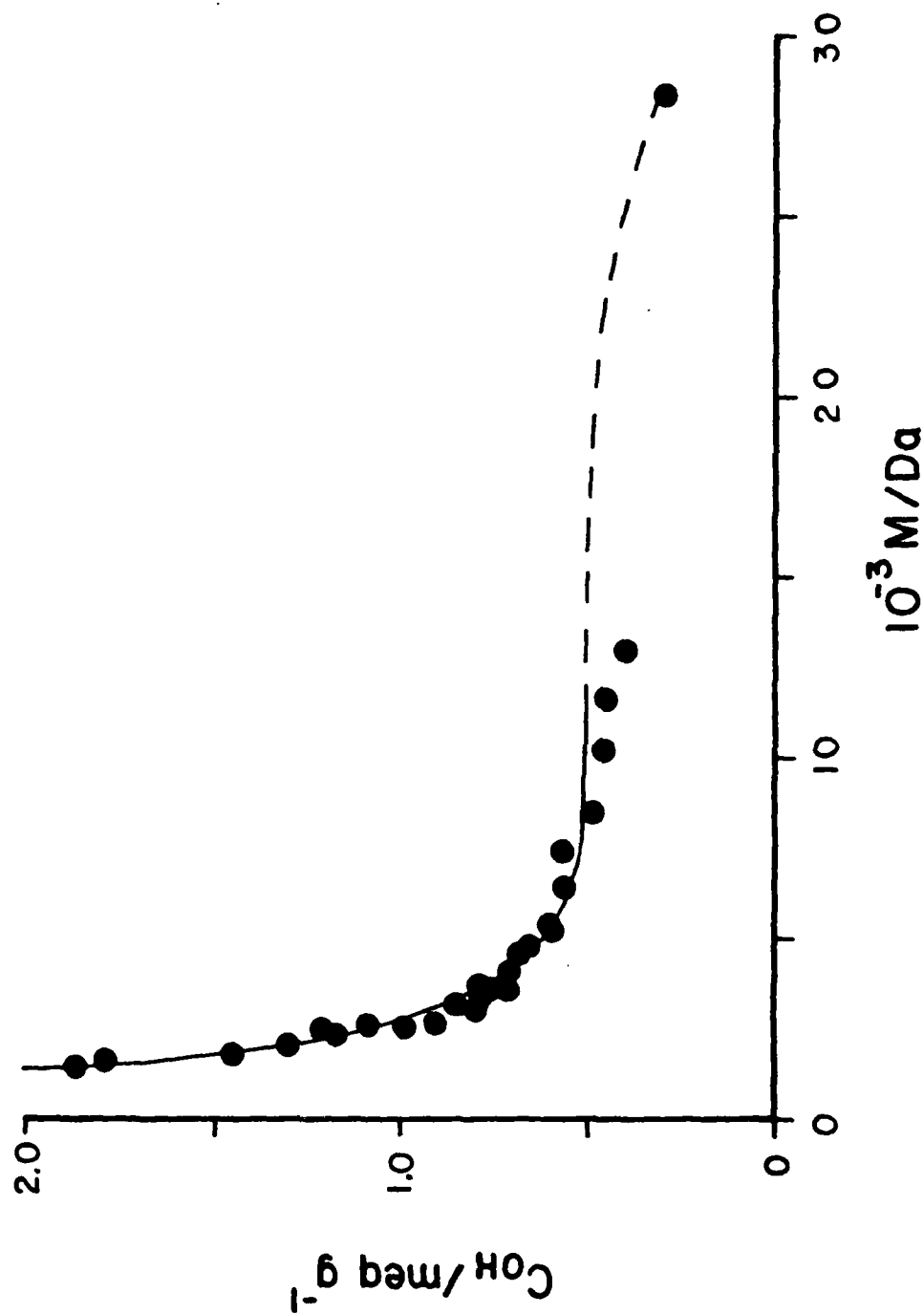


FIGURE 42. Plot of hydroxyl content $C_{OH} / \text{meq g}^{-1}$ of R-45M fractions against GPC molecular weight M / Da .

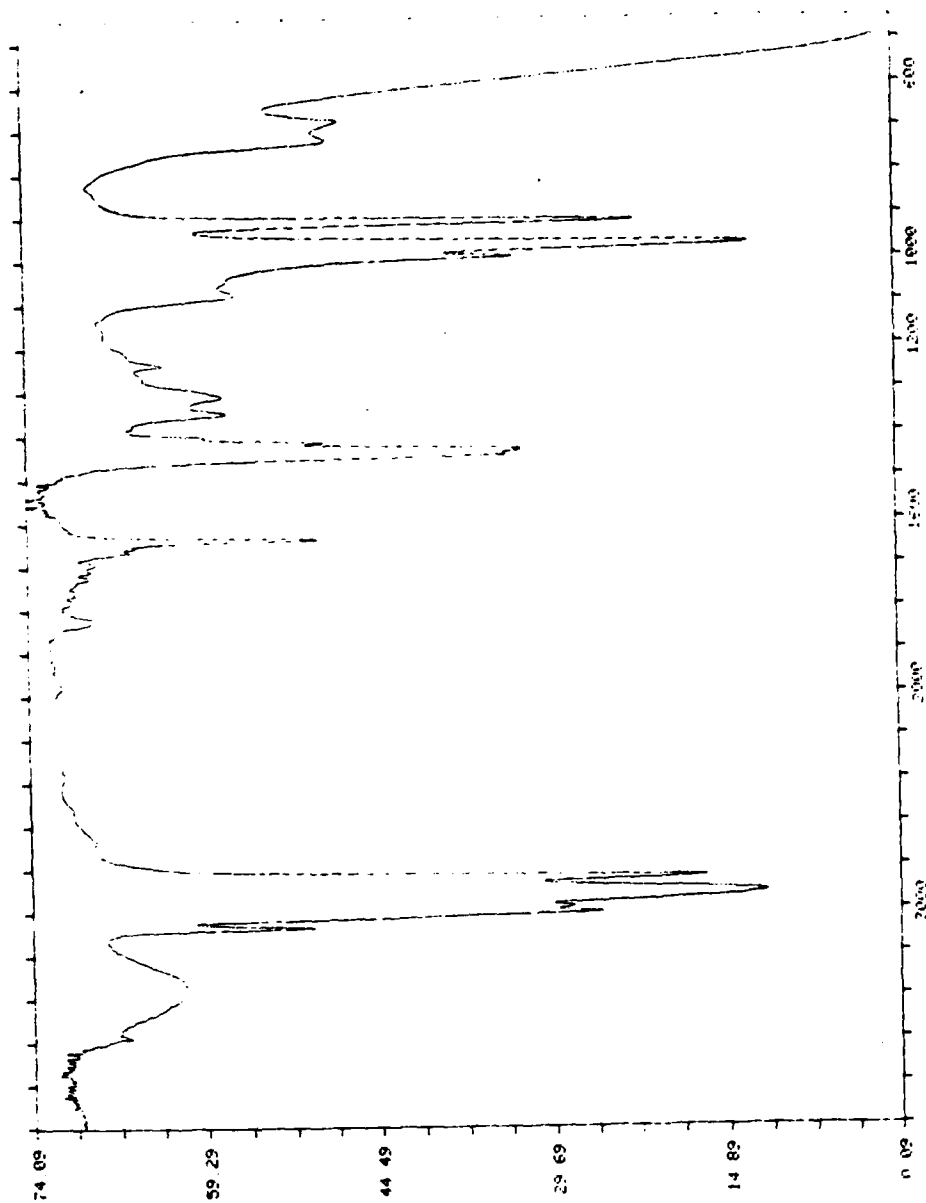


FIGURE 43. Thin-film FT-IR spectrum of neat underivatized R-45M.

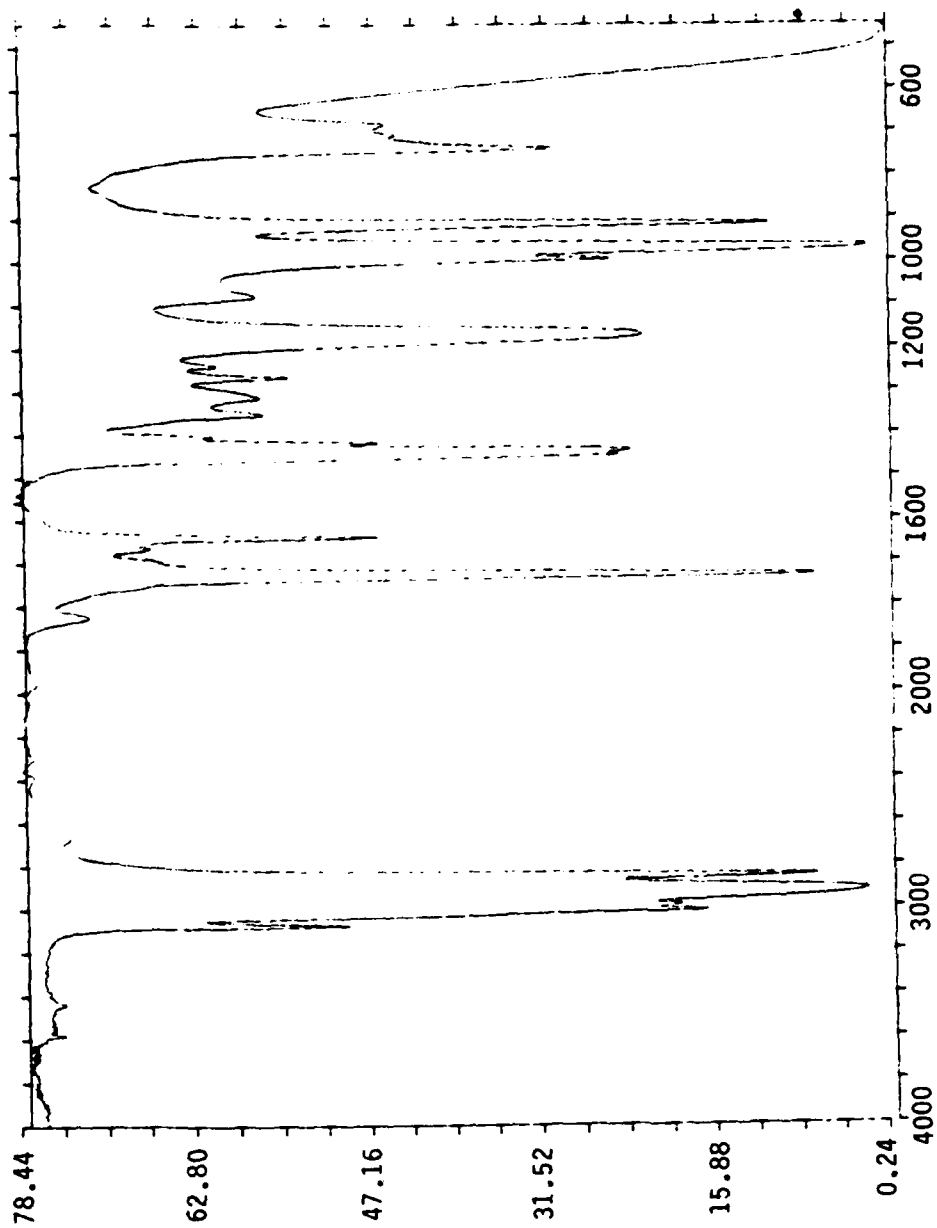


FIGURE 44. Thin-film FT-IR spectrum of R-45M derivatized with formic acid.

Having established that the derivatization procedure was virtually quantitative for bulk materials, several fractions were next examined. The FT-IR spectra of derivatized fraction nos. 1A, 1B, 4A, 7A, and 9A showed that all have been successfully reacted, and that the derivatization procedure did indeed appear to be quantitative.

NMR of R-45M Derivatized with Trichloroacetyl Isocyanate. The trichloroacetyl isocyanate derivatization procedure (31-37) was evaluated at this point to determine the hydroxyl content of fractionated R-45M.

6-Undecanol Standard. The procedure employed in a test attempt to determine the hydroxyl content of this material was as follows. The sample was made up in CCl_4 in a concentration of ca. 1% w/v; roughly $0.5\text{--}0.8\text{ cm}^3$ was added to an NMR tube; and a spectrum was then taken. Next, ca. 10 mm^3 of TCI was pipetted into the NMR tube, the solution shaken, and allowed to stand for 5 min at room temperature. A spectrum of the derivatized material was then recorded.

Figure 45 presents the NMR spectrum of underivatized 6-undecanol, which also shows the peak integrations. Note that, as shown here, integration with FT-NMR is in fact less accurate than integration with conventional NMR, which is a result of the inaccuracy in representation of peak tails with the former technique. Even so, the integration gives close to the correct values, viz., $-(\text{OH})_1$, $-(\text{CH})_1$, $-(\text{CH}_2)_8$, and $-(\text{CH}_3)_2$.

The spectrum of TCI-derivatized 6-undecanol is shown in Figure 46. Notice that the $-\text{OH}$ proton signal at ca. 3.4 ppm in Figure 45 has disappeared; and that a new quintuplet, due to $-(\text{CH})$, has appeared at ca. 5 ppm. The $-\text{NH}$ proton has also appeared at 8.7 ppm.

The quintuplet portion of the spectrum integrated as expected to 1. In addition, the new singlet band due to the amide proton also integrated to ca. unity. Overall, therefore, 6-undecanol was found to be a well-behaved model system, and did in fact undergo derivatization as expected.

R-45M Fraction 2A. In contrast to the above, the spectra of underivatized as well as derivatized fractionated R-45M were puzzling. For example, the spectrum following the addition of TCI not only indicated the presence of residual OH, but two new doublets appeared in addition to the amide band. Trifluoroacetic anhydride has been reported by Goldwasser and Adolph (36) to be superior to TCI as a derivatizing agent for R-45M hydroxyls. Imidazol reagents have also been recommended. However, formic acid is superior to both, as described in the Sections that follow.

NMR of R-45M Derivatized with Formic Acid. Having established that TCI and related methods gave ambiguous results, and that formic acid gave virtually complete derivatization of R-45M hydroxyls by FT-IR, the utility of NMR was evaluated as a means of determining this functionality with the latter reagent. The CW-NMR spectrum of formic acid-derivatized R-45M showed, first, some residual HCOOH . Secondly, adjusting the abscissa to zero for TMS, the formate band was thought to occur slightly downfield from 5 ppm. Unfortunately, however, there was not quite sufficient resolution between this band and the broad polymer band next to it for accurate integration. Accordingly, FT-NMR at 220 MHz was evaluated. The FT-NMR spectra showed resolution of the formate peak that was just sufficient to give good integration. Derivatization with formic acid thus appeared to be satisfactory as a complementary tool to FT-IR for determination of the hydroxyl content.

^{13}C FT-NMR. As a matter of general interest, and because of some overlap with proton NMR bands (see later, however), ^{13}C FT-NMR was also carried out on several samples of R-45M. The spectrum of derivatized R-45M gave a band at ca. 143 ppm due to the formate carbon. The resolution of this band was particularly encouraging as regards quantitation of the hydroxyl content by peak integration.

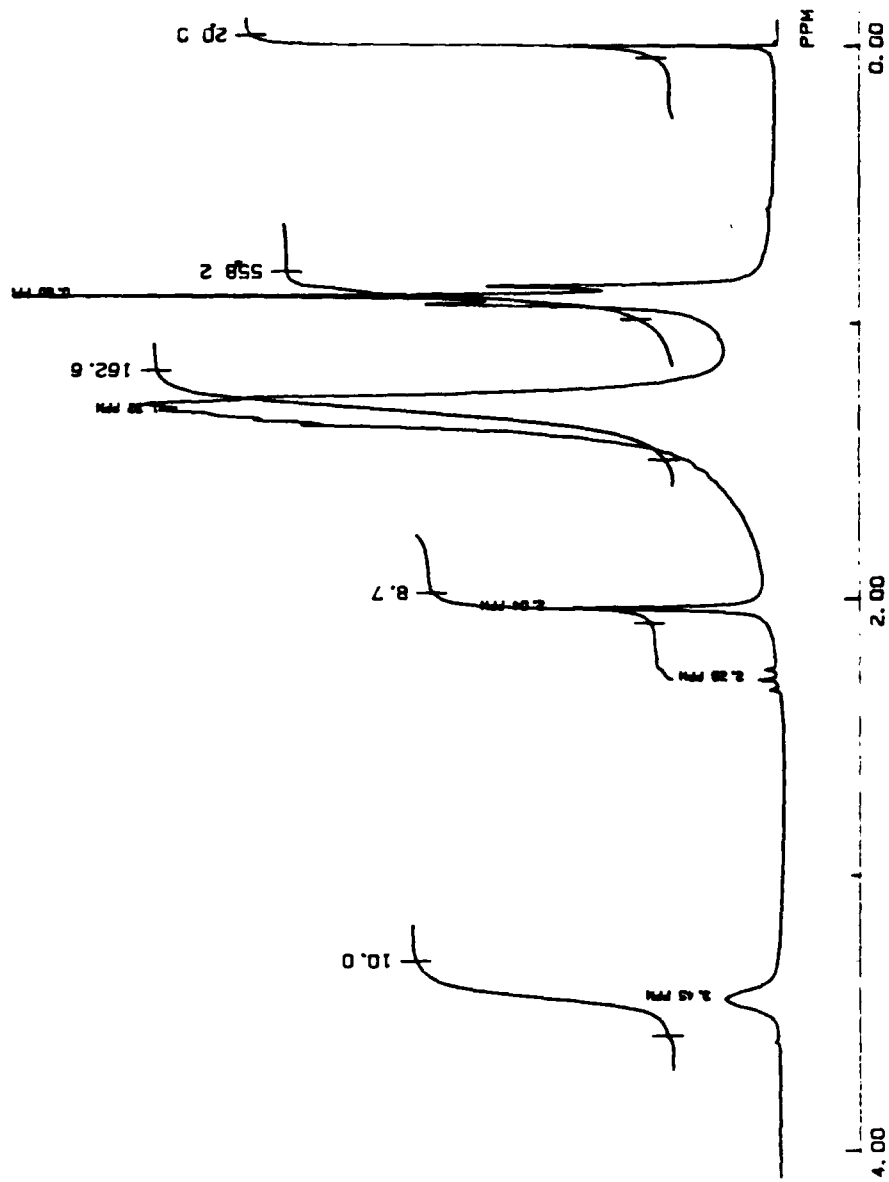


FIGURE 45. NMR spectrum of 6-undecanol in CCl_4 showing peak integrations.

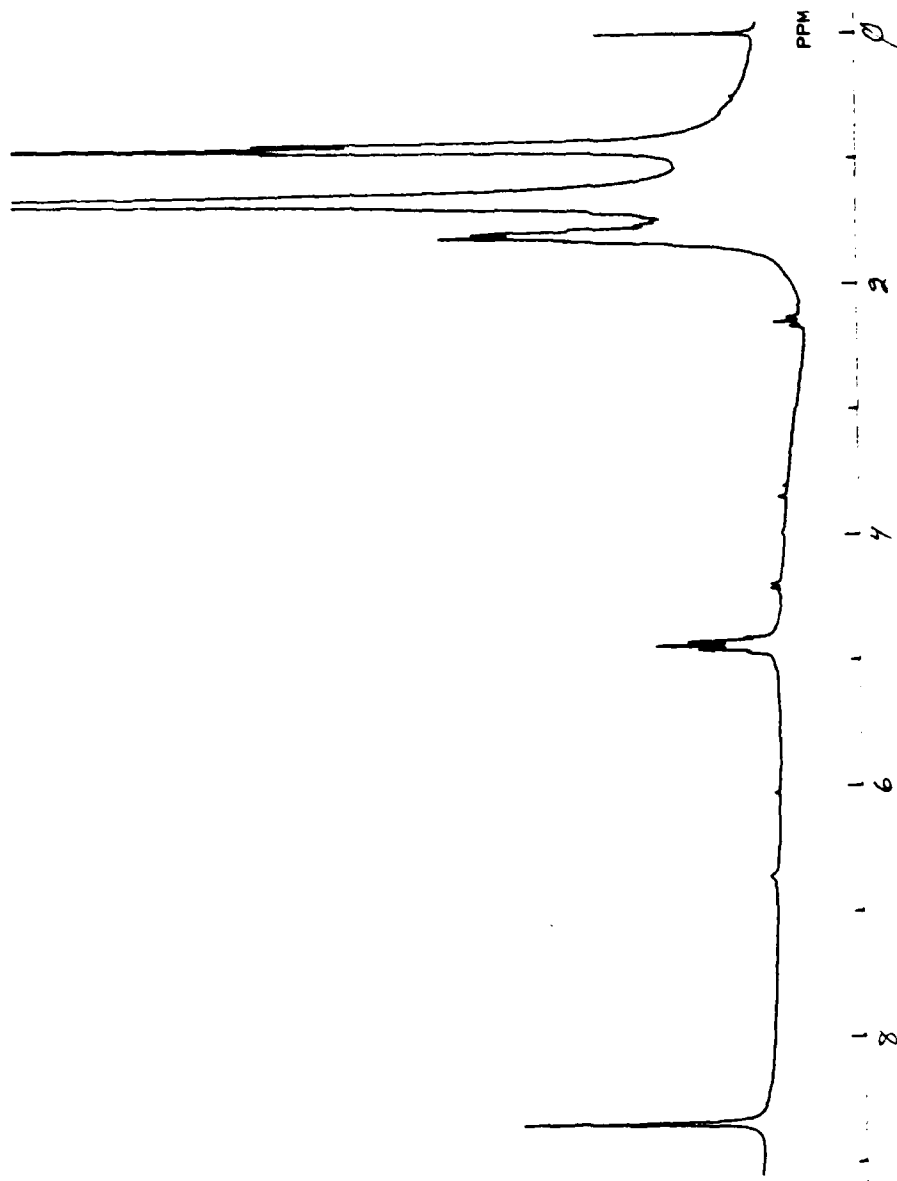


FIGURE 46. NMR spectrum of TCI-derivatized 6-undecanol.

¹H FT-NMR. The formate ester band occurred much further downfield than originally supposed, at ca. 8 ppm. (There was also a chloroform band just upfield from this at 7.3 ppm, but this was well resolved and did not interfere with the formate peak.) The peak assignment is shown in the spectrum given in Figure 47.

The spectra indicate that integration of the formate band can be used for the quantitation of R-45M prepolymer hydroxyl content. Also, because of the high degree of resolution of the proton bands, the capability of ¹³C FT-NMR, although today quite commonplace in most laboratories, does not in fact appear to be required for use of the formate ester technique.

¹H CW-NMR. Because of the enhanced resolution of the proton bands as shown above, a simple continuous-wave NMR was also evaluated for quantitation of the R-45M hydroxyl content by the formate ester technique. The ¹H CW-NMR spectrum of underivatized R-45M obtained at 90 MHz with a Varian EM-390 spectrometer gave excellent resolution of the formate proton, there being no other band within 1 ppm of it. Integration of its area was therefore straightforward. Moreover, this was also true for a 60 MHz instrument. Derivatization with formic acid thus appears to be a simple means of quantitating the hydroxyl content of R-45M, particularly since a simple proton NMR can be employed for the work.

Other Derivatizing Agents. The efficacy of methyl orthoformate, $\text{H}-\text{C} \begin{smallmatrix} \text{O} \\ \text{=} \\ \text{OMe} \end{smallmatrix}$, was also evaluated. However, it failed to react with bulk R-45M, as verified by FT-IR. Methyl orthochloroformate, $\text{Cl}-\text{C} \begin{smallmatrix} \text{O} \\ \text{=} \\ \text{OMe} \end{smallmatrix}$, was then tried. This material reacted readily with R-45M; however, the $-\text{CH}_3$ proton band fell at ca. $\frac{3}{2}$ ppm, just underneath a large peak of the polymer. This reagent therefore does not appear to be useful for quantitation purposes at this time. It reacts quickly, however, and with a high degree of completion (ca. 100% in a few minutes).

Other Alcohols. Because of the wide range of types of prepolymer hydroxyls that AFAL may be interested in quantitating, a brief experimental survey was carried out of other kinds of alcohols for which formic acid might be useful in producing formate esters (thereby permitting their analysis by proton NMR). The reagent was found to yield complete esterification of sterols; of the primary alcohols 2-methyl-1-propanol (iso-butyl alcohol) and n-dodecanol; and of the secondary alcohols 2-butanol (sec-butyl alcohol), 4-methyl-2-pentanol, and 6-undecanol. It should therefore be of use in the hydroxyl analysis of a wide range of types of prepolymers of interest to the Air Force.

DSC of R-45M. DSC studies of derivatized R-45M fractions were also carried out, with the view of correlating glass transitions at least with molecular weight and, potentially, with hydroxyl content as well. For example, it has been reported (38) that polymer glass transitions T_g vary with molecular weight M in accordance with the relation:

$$T_g = T_g^\circ - K_g M^{-1}$$

where T_g° is the limiting glass transition at infinite polymer molecular weight; and where K_g is a constant only for a particular polymer type, as pointed out by Boyer (39). However, for some polymers, e.g., hydroxy-terminated poly(propylene oxide), K_g is zero, or nearly so, as confirmed by Faucher (40). Accordingly, the variation of T_g for several polybutadiene (PBD) standards as well as representative R-45M fractions were investigated by differential scanning calorimetry (DSC).

The DSC traces for 500M, 1000M, and 22 000M PBD gave glass transitions of -113.2° , -100.6° , and -94.85°C . Thus, T_g increased as expected with molecular weight. Next, the traces for bulk and derivatized R-45M, as well as fractions 1A, 2A, 3A, 5A, 7A, 9A, and

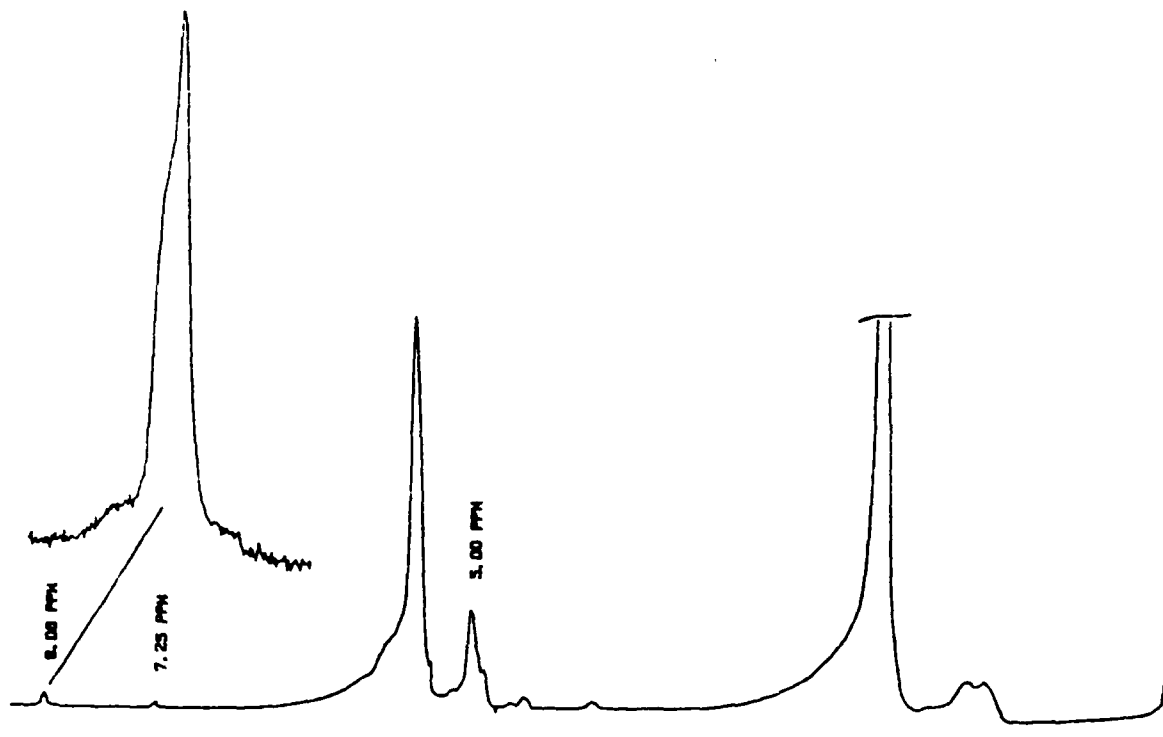


FIGURE 47. ^1H FT-NMR spectrum of derivatized R-45M. The formate band occurs at ca. 8 ppm.

10A gave glass transitions of -78.2° , -80.7° , -77.7° , -79.2° , -78.6° , -79.6° , -78.4° , -77.8° , and -79.9° C. These prepolymers therefore give K_g of zero. This is in fact quite fortunate, since T_g is also known to vary with chain branching. That is, there is the possibility that appropriate derivatization of the R-45M fractions (e.g., with formic acid) would allow changes in T_g to be observed independently of the effects of the hydroxyl content.

Phase III, Task 2. Analysis of Lots of R-45M.

During the period corresponding to the final stages of Phase III, several lots of R-45M were characterized by density and by viscosity.

Density Analysis. The densities of a number of test lots of R-45M were measured over the temperature-range $0-80^{\circ}$ C with the Mettler-Paar DMA-45 density meter, as described in the Experimental Section, a sample of the data being presented below in Tables 32 and 33. (The densities were required in any event for conversion of inverse gas-chromatographic specific retention volumes to thermodynamic quantities of solution, such as entropies, enthalpies, and Gibbs free energies, work which is being carried out in a separate Contract.) There are a number of aspects of density measurements that have an immediate bearing on the characterization of R-45M. For example, the density of a polymer is of interest in terms of molecular weight: simply, molecules of lower molecular weight pack more tightly and, hence, give higher densities than do polymers of higher molecular weight. However, the polymer density does not decrease to zero as the molecular weight increases to infinity, but rather, asymptotically approaches a lower limit. The molecular weights of small- to moderate-sized polymers can therefore be determined from their densities. The results of such an approach are presented and discussed in the Sections that follow.

TABLE 32. Experimentally-Observed Densities for Indicated Lots of R-45M at $30-65^{\circ}$ C

Parameter	R-45M Lot				
	10LM	14LM	20LM	25LM	120HM
M_n/Da	1,040	1,420	1,350	1,630	3,335
density $r/g\ cm^{-3}$					
30° C	0.9056	0.9035	0.9036	0.9028	0.8977 0.8978
40° C	0.8993	0.8975	0.8976	0.8968	0.8917 0.8919
50° C	0.8932	0.8914	0.8916	0.8909	0.8859 0.8858
60° C	0.8872	0.8854	0.8857	0.8852	0.8802 0.8802
65° C	0.8843	0.8826	0.8830	0.8828	0.8774 0.8774

TABLE 33. Experimentally-Observed Densities and Linear Least-Squares Fitting Parameters for Indicated Lots of R-45M at 20-65°C

Lot No.	t/°C							a	-10 ⁴ b	r
	20°C	30°C	40°C	50°C	60°C	65°C				
1A-200	0.9042	0.8981	0.8920	0.8861	0.8803	0.8775	0.9159 ₂	5.937 ₅	0.9999 ₁	
1B-108	0.9027	0.8965	0.8907	0.8846	0.8789	0.8762	0.9143 ₁	5.895 ₉	0.9998 ₆	
2A-404	0.9031	0.8970	0.8910	0.8851	0.8795	0.8765	0.9147 ₂	5.891 ₅	0.9999 ₁	
403225	0.9042	0.8980	0.8920	0.8861	0.8802	0.8774	0.9159 ₄	5.937 ₅	0.9999 ₃	
602185	0.9031	0.8970	0.8909	0.8849	0.8792	0.8764	0.9148 ₂	5.941 ₄	0.9998 ₈	
810255	0.9154	0.9092	0.9031	0.8972	0.8913	0.8886	0.9271 ₄	5.963 ₈	0.9998 ₇	
	0.9153	0.9092	0.9031	0.8972	0.8913	0.8886	0.9270 ₅	5.948 ₀	0.9999 ₀	
810265	0.9059	0.8997	0.8937	0.8878	0.8820	0.8793	0.9175 ₂	5.914 ₅	0.9998 ₆	
905175	0.9040	0.8979	0.8916	0.8856	0.8799	0.8772	0.9157 ₇	5.978 ₁	0.9997 ₆	

Experimental Sources of Error. Use of the DMA-45 requires that ca. 1 cm³ of the (degassed) liquid sample be injected into a U-tube of approximately 2 mm i.d. (It is important that no air bubbles be introduced at the same time, as these would adversely affect the accuracy of the measurements.) R-45M is of course quite viscous at room temperature and so, some difficulty was encountered in getting the samples into the density meter. Ultimately, it was found that prepolymers had to be injected into the U-tube very slowly, typically over a period of 15 min or so, such that no air bubbles were introduced at the same time.

Cleaning the density meter following a series of measurements on a given sample also posed some difficulty. It was found that the system required flushing with many volumes of chloroform or methylene chloride, followed by drying with a stream of nitrogen. It was judged clean when the density meter read ca. 0.0010 g cm⁻³ when empty, i.e., the density of dry air at 20°C. Interestingly, cleaning the density meter proved nearly as difficult as cleaning the viscometer tube (see earlier Sections), that is, there was left behind a thin film of prepolymer coating the inside of the glass U-tube if it was not flushed with sufficient solvent. Moreover, the presence of a coating of prepolymer was easily detected simply by turning on the density meter (values of 0.0080 g cm⁻³ were common for incomplete cleaning). It was also found that multiple cleanings were required; that is, several volumes of chloroform were passed through the system, it was blown dry, several more volumes of chloroform were passed through the U-tube, it was blown dry again, and so on. (It was generally necessary to go through four or five such cycles before the tube was thoroughly cleaned.)

Reproducibility. The sixth column of Table 32 presents replicate measurements of the densities of Lot 120HM, where the reproducibility is seen to be on the order of two parts per ten-thousand. A similar comparison, with similar findings, was made for prepolymer no. 810255 in Table 33. However, the former set of data were taken as the temperature was increased; that is, a density measurement was made at 30°C, the thermostat was changed to 40°C, the density at the new temperature was measured, and so on. The question therefore arises as to the reproducibility of the density data were the temperature to be changed from higher to lower values. In addition, it might be thought that the densities at the higher temperatures would be erroneous because of changes that might take place with R-45M at, say, 60°C. Accordingly, the densities of Lot 14LM of R-45M were also measured both as the temperature was increased and decreased. The results are shown below in Table 34 and not only verify the reproducibility of the densities, but also confirm that the density data are independent of the manner of temperature change.

TABLE 34. Comparison of Densities Observed Experimentally for R-45M Lot 14LM at Increasing and Decreasing Temperatures over the Range: 20-65°C

t/°C	r/g cm ⁻³		
	Increasing Temperature		Decreasing Temperature
	Trial 1	Trial 2	
20	-	0.9098	0.9099
30	0.9035	0.9034	0.9036
40	0.8975	0.8975	0.8977
50	0.8914	0.8914	0.8916
60	0.8854	0.8855	0.8856
65	0.8826	0.8827	0.8827

Linearity of Density with Temperature. Ordinarily, density regresses very nearly linearly with temperature for low molecular-weight organic liquids. However, it is not unusual to find that the regression is not linear for polymers, since volume expansion with temperature can result from several factors, among them chain-tangling phenomena. Variations of the density of lots of R-45M were therefore assessed with both linear and quadratic expressions of the forms, respectively:

$$r = a + b t$$

$$r = a' + b' t + c' t^2$$

where a , a' , b , b' , c , and c' are empirical fitting constants. The best-fit values of a and b are given in Table 35, together with the correlation coefficient r and standard deviations s_a and s_b for each data set; while the corresponding nonlinear regression values of a' , b' , and c' are provided in Table 36. Comparisons of the densities calculated from each with those observed experimentally are then made in Table 37.

The data show that both linear and quadratic regressions provide excellent fits of the densities. However, the regressions obtained with the quadratic appear to be specious: the standard deviations s_c are the same order of magnitude as the values of c , which is usually taken as an indication that the parameter is meaningless. Accordingly, the densities do in fact regress linearly with temperature, and the values of a in Table 35 do indeed correspond to the densities of the lots of R-45M at 0°C.

Regression of the Density Data with Temperature. Figure 48 provides a representative plot of the regression of density $r/g\text{ cm}^{-3}$ with temperature $t/^\circ\text{C}$. Note that the experimental error on each point is smaller than the size of the symbol. There appears to be little question of the linearity of these data.

Regression of the Density Data with Prepolymer Molecular Weight. Plots of the prepolymer density at 0°C against M_n for the ARCO materials obviously regressed nonlinearly and so, semilog data reduction was applied. The most successful mode was the form: $\log M_n$ against r , as shown in Figure 49. The slope and intercept of the line are -59.667_7 and 58.117_0 , respectively, with a correlation coefficient of 0.996. The goodness of fit strongly suggests that the number-average molecular weight of a lot of R-45M can be determined simply from this nomograph and its density at 0°C.

Application to Other Lots of R-45M. Also measured were bulk lots of R-45M that were furnished by AFAL, and which were labeled as nos. nos. 1A-200, 1B-108, 2A-404, 403225, 602185, 810255, 810265, and 905175. The nomograph of $\log M_n$ against density derived above was employed; the results are provided below in Table 38.

Viscosity Analysis. The intrinsic viscosities of five of the test lots of R-45M were also determined. The solvent was tetrahydrofuran (THF), and the temperature was 30°C. The raw data recorded during the viscosity measurements are presented in Table 39 together with the slopes and intercepts of the regressed data (the intercepts being equal to the intrinsic viscosities).

Note that only one temperature was employed for most of the determinations, since it had been determined previously that THF is a "good" solvent for R-45M, that is, the intrinsic viscosity data are temperature-independent at least over the range 20-50°C. One set of data was nevertheless replicated at 40°C to ensure that the procedures employed yielded reproducible results. The intrinsic viscosity data thereby obtained agreed to within 0.4%.

Table 35. Best-Fit Linear Regression Parameters for Density Data of Table 32

Parameter	R-45M Lot				
	10LM	14LM	20LM	25LM	120HM
a	0.9237 ₃	0.9214 ₁	0.9212 ₁	0.9197 ₉	0.9149 ₇ 0.9152 ₄
$\pm 10^4 s_a$	2.3	1.7	2.3	4.7	2.0 2.9
$-10^4 b$	6.084 ₂	5.990 ₂	5.903 ₇	5.731 ₇	5.793 ₉ 5.840 ₂
$\pm 10^6 s_b$	4.5	3.4	4.6	9.2	4.0 5.7
r	0.9999 ₂	0.9999 ₈	0.9999 ₄	0.9997 ₂	0.9999 ₃ 0.9998 ₆

Table 36. Best-Fit Quadratic Regression Parameters for Density Data of Table 32

Parameter	R-45M Lot				
	10LM	14LM	20LM	25LM	120HM
a	0.9254 ₂	0.9223 ₀	0.9226 ₈	0.9229 ₆	0.9164 ₇ 0.9170 ₀
$\pm 10^4 s_a$	1.5	7.1	6.9	11.	8.6 1.4
$-10^4 b$	6.847 ₂	6.377 ₈	6.556 ₆	7.145 ₃	6.473 ₈ 6.636 ₆
$\pm 10^5 s_b$	0.66	3.1	3.1	5.1	3.8 0.60
$10^7 c$	8.001 ₆	4.012 ₇	6.796 ₂	14.631 ₂	7.129 ₀ 8.350 ₅
$\pm 10^7 s_c$	0.69	3.3	3.2	5.3	4.0 0.63

TABLE 37. Comparison of Experimentally-Observed Densities with Values Calculated from Best-Fit Linear and Quadratic Relations (Cf. Text) for Indicated Lots of R-45M at 30-65°C

R-45M Lot	t/°C				
	30°C	40°C	50°C	60°C	65°C
10LM					
Exptl.	0.9056	0.8993	0.8932	0.8872	0.8843
Linear	0.9054 ₈	0.8994 ₀	0.8933 ₁	0.8872 ₃	0.8841 ₉
Quadr.	0.9056 ₀	0.8993 ₁	0.8931 ₈	0.8872 ₂	0.8842 ₉
14LM					
Exptl.	0.9035	0.8975	0.8914	0.8854	0.8826
Linear	0.9034 ₄	0.8974 ₅	0.8914 ₆	0.8854 ₇	0.8824 ₈
Quadr.	0.9035 ₃	0.8974 ₃	0.8914 ₁	0.8854 ₈	0.8825 ₄
20LM					
Exptl.	0.9036	0.8976	0.8916	0.8857	0.8830
Linear	0.9034 ₉	0.8975 ₉	0.8916 ₈	0.8857 ₈	0.8828 ₃
Quadr.	0.9036 ₂	0.8975 ₄	0.8916 ₀	0.8857 ₉	0.8829 ₃
25LM					
Exptl.	0.9028	0.8968	0.8909	0.8852	0.8828
Linear	0.9025 ₉	0.8968 ₆	0.8911 ₃	0.8854 ₀	0.8825 ₃
Quadr.	0.9028 ₄	0.8967 ₂	0.8908 ₉	0.8853 ₅	0.8827 ₀
120HM: Trial 1					
Exptl.	0.8977	0.8917	0.8859	0.8802	0.8774
Linear	0.8975 ₉	0.8918 ₀	0.8860 ₀	0.8802 ₁	0.8773 ₁
Quadr.	0.8976 ₉	0.8917 ₂	0.8858 ₉	0.8802 ₀	0.8774 ₁
120HM: Trial 2					
Exptl.	0.8978	0.8919	0.8858	0.8802	0.8774
Linear	0.8977 ₂	0.8918 ₈	0.8860 ₄	0.8802 ₀	0.8772 ₈
Quadr.	0.8978 ₄	0.8917 ₉	0.8859 ₁	0.8801 ₉	0.8773 ₉

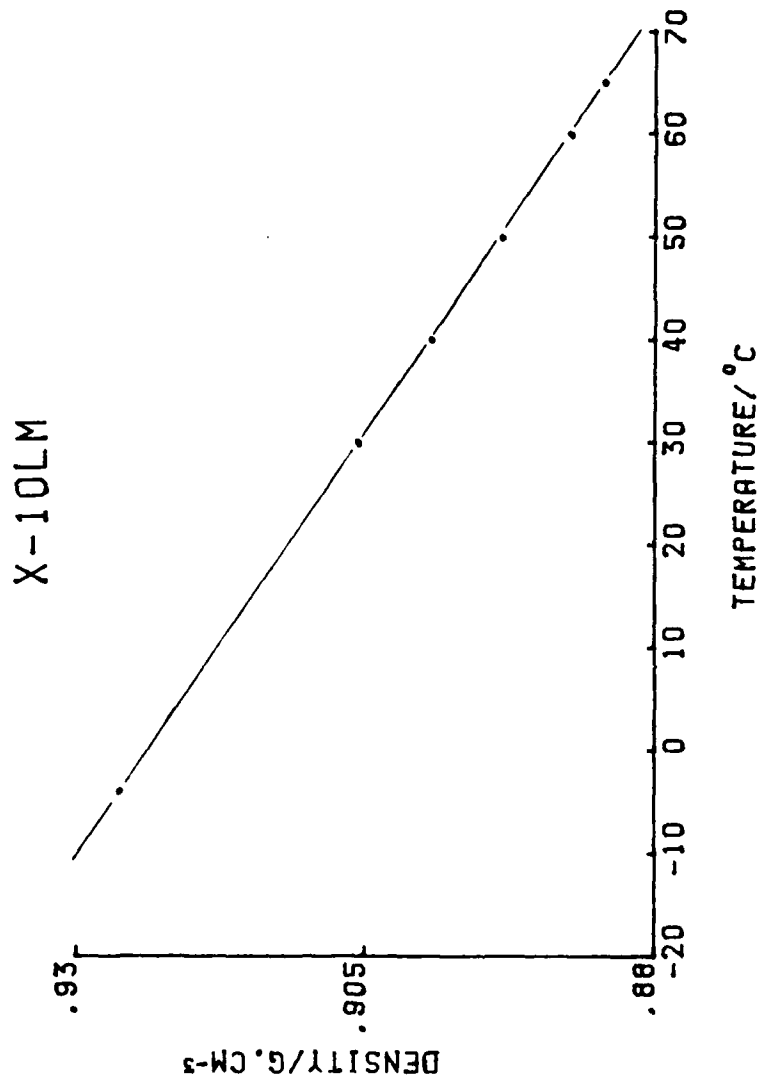


FIGURE 48. Plot of density against temperature for R-45M Lot 10LM.

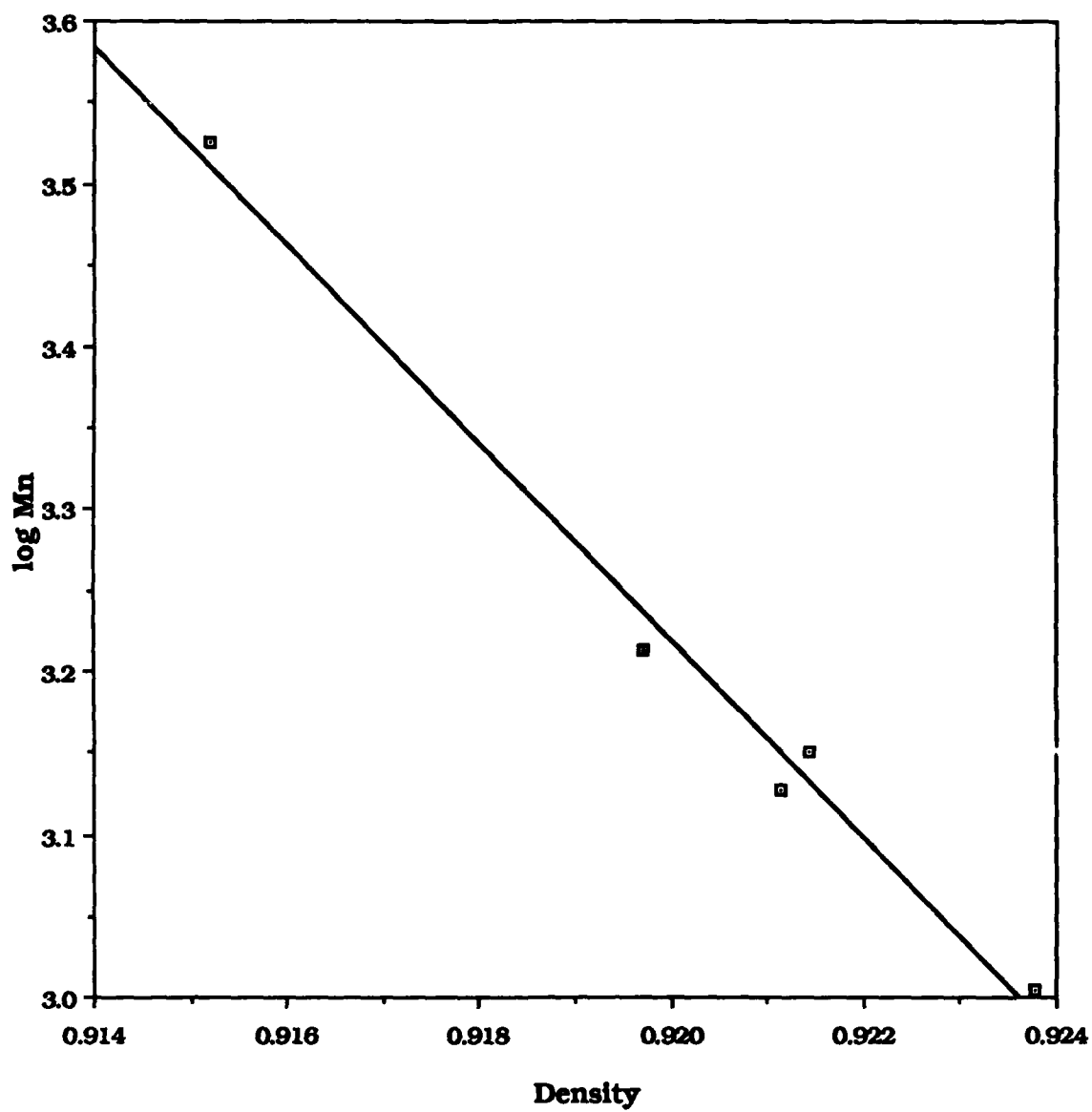


FIGURE 49. Plot of $\log M_n$ against density for lots of R-45M.

Table 38. Apparent Number-Average Molecular Weights M_n/Da of Indicated Lots of R-45M Calculated from Data of Table 33

<u>Lot No.</u>	<u>M_n/Da</u>
1A-200	2 926
1B-108	3 650
2A-404	3 450
403225	2 918
602185	3 403
810255	630 \pm 4
810265	2 349
905175	2 987

TABLE 39. Raw Viscosity Data for Indicated Lots of R-45M at 30° Except as Noted

<u>A. Lot 403225</u>	<u>C/g cm⁻³</u>	<u>t/sec</u>	<u>(t - t₀)/(t₀ C)</u>	<u>r/g cm⁻³</u>	<u>n/cm³ g⁻¹</u>
	0.0312	273.80	16.6806	0.8786	
	0.0409	312.42	17.9681	0.8786	
	0.0521	354.60	18.6012	0.8794	
	0.0681	435.28	20.8098	0.8796	
	0.0873	528.48	22.1615	0.8804	13.7318
<u>B. Lot 602185</u>					
	0.0328	283.04	17.4313	0.8784	
	0.0361	300.76	18.5636	0.8786	
	0.0547	373.50	19.6358	0.8792	
	0.0599	406.56	20.9960	0.8795	
	0.0914	576.90	23.5623	0.8803	14.5667
<u>C. Lot 602185 (40°C)</u>					
	0.0331	260.46	17.4383	0.8679	
	0.0382	281.52	18.4486	0.8679	
	0.0552	342.58	19.4653	0.8688	
	0.0636	385.64	20.9942	0.8690	
	0.0922	518.82	23.2288	0.8702	14.5135
<u>D. Lot 810255</u>					
	0.0278	289.68	21.8927	0.8786	
	0.0396	352.70	24.2064	0.8792	
	0.0464	386.88	24.7495	0.8796	
	0.0664	521.44	28.5482	0.8805	
	0.0777	598.74	29.9209	0.8810	17.4917

TABLE 39 (Continued)**E. Lot 810265**

0.0303	276.80	17.7259	0.8784	
0.0356	300.76	18.8243	0.8787	
0.0507	360.48	19.7589	0.8792	
0.0595	410.02	21.4601	0.8795	
0.0855	543.42	23.5983	0.8803	14.8222

F. Lot 905175

0.0270	263.38	17.1323	0.8785	
0.0326	286.70	18.1617	0.8788	
0.0450	333.72	18.9595	0.8793	
0.0546	381.06	20.4407	0.8796	
0.0753	479.24	22.0619	0.8803	14.6521

This work completed the technical effort of this Contract.

SUMMARY AND CONCLUSIONS

Gel-permeation chromatographic fractionation of low molecular-weight prepolymers was found to be of limited utility even on the analytical scale for the separation of individual homologs of PS and HTPB. The method of fractional solution was therefore employed instead, where samples were deposited at the head of a reverse-phase LC column followed by programming the solvent from very "poor" to very "good". Resolution of the homologs of 680M polystyrene was considerably greater than baseline. However, the separation of polystyrenes above ca. 1500 Da or so was determined to be an "all-or-nothing" phenomenon, that is, the polymers were either freely separable (or completely inseparable) in the solvent, depending upon its composition. Further, the break-point of solubility appears to be sharply defined for higher molecular-weight materials, much like the titration curve of a strong acid with a strong base where the slope of the curve at the equivalence point is infinite.

Semi-preparative scale (9.4-mm i.d. by 50 cm length) reverse-phase column LC was then used for separation of the homologs comprising 526M, 680M, and 946M polystyrenes. However, injections of 150-mm³ of solution containing as little as 18 mg cm⁻³ of sample overloaded the column. Further, the situation only worsened with polystyrene standards of higher molecular weight, that is, the overload level amounted to ca. 1 mg total sample weight. Gram-scale fractional solution of polystyrene standards was therefore carried out with a much larger preparative-scale LC column (2.5 cm i.d.). Following clean-up, the fractions were characterized by analytical-scale liquid chromatography. Each was found to contain varying amounts of the first 20 homologs of polystyrene, as verified by mass spectrometry.

Fractionation of polybutadiene (PBD) prepolymer was investigated next, as the LC separation of the homologs of this material was considered to represent a degree of difficulty intermediate between polystyrene and HTPB. The results were not satisfactory insofar as there was little resolution. The LC separation of molecular-weight homologs of HTPB was equally disappointing, nor did reverse-phase liquid

chromatography of HMDS-derivatized HTPB show any substantial improvement. The failure to resolve crude HTPB by reverse-phase LC was said to be analogous to the failure of separation of PS that exceed a certain molecular weight (ca. 2000 Da). As noted earlier, this is a critical molecular-weight phenomenon where, for mixtures of homologs that exceed M^c , the polymer chains cannot not be resolved with reverse-phase LC systems even if the sample contains low molecular-weight homologs that are, by themselves, otherwise separable.

Bulk-scale solvent/no-solvent fractional solution of R-45M was employed next, with considerable success. Very many fractions both of silylated as well as unsilylated materials were collected. Each was then characterized further according to molecular weight and hydroxyl content by gel-permeation chromatography, vapor-phase osmometry, viscosity, Fourier-transform infrared and nuclear magnetic resonance spectroscopy, density, and gas chromatography. Relative chain-branching functions, as well as cis-, trans-, and vinyl contents, were also determined.

Gel-permeation chromatography of the fractions was carried out with nomographs of $\log M$ against retention volume constructed from data obtained both with polybutadiene and polystyrene standards. Differences between the calibration curves resulted in a doubling of the apparent molecular weights of the samples. The results emphasized that appropriate standards must be employed to calibrate GPC columns if meaningful data are to be derived from the technique.

A Knauer vapor-phase osmometer was used next for the measurement of M_n of several of the bulk (unfractionated) and fractionated polystyrenes and HTPB. The overall assessment of the VPO technique with the instrument to hand was that the precision that could be expected was no better than $\pm 20\%$. Also, and in addition to random instrument errors, there exists a systematic error inherent in the VPO technique, namely, deviations from unity of the solvent activity coefficient in the solute-solvent mixture. It was concluded that calibration of VPO apparatus must therefore be carried out with the same polymer that is to be measured, namely, polystyrene calibration for polystyrenes; HTPB standard for HTPB polymers, and so forth. Large errors approaching hundreds of percent can otherwise be anticipated. (The situation was said to be analogous to calibrating GPC columns with standards that have much different hydrodynamic volumes than the polymers of interest.)

The measurement of viscosity was explored next in very great detail, since such data, together with GPC peak-maximum molecular weights, were required for calculation of relative chain-branching functions. Several major sources of error were identified. For example, while pure solvents gave results that agreed to at least within $\pm 0.15\%$ of the manufacturer's values, the apparent viscosities of solutions of R-45M given by repeated measurements (solution taken up into the capillary arm, allowed to fall, taken up again, and so on) would nearly double over the course of 15 runs. Contamination of the viscometer-tube capillary walls was found to be the source of the error, which necessitated extensive cleaning procedures (fresh hot cleaning solution) between each run. Also, at least five solutions of concentration greater than ca. 0.03 g cm^{-3} , but less than 0.1 g cm^{-3} , were required in order to define the linear portion of the plots of $(1/c)(t - t_0)/t_0$ against $1/c$. Since at least 25 cm^3 of each solution was required, a total of 5 g of material was needed for a viscosity determination. THF was shown to be a "good" solvent, with which the intrinsic viscosities (hence the Mark-Houwink constants K and a) were temperature-independent.

The intrinsic viscosities for PBD (500, 1000, and 22,000 Da) were 2.0356, 3.4423, and $39.1161 \text{ cm}^3 \text{ g}^{-1}$, respectively (THF; 30°C), which gave Mark-Houwink values, $[n] = K M^a$, of: $a = 0.7811$ and $K = 0.0159$. Several iterations with different fractions of untreated R-45M yielded the Mark-Houwink constants: $K = 0.0490$ and $a = 0.6510$. Also, the constants for silylated R-45M were found to be: $K = 0.0510$ and $a = 0.6440$ (the viscosities of bulk

and fractionated R-45M ranged from 5-23 cm³ g⁻¹). Thus, there was not much difference between the two data sets. And, while it was originally supposed that the hydroxyl content of R-45M might be determined simply by measuring the viscosity difference between silylated and untreated materials, the average hydroxyl content is apparently too small to affect the viscosity of R-45M by more than ca. 10%.

The above data were used to derive the branching parameter n for silylated fractions of R-45M. However, the values did not vary in a consistent manner, as has been found to be the case also by others. Thus, fraction 1C gave 1×10^{-4} ; fraction 2C gave 2×10^{-4} ; fraction 9A gave 1×10^{-5} , and so on. Overall, the values averaged ca. 5×10^{-5} .

DSC studies of derivatized R-45M fractions were carried out with the aim of correlating glass transitions T_g at least with molecular weight and, potentially, with branching as well, where $T_g = T_g^\infty - K_g M^{-1}$. Accordingly, the variation of T_g for several polybutadiene (PBD) standards as well as representative R-45M fractions were investigated. The DSC traces for 500M, 1000M, and 22 000M PBD gave glass transitions of -113.2°, -100.6°, and -94.85°C. Thus, T_g increased as expected with molecular weight. Next, the traces for bulk and derivatized R-45M, as well as fractions 1A, 2A, 3A, 5A, 7A, 9A, and 10A, gave glass transitions of -78.2°, -80.7°, -77.7°, -79.2°, -78.6°, -79.6°, -78.4°, -77.8°, and -79.9°C. K_g was therefore shown to be zero for this prepolymer.

A critical examination of the ARCO method for determination of the cis-, trans-, and vinyl-contents of the silylated fractions was carried out. The absorption spectrum of the silylated fractions was strongly solvent-dependent, that is, use of a different solvent gave very different results. An alternative technique using attenuated total reflectance (ATR) was therefore developed, which was found to be ideal for bulk untreated as well as silylated R-45M fractions (these tacky fluids wet ATR crystals well; also, cleaning the cell amounts simply to washing the crystal face with chloroform). The trans/vinyl ratios of fractionated R-45M were shown to be approximately constant, as was the cis content. The cis-, trans-, and vinyl-contents of Thiokol lots of R-45M also appeared to be invariant. The respective types of unsaturation were: 32.6, 33.6, and 33.9% (cis-content; lots 1A-200, 1B-108, and 2A-404, respectively); 24.6, 24.1, and 24.2% (vinyl-content); and 42.8, 42.3, and 41.9% (trans-content). These values compared very favorably with the averages of those found for fractionated HMDS-treated R-45M, viz., $35.4 \pm 1.9_5$ (\pm standard deviation), $23.4 \pm 0.6_6$, and $41.2 \pm 1.5_4$ % for the cis-, vinyl-, and trans-contents, respectively.

In determining hydroxyl content by FT-IR, the calibration plot of the absorbance of 6-undecanol at 3628 cm⁻¹ against millimolar concentration of OH was found to be absolutely linear over the concentration range 20-100 meq dm⁻³. The equation of the line was: $Y = 0.001482 X + 0.01768$, while the linear least-squares correlation coefficient was 0.9999₃. The hydroxyl contents of the R-45M fractions were found to decrease exponentially with increasing molecular weight. The equation of the curve describing the data was:

$$C_{OH} = 4.04 e^{-7.47 \times 10^{-4} M} + 0.473$$

The hydroxyl content calculated with this relation agreed with those determined experimentally on average to no worse than $\pm 10\%$.

It was originally intended to verify the hydroxyl data by selective derivatization of R-45M fractions, followed by quantitation of the derivatization group (thence the hydroxyl content) by NMR. Several derivatizing reagents and procedures were investigated, where the effectiveness of each was gauged by the disappearance of the hydroxyl band (FT-IR) at ca. 3500 cm⁻¹. It was eventually found that formic acid, a very powerful derivatizing agent for prepolymer hydroxyls, was the most useful. The formate ester proton band occurs at ca. 8 ppm, the integrated area of which correlated well with the R-45M prepolymer hydroxyl content. Further, because of the excellent resolution of

the proton band, simple continuous-wave 60- and 90-MHz NMR spectrometers could also be employed. Thus, ^{13}C FT-NMR, although commonplace in most laboratories, was not required (the formate carbon occurs at 143 ppm).

During the period corresponding to the final stages of the work, several lots of R-45M were characterized by density. Plots of the prepolymer density at 0°C against M_n for standard ARCO materials regressed nonlinearly and so, semilog data reduction was applied. The most successful mode was the form: $r = f(\log M_n)$. The slope and intercept of the resultant line were -59.667_7 and 58.117_0 , respectively, with a correlation coefficient of 0.996. The goodness of fit strongly suggested that the number-average molecular weight of R-45M could be determined simply from this nomograph and the density of a sample extrapolated to 0°C . It was applied to several lots of R-45M furnished by AFAL, one of which was shown to be highly anomalous.

The potential utility of inverse GC was also evaluated as an alternate method of characterizing Defense-related prepolymer materials in general, and R-45M in particular. The specific retention volumes of a bank of 23 solutes, comprised of normal- and branched aliphatic, aromatic, alicyclic, heterocyclic, and heterofunctional hydrocarbons, were therefore determined over the temperature-span $30\text{--}80^\circ\text{C}$ with several lots of R-45M, as well as with a number of the fractions obtained by fractional solution. The prepolymer was found to be ideally suited as a stationary phase insofar as no column bleed was observed at the maximum temperature (90°C) of the system thermostat and at maximum sensitivity of the thermal conductivity detector. In addition, repeated cycling of the temperature, coupled with reinjection of several of the solutes, demonstrated that the stationary packings remained invariant over the course of individual experiments. Finally, the retentions of several solutes with several bulk and fractionated lots of R-45M demonstrated that the probe-solute GLC technique offers much promise as a means of characterizing hydroxy-terminated polybutadiene prepolymer.

REFERENCES

1. Carver, J. G., Improved Specifications for Composite Propellant Binders for Army Weapon Systems, Technical Report T-79-76, U.S. Army Missile Command, Redstone Arsenal, Alabama, July 1979.
2. Carver, J. G., Rapid Method for Determination of Functionality Distribution in Hydroxy-Terminated Polymers, Paper presented at the Tenth JANNAF Symposium on Propellant Characterization, October 1980; Publication 333, Chemical Propulsion Information Agency, Laurel, Maryland, October 1980.
3. Thompson, G., and Daly, E. E., Development of HTPB Propellant for Ballistic Missiles, Final Technical Report TWR-8618, Vol. II (AFRPL-TR-75-23, Vol. II), November 1974.
4. Law, R. D., An Evaluation of Derivatives of HTPB Used in the One-Step Determination of Average Functionality Profile, Paper presented at the Tenth JANNAF Symposium on Propellant Characterization, October 1980; Publication 333, Chemical Propulsion Information Agency, Laurel, Maryland, October 1980.
5. Christian, T. W., Chemical Characterization of HTPB Prepolymers, Report No. LS79-29, Chemical Propulsion Information Agency, Laurel, Maryland, June 1979.
6. Brown, R. D., Literature Survey on Hydrocarbon Binders for Solid Rocket Propellants, Publication 251, Chemical Propulsion Information Agency, Laurel, Maryland.

7. Myers, G. E., Optimization of HTPB Binder, Final Technical Report LPC-436-F (AFRPL-TR-71-123), January 1972.
8. Grubisic, Z., Rempp, R., and Benoit, H., Journal of Polymer Science, Part B, Vol. 5, p. 753, 1967. See also: Cantow, M. J. R., and Johnson, J. F., Journal of Applied Polymer Science, Vol. 11, p. 1851, 1967; Journal of Polymer Science, Part A-1, Vol. 5, p. 2835, 1967.
9. Cantow, M. J. R., Porter, R. S., and Johnson, J. F., Journal of Polymer Science, Part A-1, Vol. 5, pp. 987, 1301, 1967.
10. Ramey, K. C., Characterization of Hydroxy-Terminated Prepolymer R-45M, Paper presented at the Fifth JANNAF Symposium on Propellant Characterization, October 1974; Publication 258, Chemical Propulsion Information Agency, Laurel, Maryland, October 1974.
11. Blanks, J. W., Shephard, I. G., and Stephens, W. D., Comparison of R-45M Fractionation Methods, Paper presented at the Sixth JANNAF Symposium on Propellant Characterization, September 1975; Publication 269, Chemical Propulsion Information Agency, Laurel, Maryland, September 1975.
12. Dilts, R. D., Ghilarducci, H. E., Van Vleck, L. D., Mastrolia, E. J., Bills, K. W., Frost, C. B., Epstein, R. H., Dankman, H. S., and Klotz, M. A., Advanced Technology Studies Under Production Support Program, Vol. I, Optimized Binder for High-Performance Solid Propellants, Final Technical Report BSD-TR-66-28, September 1965.
13. Muenker, A. H., and Hudson, B. E., Functionality Determination of Binder Prepolymers, Final Technical Report GR-8-FBP-68 (AFRPL-TR-68-237), October 1968.
14. Johnson, K. E., Functionality, Molecular Weight, and Solution Properties of Hydroxyl- and Carboxyl-Terminated Polybutadienes, Technical Report S-193, November 1969.
15. Yau, W. W., Kirkland, J. J., and Bly, D. D., Modern Size-Exclusion Liquid Chromatography, Wiley-Interscience, New York, 1979, Ch. 1
16. Kremmer, T., and Boross, L., Gel Chromatography, Wiley, Chichester, England, 1979.
17. Cazes, J., and Dobbins, R. J., Journal of Polymer Science, Part B, Vol. 8, p. 785, 1970.
18. Drott, E. E., In Liquid Chromatography of Polymers, Cazes, J., Ed., Dekker, New York, 1977, p. 161.
19. Anderson, W. S., Hyer, H. J., Nehr Korn, D. W., Sawyer, J. M., Saunders, M. E., and Wong, M. W., Characterization of Hydroxy-Terminated Polybutadiene, Paper presented at the Tenth JANNAF Symposium on Propellant Characterization, October 1980; Publication 333, Chemical Propulsion Information Agency, Laurel, Maryland, October 1980.
20. Coleman, M. M., and Fuller, R. E., Journal of Macromolecular Science, Part B, Physics, Vol. 11, p. 419, 1975.

21. Law, R. D., Journal of Polymer Science, Part A-1, Vol. 9, p. 589, 1971.
22. Muenker, A. H., Determination of Prepolymer Functionality and Its Relationship to Binder Properties, Final Technical Report GR-10-FBP-70 (AFRPL-TR-70-30), February 1970.
23. DiMilo, A. J., The Development and Evaluation of a Hydrocarbon Binder for High Energy Solid Propellants, Final Technical Report 1030-82F (AFRPL-TR-68-238), November 1968.
24. Consaga, J. F., Journal of Applied Polymer Science, Vol. 14, p. 2157, 1970.
25. Ramey, K. C., Characterization of R-45M, Final Technical Report AFRPL-TR-74-64, September 1974.
26. Dee, L. A., Biggers, B. L., and Fiske, M. E., Analytical Chemistry, Vol. 52, p. 572, 1980.
27. Laub, R. J., Purnell, J. H., Williams, P. S., Harbison, M. W. P., and Martire, D. E., Journal of Chromatography, Vol. 155, p. 233, 1978.
28. Emanuel L. J., and Dee, L. A., Semi-Micro Hydroxyl Equivalent Weight Methods, Technical Report AFRPL-TR-82-041, Air Force Astronautics Laboratory, Edwards Air Force Base, California, July 1982. See also: Emanuel, L. J., and Park, T. W., A Hydroxyl Equivalent Weight Interlaboratory Study, Technical Report AFRPL-TR-84-088, Air Force Astronautics Laboratory, Edwards Air Force Base, California, December 1984.
29. Tserng K.-Y., and Klein, P. D., Steroids, Vol. 29, p. 635, 1977.
30. Laub, R. J., and Pecsok, R. L., Physicochemical Applications of Gas Chromatography, Wiley-Interscience, New York, 1978.
31. Goodlett, V. W., Analytical Chemistry, Vol. 37, p. 431, 1965.
32. Mark, H. D., and Rogers, M. G., Analytical Chemistry, Vol. 44, p. 837, 1972.
33. Rogers, M. G., Journal of Applied Polymer Science, Vol. 16, p. 1953, 1972.
34. Hammerich, A. D., and Willeboordse, F. G., Analytical Chemistry, Vol. 45, p. 1696, 1973.
35. Batzer, H., and Zahir, S. A., Journal of Applied Polymer Science, Vol. 19, p. 601, 1975.
36. Goldwasser, J. M., and Adolph, H. G., Hydroxyl Group Determination in Prepolymers by ¹H NMR Spectroscopy, Paper presented at the Sixteenth JANNAF Symposium on Propellant Characterization October 1985; Publication 435, Chemical Propulsion Information Agency, Laurel, Maryland, October 1985.
37. Senger, J. S., Subramanian, R., Ward, T. C., and McGrath, J. E. Polymer Preprints, Vol. 27, p. 144, 1986.
38. Fox, J., and Flory, P. J. Journal of Applied Physics, Vol. 21, p. 581, 1950; Journal of Polymer Science, Vol. 14, p. 315, 1954.

39. Boyer, S. K., Macromolecules, Vol. 7, p. 142, 1974.
40. Faucher, M. Polymer Letters, Vol. 3, p. 143, 1965.